UNIVERSITY OF CAPE COAST

OPTIMIZATION OF PATIENT RADIATION PROTECTION IN DIGITAL DIAGNOSTIC RADIOGRAPHY EXAMINATIONS IN GHANA

EMMANUEL GYAN

2020

UNIVERSITY OF CAPE COAST

OPTIMIZATION OF PATIENT RADIATION PROTECTION IN DIGITAL DIAGNOSTIC RADIOGRAPHY EXAMINATIONS IN GHANA

BY

EMMANUEL GYAN

Thesis submitted to the Department of Physics of the School of Physical Sciences, College of Agriculture and Natural Sciences, University of Cape Coast, in partial fulfilment of the requirements for the award of Doctor of Philosophy degree in Physics

APRIL 2020

DECLARATION

Candidate's Declaration

I hereby declare that this thesis is the result of my own original research and that no part of it has been presented for another degree in this University or elsewhere.

Candidate's Signature …….. Date ……

Name: Emmanuel Gyan

Supervisors' Declaration

We hereby declare that the preparation and presentation of the thesis were supervised in accordance with guidelines on supervision of thesis laid down by the University of Cape Coast.

Principal Supervisor's Signature ……. Date …….....

Name: Stephen Inkoom (Ph.D.)

Co-Supervisor's Signature …….. Date ……

Name: Prof. George Amoako

ABSTRACT

The basic challenge with digital radiography systems is the large dynamic range which has the potential to increase patient radiation dose unnecessarily. The aim of this study was to optimize patient radiation protection in digital radiography systems. Entrance skin dose (ESD) of nine radiological examinations were estimated from five selected radiographic centers using mathematical equation. Anthropomorphic phantom images were acquired with different exposure factors for chest posterior anterior (PA), lumbar spine anterior posterior (AP) and lumbar spine lateral (LAT) at one of the centers. Clinical assessment of the images were done by three (3) senior radiographers to determine the optimal peak-kilo-voltage (kVp), milli-ampere seconds (mAs), Entrance skin dose and exposure indicator (EI). The average ESDs estimated were 0.66 ± 0.60, 2.47 ± 0.80, 3.77 ± 0.90, 0.47 ± 0.30, 0.49 ± 0.30, 1.37 ± 0.60, 1.29 ± 0.50, 1.74 ± 0.80 and 2.15 ± 0.90 mGy for chest PA, lumbar spine AP, lumbar spine LAT, cervical spine AP, cervical spine LAT, skull PA, skull LAT, pelvis AP, and abdomen AP respectively. The optimal exposure factors were 90 kVp, 2.5 mAs; 100 kVp, 2.0 mAs and 110 kVp; 1.6 mAs for chest PA. The optimal EI was obtained to be within the range of 2323 – 2355 with optimal ESD of 0.29 mGy. 70 kVp; 22 mAs with associated EI of 348 – 363 and optimal ESD of 1.97 mGy were obtained for lumbar spine AP. For lumbar spine LAT, 80 kVp; 25 mAs, and 90 kVp; 20 mAs, with EI values of 895 – 1005 were obtained. The optimal ESD obtained for lumbar spine LAT were 3.20 and 3.30 mGy. In conclusion, model equation of EI, mAs, and kVp, as well as optimization management flow chart were developed to help reduce patient radiation dose in digital radiography.

KEY WORDS

Digital radiography

Entrance skin dose

Exposure factors

Optimal factors

Optimization

Radiation

ACKNOWLEDGEMENTS

I am very grateful to Ghana Education Trust Fund (GETfund) for the financial support towards this Ph.D studies. I am equally thankful to Norwegian Partnership Programme for Global Academic Cooperation (NORPART- project, Ghana-Norway Collaboration in Medical Physics and Radiography Education) and the NORPART coordinators both in Ghana and Norway for giving me the opportunity to continue this research at the Norwegian University of Science and Technology at Trondheim.

My heartfelt gratitude goes to my supervisors; Dr. Stephen Inkoom of the Radiation Protection Institute, Ghana Atomic Energy Commission, Prof. George Amoako, Head of Physics Department, University of Cape Coast for their contributions, advisors, encouragements and guidance. Infact with their hardwork and dedication, this research has been completed on schedule.

Special gratitude to Prof. Erik Pal Goa at the Department of Physics, Norwegian University of Science and Technology for his contribution and support to this work.

I am also thankful to Leonard Quansah at Philips Medical Systems-Ghana for his support. Also, I am grateful to Linn Rolstadaas, Sven-Erik Ivan Johnsson and Tommy Berglund- Medical Physicists at St. Olav's hospital-Norway and Sykehnsinnkjop H.F. respectively for their professional advice, contributions and guidance.

Finally, my special thanks go to my family and friends especially my wife and Kinsley Agyemang for their support, contributions and encouragement throughout my Ph.D. studies.

DEDICATION

To my wife Harriet Nyarko and my children; Lorena Baabea-Gyan, Lawrence Gyan and Vincent Nhyira-Gyan.

TABLE OF CONTENTS

LIST OF TABLES

LIST OF FIGURES

LIST OF ACRONYMS

AAPM	American Association of Physicists in Medicine
AEC	Automatic Exposure Control
ALARA	As Low As Reasonably Achievable
AP	Anterior – Posterior
AUC	Area Under Curve
CD	Capacitor Discharge
CEC	Commission of European Communities
CNR	Contrast to Noise Ratio
CR	Computed Radiography
CT	Computed Tomography
DAP	Dose Area Product
DDR	Direct Digital Radiography
DI	Deviation Index
DICOM	Digital Imaging and Communications in Medicine
DNA	Deoxyribonucleic Acid
DQE	Detective Quantum Efficiency
DR	Digital Radiography
DRL	Diagnostic Reference Levels
EI	Exposure Indicator
ED	Effective Dose
ESD	Entrance Skin Dose
FRD	Focus to Receiver Distance
FSD	Focus to Skin Distance
QC	Quality Control
HVL	Half Value Layer
IAEA	International Atomic Energy Commission
ICS	Image Criteria Score
ICRP	International Commission of Radiological Protection

ICRU	International Commission on Radiation Units and Measurements
IEC	International Electroctechnical Commission
K_{IND}	Indicated equivalent air kerma
K_{TGT}	Target equivalent air kerma
KUB	Kidney Ureter Bladder.
kV	Kilo Voltage
kVp	Peak kilo Voltage
LAT	Lateral
LNT	Linear -no -Threshold
LSF	Line Spread Function
mAs	milli Ampere seconds
MTF	Modulation Transfer Function
MRI	Magnetic Resonance Imaging
NCRP	National Commission on Radiation Protection and Measurements
NEQ	Equivalent Number of Quanta
NRA	Nuclear Regulatory Authority
NRPB	National Radiological Protection Board
OBL	Oblique
PA	Posterior-Anterior
PSF	Point Spread Function
Q	Quantity of Charge
PACS	Picture Archiving and Communication Systems
ROC	Receiver Operating Characteristics
SID	Source to Image Distance
SNR	Signal to Noise Ratio
TFT	Thin Film Transistor
TLD	Thermolumences Dosimeter
UK	United Kingdom
UNSCEAR	United Nations Scientific Committee on the Effects of Atomic Radiation

V	Applied Voltage
VGA	Visual Grading Analysis
VGAS	Visual Grading Analysis Score

CHAPTER ONE

INTRODUCTION

1.0 Introduction

Ionizing radiation has significant applications in medicine for producing radiographs for diagnostic and therapeutic purposes. However, the use of ionizing radiation is associated with risks of stochastic and deterministic effects to patients. In order to minimize its harmful effects and to ensure its safe applications in radiography, optimization of the patient radiation dose is necessary. This chapter covers background of the study, statement of the problem, purpose of the study/research objectives, significance of the study, limitations of the study and organization of the study.

1.1 Background to the Study

1.1.1 X-ray equipment

Basically, medical X-ray equipment is made up of the generator and the tube (Khan, 2003; Seibert, 2004). The X-ray tube converts the kinetic energy of the highly accelerated electrons into X-rays. Its main components are the cathode and the anode assemblies, the tube envelop, the rotator and the stator, and the tube housing (Martin, 2006). The design of X-ray tube greatly affects beam characteristics such as focal spot size, X-ray field uniformity and X-ray energy spectrum. Radiological parameters like patient dose, image contrast and spatial resolution also depend on these basic beam characteristics (Zink, 1997). The X-ray generator is mainly a high voltage transformer circuit which allows the operator to select X-ray energy (kilovoltage peak), quantity

of X-ray to be produced, exposure time and focal spot size (Seibert, 2004). There have been many types of X-ray generators over the years which include; single phase self-rectified, single phase full-wave rectified, three phase, three phase six pulse, three phase twelve pulse, constant potential, high frequency and capacitor discharge (CD) mobile generators (Nickoloff & Berman, 1993). The X-ray generator supplies high voltage that is applied between the cathode and the anode of the X-ray tube which is needed for the production of X-rays. This high voltage determines the energy and the quality of the X-rays produced. The X-ray generator again, has a low voltage circuitry that provides the filament current. The filament current causes electrons emission from the cathode to the anode. The number of electrons emitted from the cathode depends on the filament current (Seibert, 1997).

1.1.2 X-ray production

X-rays are produced when the kinetic energy of accelerated electrons from the cathode is converted into electromagnetic radiation when the electrons collide with the anode (Martin, 2006). When the accelerated electrons from the cathode hit the anode, energy is imparted to the anode and in the process, X-rays are produced. The two types of X-rays produced in this process are characteristic X- rays and the Bremsstrahlung (braking radiation) (McCollough, 1997). Characteristic X-rays are produced when an incoming electron dislodges an electron from the inner K shell of the atom of the anode. When this happens, a hole is created in the inner K shell; an electron from the higher L shell will move to fill this hole in the K shell. Kinetic energy is lost in the process and characteristic X-rays are produced. Other transitions such as from M shell to the K shell and N shell to the K shell are also possible. The

binding energy of K shell electron to the nucleus in tungsten which is always used as the anode material in medical X-ray equipment is above 70 kV (Nickoloff, & Berman, 1993). It therefore means that to eject electron from K shell in tungsten requires energy greater than 70 kV. This implies that energies below 70 kV will produce entirely Bremsstrahlung radiation (Podgorsak, 2006).

Bremsstrahlung radiation is produced when an electron passes close to the atomic nucleus of the anode material; the positively charged nucleus decelerates the negatively charged electron thereby causing change in path and loss of kinetic energy. X-rays are produced in the process which is proportional to the loss of the energy (Podgorsak, 2005). The process of X-rays production is highly ineffective as only one percent (1%) of the total kinetic energy is converted to useful X-rays while the remaining ninety nine percent (99%) is wasted as heat (Zink 1997; Slapa et al., 2002).

1.1.3 Application of X-rays in medicine

The discovery of X-rays in 1895 by William Conrad Roentgen (Panchbhai, 2015; Kemerink et al., 2012; Mould, 1995) has impacted positively on health care delivery across the world (Oluwafisuye et al., 2010). It has provided an opportunity for physicians and surgeons to see through the human body without cutting them. It has also facilitated diagnosis, treatment and management of patients (Ibrahim et al., 2014).

The application of X-rays in medicine started immediately after Roentgen's discovery, where a radiograph of his wife's hand was produced. Within a year of its discovery, the first radiology department was established in Glasgow hospital where kidney stones and a penny lodged in a child's

throat were radiographed (Waters, 2011). This development established a new specialty in medicine called radiology. Diagnostic radiology comprises of different imaging modalities such as conventional radiography, computed tomography (CT), ultrasound, magnetic resonance imaging (MRI), mammography, dental radiography and nuclear medicine for diagnosis and treatment. However, MRI and ultrasound use non-ionizing radiation. Although there are different types of imaging modalities in radiology, the decision to employ a modality for an examination is usually influenced by the diagnostic information required and the availability of the modality. It is therefore important that medical practitioners abreast themselves with the limitations and the advantages of these modalities in clinical applications. Improper selection of modality could greatly impair the diagnostic information sought for and could possibly increase patient radiation dose unnecessarily.

Computed tomography is an imaging modality that utilizes X-ray photons to produce images. It combines multiple X-ray projections taken from different angles to produce detailed cross-sectional images of the region of interest in the human body. The use of CT in medicine has drastically increased since its introduction in the 1970s. It is estimated that, the annual CT examinations in United States increased from approximately 3 million in 1980 to about 70 million in 2007 (Smith- Bindman et al., 2009). Computed tomograph has an advantage of producing three- dimensional views of the organ or body region of interest. It also has high contrast sensitivity which helps in visualizing soft tissues. However, CT delivers substantial amount of dose to the body organs than the conventional radiography (Brenner & Hall 2007).

Conventional radiography uses X-rays which are ionized. It is useful to detect pathologies of the skeletal systems as well as the adjacent soft tissues. Conventional radiography still remains the first line of modality in some clinical inductions such as fractures. It is also effective in evaluating the chest for conditions like pneumonia, lung cancers, tuberculosis, congenital cardiac failure etc. Conventional radiography is however limited in the radiological demonstration of soft tissues such as brain, spinal cord and muscles.

The introduction of computers in medicine has significantly changed detector technology from the screen-film radiology to digital radiology. It is now possible to convert analogue images into digital form which can be monitored on computer and transmitted electronically. This development has improved the capabilities of conventional radiography into what is now called digital radiography. Digital radiography is further classified as computed radiography (CR) and direct digital radiography (DDR). The details of these systems have been given in chapter two of this thesis. Conventional radiography is still useful due to its low cost, availability, and relatively low radiation dose as compared with CT.

Medical exposure of ionizing radiation is the largest source of man-made exposure to ionizing radiation (Moores et al., 2012). It includes exposure of patients as part of their medical diagnosis or treatment, exposure of individuals as part of health screening programs and exposure of healthy individual voluntarily participating in medical, biomedical diagnostic or therapeutic research program (UNSCEAR, 2008). Collective and individual doses to patients from medical exposure keep increasing significantly from year to year (Moores, 2012). It accounts for about 96% of all man-made

radiation exposure to humans and expected to increase significantly (Sulieman, 2015). Technological improvement of X-ray equipment will continue to drive its application in medicine. It is estimated that more than ten million diagnostic examinations are performed in a day worldwide (Larcher et al., 2008). Generally, radiography still accounts for about two-thirds of all X-ray imaging (Larcher et al., 2008). In 1982, the per capita dose among US population was estimated at 0.54 mSv while the collective dose was 124,000 person-Sv. However, according to the preliminary estimates of the National Council on Radiation Protection and Measurements (NCRP) scientific committee 6-2 medical subgroup, the per capita dose from medical exposure (excluding dental and radiotherapy) had increased by 600% to about 3.0 mSv while the collective dose had also increased over 700% to 900, 000 person-Sv in 2006 (Mettler, 2008). In the United Kingdom (UK), 41.5 million medical and dental X-ray examinations are performed each year which puts the annual per capita effective dose to 330.0 µSv (Hart &Wall, 2002).

1.1.4 Overview of radiation protection

X-rays are part of the electromagnetic waves with high frequency, high energy and short wavelength (Aichinger et al., 2012). The energy associated with X-rays is high enough to remove electrons from atoms or molecules and hence causing ionization. The ionizing effect of X-rays has potential to cause damage to biological tissues and therefore radiation protection measures must be instituted to minimize its effects. Another reason why radiation protection in medical diagnostics should be taken seriously is the large numbers of population being exposed to X-rays. For instance, it has been reported that medical exposure to Americans has increased by seven folds from 1980s to

2006 (Schauer & Linton 2009). Again, inappropriate radiological examinations have been reported in clinical practice which justify radiation protection in diagnostic radiology. Reports in literature indicated that about 20 to 50% of radiological examinations might not be appropriate (Malone et al., 2012). Insufficient knowledge of both referring and radiological practitioners about radiation doses and its associated risks to patients has been largely reported as the cause of inappropriate radiological examinations (Sukumar, & Ricketts, 2013). Early radiation protection recommendations by International Commission on Radiological Protection (ICRP) focused only on the protection of X-ray and radium workers in medical facilities and to provide advice on how to avoid harmful skin reactions (ICRP 2016). However, as the harmful effect of X-rays became public health issues, recommendations were extended to the public and patients. Radiation protection involves implementation of good practice to reduce exposure to patients, radiation workers and the general public.

The ICRP stated that 'the overall objective of radiation protection is to provide an appropriate standard of protection for man without unduly limiting the beneficial practices giving rise to the radiation exposure' (ICRP, 1991). NCRP report (No 116) also stated that "the goal of radiation protection is to prevent the occurrence of serious radiation induced conditions (acute and chronic deterministic effects) in exposed persons and to reduce stochastic effects in exposed persons to a degree that is acceptable in relation to the benefits to the individual and to society from the activities that generate such exposure" (Grover, Kumar, Gupta, & Khanna, 2002; NCRP, 1993).

The principles of radiation protection as recommended by ICRP are justification of practice, optimization of procedures and techniques and dose limitation. Detailed explanation of these principles are given in section 2.8. The radiation protection principles and recommendations are set by international organisations such as ICRP and International Atomic Energy Agency (IAEA) (Grover et al., 2002). The principles and recommendations flow down to national and regional regulators such National Commission on Radiation Protection and Measurements (NCRP) in United State of America, Atomic Energy Regulatory Board (AERB) in India, and Nuclear Regulatory Authority (NRA) in Ghana.

1.1.5 Optimization in digital radiography

Lack of consistent feedback to radiographers and technologists regarding the use of optimal acquisition techniques and the wider dynamic range of digital systems have the potential to increase patient radiation dose (Williams et al., 2007). Over exposure of 5 – 10 times the normal exposure can occur and the image would still appear as properly exposed because of the compensation of the digital detector (Seibert, & Morin, 2011). The large dynamic range of the digital systems has been reported as the causes of dose creep in digital radiography. Dose creep is the gradual increase in X-rays exposure over time that results in increased radiation dose to patients (Gibson, & Davidson, 2012). Image contrast and brightness are no longer related to the exposure techniques due to the post-processing algorithms of the digital technology. Over exposure and under exposure cannot be easily recognized because of the large dynamic range and post processing capabilities of the digital systems (Adejoh, Ewuzie, Ogbonna, Nwefuru, & Onuegen 2016).

Eliminating dose creep is very necessary since digital systems are supposed to reduce patient radiation dose. One of the ways to achieve this, is regularly optimizing the protocols and procedures of digital radiography. Optimization of patient radiation dose is therefore as important in digital radiography as in the screen film. Understanding the factors that control image quality parameter are essential to optimize, maintain image quality and to reduce radiation dose to the patients in line with the As Low As Reasonably Achievable (ALARA) principle (Alsleem, & Davidson, 2012).

Fundamental requirement for the optimization of imaging procedures protocols and selection of technical factors is the complete understanding of the digital image structure, impact of image quality and the concept and practice of optimization. Patient radiation is normally controlled by X-rays' technical factors which include applied tube voltage (V), quantity of charge (Q), grid, source to image distance (SID), filtration, beam collimation as well as the amount of energy imparted to the body, and the size and the area of the body being irradiated (Seibert & Morin, 2011). Any of these factors can be optimized in digital radiography to reduce patient radiation dose. Some studies have used tube potential (V, Q, and filtration) for the optimization (Geijer, Norrman, & Persliden 2009). Optimization is not only about reducing patient radiation dose but also to produce quality images to accomplish particular clinical task. Therefore, factors which influence image quality (noise, resolution and contrast) can also be quantified to guide the optimization protocols. These physical parameters have been quantified in terms of detective quantum efficiency (DQE), signal to noise ratio (SNR), contrast to noise ratio, (CNR), and modulation transfer function (Alves et al., 2016). The

automatic exposure control (AEC), and the exposure indicator (EI) are some of the components in digital radiography that can be optimized to help reduce radiation dose and achieve good image quality (Allen, et al., 2012; Batista 2016). Optimizing the EI is closely related to optimizing kV and mAs (Seeram, Bushong, Davidson & Swan 2016). The purpose of AEC is to deliver consistent, reproducible exposures across a wide range of anatomical thicknesses and tube potential.

1.2 Statement of the Problem

Digital radiography is rapidly replacing screen-film systems in medical imaging. This technology has many advantages over screen-film radiography which include wider dynamic range and post processing algorithm. These advantages which are supposed to reduce patient radiation dose equally have the potential to increase patient dose significantly. The wider dynamic range of digital systems contributes to overexposure with no adverse effect on the image quality which results in dose creep. This results in unnecessary exposure of patients to ionizing radiation which has the potential to cause harmful effects. Exposure to ionizing radiation is associated with potential risk of cancer and other hereditary disorders and therefore its use must be optimized to minimize the risks to patients who undergo radiographic examinations. In screen-film radiography, the optical density easily serves as a visual feedback to the radiographers regarding the level of exposure to the detector and the patient. Overexposure is easily recognized by just looking at film blackening. However, in digital radiography overexposure is hardly identified. The optical density is not directly related to the patient exposure in

digital radiography, therefore EI was developed by digital systems manufacturers to serve as feedback regarding the levels of exposure to the detector. This EI is not directly related to patient dose but rather a measure of exposure to the detector. How well EI could be used as proper feedback to check patient radiation dose is not well understood by researchers. The relationship between the patient radiation dose and the EI is still not well understood. Exposure indicator has not been well optimized to establish the optimal ranges that produce quality image that obey the ALARA principle. Further research is required to properly understand the EI effectiveness as a feedback mechanism and its relationship to the patient radiation dose.

Exposure parameters significantly affect patient radiation dose and image quality. The selection of exposure factors is one of the basic challenges often encountered at radiology departments. An experienced radiographer sometimes finds it difficult to select the correct exposure factors for optimal image quality and low dose. Some digital radiography systems have AEC device which helps in the selection of the technical factors. However, due to lack of better understanding in the use of this AEC and its inherent challenges make it difficult for some radiographers to fully make use of it. Recommended alternative is to optimize these technical factors and develop exposure charts which could clearly be displayed at the radiology department. This thesis is therefore seeking to fill the gap in the exposure indicator, optimize exposure factors for chest PA, lumbar spine AP and lumbar spine LAT. It is to establish clearly the relationship between EI and patient radiation dose and how truly the EI reflects the true exposure to the detector.

1.3 Purpose of Study/ Research Objectives

The purpose of this study was to optimize the patient radiation dose while maintaining image quality that would provide necessary diagnostic information. The specific objectives of this research work included:

1. To perform five quality control tests on five (5) X-ray equipment used for the study.
2. To estimate average patient entrance surface dose for chest Posterior-anterior (PA), lumbar spine anterior-posterior and lateral (AP &LAT), skull (AP & LAT), pelvis (AP), cervical spine (AP,& LAT), and abdomen (AP) radiographic examinations using CR.
3. To perform dose-image quality analysis using visual grading analysis on anatomical structure visualization to determine optimal dose, quantity of charge, applied voltage, and related EI for chest (PA), lumbar spine (AP and LAT) examinations.
4. To model mathematical relationship relating EI, Q and V for chest PA examination.
5. To develop EI based on optimization management strategy to help reduce unnecessary radiation exposure to patient.

1.4 Significance of the Study

In Ghana, digital radiography is rapidly replacing the conventional screen-film radiography in medical imaging. Digital radiography has the potential to either reduce or increase the patient radiation dose and therefore patient radiation dose must be monitored to avoid the potential risks associated with ionizing radiation. The first task of this work was to determine the patient

radiation dose (entrance surface dose) in some digital radiography projections. This dose survey on digital systems would provide background information for radiographers, radiologists, medical physicists, researchers, policy makers, regulatory authorities and other bodies in Ghana. This would also help to streamline the radiation protection of patients in diagnostic radiographic examinations in Ghana through proper application of optimization protocols.

The other aspect of this work would concentrate on dose-image quality optimization to determine optimal exposure factors (V, Q, and EI) for chest PA, lumbar spine AP and lumbar spine LAT which would help radiographers and technologists in selecting optimum exposure factors for these examinations. The availability of optimization strategy flow chart would significantly help to curtail dose creep which is a major challenge in the practice of digital radiography regarding radiation dose. The work would also contribute to the existing literature knowledge on EI as feedback mechanism to radiographers, how EI is linked with patient dose and how well it represents the exposure to the detector to ensure patient safety in digital systems.

1.5 Delimitations of the Study

This research will be limited to the following areas.

1. It would cover digital radiography both CR and DDR for the entrance skin dose survey but dose-image quality optimization would be done using CR. The study would not be applicable to screen-film radiography, fluoroscopy and CT.
2. The radiographic examinations covered under this study included chest (PA), abdomen (AP), skull (AP & LAT), cervical spine (AP & LAT),

lumbar spine (AP & LAT), and pelvis (AP). No interventional radiography will be considered under this study.

3. The patient dosimetric quantity to be considered in this study was the entrance skin doses. Organ dose, effective dose, and equivalent dose would not be considered in this study.
4. The exposure factors to be optimized in this study would be V, Q and EI. The study would not include other parameters such as filtration, source to image distance, half value layer and collimation which could also be optimized.
5. The image quality metric to be used for this study in determining the image quality will be the absolute visual grading analysis. Receiver operating characteristic (ROC) will not be applicable in this study.
6. The study will also cover the quality control test on the X-ray equipment which will include kVp accuracy and reproducibility, Dose-kVp linearity test, X-Ray tube output. Beam and collimation alignments would not be considered in this study.

1.6 Limitations of the Study

The following limitations were encountered but did not affect the accuracy and timely delivery of the research results;

1. Scattered nature of the study areas was a challenge for smooth data collection.
2. Effect of different patient thicknesses on patient radiation dose could not be evaluated since there was no access to different anthropomorphic phantom thickness. Therefore, all equations,

relationships and models established in this study are reliable only on the average patient thickness of 23 cm for chest PA, Lumbar spine AP and 25 cm for lumbar spine LAT.

3. The image quality assessments were done by only senior radiographers due to lack of availability of radiologists.

1.7 Organization of the Study

This thesis consists of five chapters. Chapter one is the introduction to the study. It focuses on the background to the study which examines the application of X-rays in medicine and other issues on optimization in digital radiography. It also discusses the purpose of the study and the research objectives. The significance of the study as well as the delimitations of the study are discussed under this chapter.

Chapter two is about the literature review. This chapter reviews existing literature that are linked with the study area. It discusses screen-film radiography, computed and direct digital radiography. Literature on biological effects of ionizing radiation, principles of optimization, patient radiation dosimetry, quality control in diagnostic radiography systems, image quality assessment, estimation of patient radiation dose and diagnostic reference levels have been reviewed.

Chapter three covers the methodology of the study. This chapter describes fully the materials and methods of this research study. It presents in details the data collection instrument, data collection procedures and the processing and analyses. It will also explains the study design and how the experimental procedures were carried out.

Chapter four presents the results and discussion. The results on the experimental procedures are presented in this chapter. The results of average entrance skin dose, the EI, image quality analysis, and the optimal exposure factors for chest PA, lumbar spine AP and lumbar spine LAT are presented. The model linking V, Q and inverse EI for chest PA as well as the optimization strategy flow chart are also presented.

The final chapter is the summary, conclusion and recommendations. This chapter summarizes the entire research work and discuss its findings as well as the recommendations for further action.

1.8 Chapter Summary

This chapter covers the introduction to the study and examines background to the study, statement of the problem, purpose of the study/research objectives, significance of the study, limitations of the study and organization of the study.

X-ray equipment is basically made up of generator and tube. The X-ray tube converts the kinetic energy of the highly accelerated electrons into X-rays. Two types of X-rays produced through this process are characteristic X-rays and Bremsstrahlung. Application of X-rays in medicine started immediately after Roentgen's discovery which resulted in the establishment of a new speciality in medicine known as radiology. The ionizing effect of X-ray has the potential to cause biological damage to tissues. For this reason, radiation protection in diagnostic radiography becomes necessary for both the workers and the general public.

Optimization in digital radiography is necessary due to lack of consistent feedback to radiographers and technologists regarding the use of optimal acquisition techniques and the wider dynamic range of digital detectors. Consequently, overexposure in digital radiography can occur without an adverse effect on image quality. However, patient radiation dose could increase unnecessarily which has the potential to cause harmful effect in humans.

The main objective of this study was to optimize the patient radiation dose while maintaining the image quality that would provide necessary diagnostic information. The significance of the study is that, background information on patient radiation dose that to be estimated would be useful information for radiographers, radiologists, medical physicist, researchers, policy makers, regulatory authorities and other bodies in Ghana. It will also contribute to the existing literature knowledge on EI as a feedback mechanism to radiographers. The scattered nature of the study areas and the use of only senior radiographers for assessing the image quality due to lack of availability of radiologists were some of the limitations to this study.

CHAPTER TWO

LITERATURE REVIEW

2.0 Introduction

This review covers screen-film radiography, physics of digital radiography systems, quality control in diagnostic radiography, Exposure indicator, biological effects of ionizing radiation, principles of radiation protection, principles of optimization, optimization in digital radiography, patient radiation dosimetry, diagnostic reference levels (DRLs), image quality assessment and gaps in literature.

2.1 Screen-Film Radiography

The screen-film system was employed in radiography immediately following the discovery of X-rays and are still widely used in many countries around the world. However, it is being replaced by digital imaging systems due to its limited linear response to radiation. Thus, it cannot tolerate a wide range of radiation exposure without getting saturated. Screen-film images become underexposed at low exposures and at higher exposures become overexposed due to its limited dynamic range (Veldkamp, Lucia, & Geleijns, 2009; Mattoon & Smith, 2004; Doi, 2006). Also, it has no post processing capabilities for error corrections and therefore repeat examinations are very common which tend to increase patient radiation dose and cost. Again, it is not compatible with picture archiving and communications systems (PACS) and requires manual transmission from one point to the other. However, conventional screen-film has higher spatial resolution than that of storage-

phosphor image plates. In terms of diagnostic values, the two image systems are almost equivalent (Uffmann & Schaefe-Prokop, 2009).

In Screen-film radiography, the radiographic film is processed using chemicals (fixer and developer) to transform the latent image into visible image which can be interpreted later. It consists of radiographic film that is sandwiched between two intensifying screens being protected by harder case called cassette. Image acquisition, display, and storage all occurred on the radiographic film in screen-film radiography. The film density is used as an exposure indicator. The appearance of film after processing provides an immediate feedback regarding exposure in screen-film radiography (Bansal, 2006). The intensifying screen converts the X-rays into light and increases the efficiency of exposure of the film as compared with the direct exposure by the X-ray beams (Ritenour, 1996). The use of intensifying screen also reduces the absorbed dose to patient (Davidson, 2006; Oborska-Kumaszнska, 2011). Fluorescent materials which have been used as intensifying screens include; calcium tungstate ($CaWCO_4$) which emits blue light, gadolinium oxysulphide; terbium activated (Gd_2O_2S; T_b) which emits green light and lanthanue oxyrrommide; thulium activated (laOBr;Tr) also emits blue light (Bushberg, 2002; Graham & Cloke, 2003).

2.2 Digital Radiography Systems

Digital radiography is not much different from the screen-film radiography except the production of the latent images and how the images are processed. Digital radiography can be subdivided into computed radiography (CR) and direct digital radiography (DR) depending on how the images are

acquired (Mothiram, Brennan, Lewis, Moran, & Robinson, 2014). The significant difference between digital radiography and screen-film technologies are image acquisition and the read-out processes. Digital radiography has some advantages over the conventional screen film systems. It has wide dynamic range which tends to decrease repeat examinations and thus reduce patient radiation dose. It is also compatible with PACS making transmission of digital images from one point to another very easy. It again has post processing capabilities which tend to improve image quality (Berkhaut et al., 2004).

2.3 Physics of Computed Radiography

Computed radiography was first introduced in diagnostic medical imaging by Fuji film medical systems in the 1980s (Korner et al., 2007). The image acquisition systems are separated from the image read out processes. The CR system is made up of image plates, plate reader, computer, and printer. The basic principle of the CR is that, it first captures the image on the plate and then transfer to a computer (Korner et al., 2007). CR image plate is composed of detective layer of photostimulable crystals containing different halogenides such as chlorine, iodine and bromide. The photostimulable phosphor (PSP) is enclosed in a protective cassette just like screen-film system (Seibert, 2004). The desired properties of PSP (imaging plate) in medical imaging applications have been described by (Schaetzing, 2003). Schaetzing outlined the following desired properties;

1. The PSP used as acquisition system must absorb the X-ray coming from the exposed object.

2. The PSP must produce latent image proportional to the absorbed aerial images and must retain the latent image for a longer period of time.
3. Be able to convert the latent image into a digital form.

The phosphor materials found to have satisfied the above properties to be used in CR technology is the barium fluorohalide family doped with europium (BaFX: Eu^{2+}) where X is Cl, Br, or I (Schaetzing, 2003). The most common commercially available image plate is the barium fluro-bromide/iodide (BaFBr/I) (Lanca and Silva, 2013). The europium known as activator is an impurity added to control the amounts of phosphor during the process of manufacturing. It significantly affects the storage properties of the phosphor and the spectrum of the emitted light.

When the image plate is exposed to X-rays, the energy of the incident radiation is absorbed and excites electrons into higher energy levels. These excited electrons will remain trapped at the unstable energy levels of the atom. The absorbed X-ray energy is stored in gaps of the altered crystal structure as latent image temporally (Nyathi, Chirwa, & Merwe, 2010). The CR plate does not store information regarding the tube current (mAs) and tube potential (kVp). The latent images acquired by CR detector can only be stored for a period of time. The amount of energy stored decreases with time. Twenty five percent (25%) of the stored signal can be lost between 10 minutes to 8 hours after exposure through spontaneous phosphorescence (AAPM, 2006). It is therefore important that readout process begins immediately after exposure. During the readout process, a laser beam with a specific wavelength scans through the image plate thereby de-excited the electrons. As the electrons fall back to their original ground states, the stored energy is converted into light

with different wave lengths from that of the laser beams (Seibert, 2009). The light is then collected by photodiodes and converted into digital image (Korner et al., 2007). Since CR is cassette based, its integration into an existing radiographic system is very easy. One significant difference between CR imaging plate and the screen-film is that, the CR imaging plate is reusable while the film in screen-film technology is not. To reuse the CR imaging plate, residual signals must be erased. Residual latent image electrons remain trapped even after reader out. This energy must be erased by using a high intensity white light source that flashes the trapped electrons from the higher energy levels to the ground state (Korner et al., 2007).

2.4 Physics of Direct Digital Radiography

Direct digital radiography can be divided into direct digital conversion and indirect digital conversion (Williams et al., 2007). Direct conversion detectors employ X-ray photoconductor such as amorphous selenium (a-S_e) to convert X-ray photons directly into electrical charges. These electrical charges are then stored in capacitors to be read out by thin film transistor (TFT) array. Indirect conversion systems use a scintillator such as gadolinium oxisulphide (Gd_2O_2S) or cesium iodide (C_SI) to convert X-rays into visible light. The visible light is then converted into electrical signal through an amorphous silicon photodiode array. The readout is again achieved through the use of TFT array (Kotter, & Langer, 2002). The digital radiography flat-plate readout increases work throughput since the readout process is very short, allowing many images to be processed within very short time. The DR performance has been found to be better than CR systems (Lanca & Silva, 2013). However, it

has been also reported that DR is susceptible to the same artifacts such as grid-related and image processing artifacts as in CR systems (Flannigan, Magnuson, Erickson, & Schneler, 2012).

Despite all the technological advancement in diagnostic radiography, avoiding unnecessary radiation exposure to patients is still a challenge in screen-film radiography due to the limited dynamic range, overexposure and underexposure frequently occur which necessitate repeat examinations thereby increasing patient radiation dose and cost. Also, in digital radiography, the wide dynamic range provides an opportunity to minimize cost by reducing repeat examinations. However, patient radiation dose can considerably be increased since overexposed images would still produce quality image. Underexposed films increase noise and degrade image quality which demand for repeat examination. One practical approach to effectively deal with this challenge of exposure is to incorporate into radiographic quality assurance program a periodic optimization of exposure factors. The use of optical density to determine radiographic technique and patient exposure is no more appropriate as a result of post processing capabilities of digital radiography (Moore et al., 2012).

2.5 Quality Control in Diagnostic Radiography

The main purpose of quality control test in diagnostic radiology is to maintain efficient and effective performance of all the components in the imaging system (Gholami, Nemati, & Karami, 2015). These programs help to produce images with high quality and administer low radiation dose to both patients and operators. Quality control also helps to detect changes in image

quality that may affect diagnosis and patient radiation dose. It minimizes costs through elimination of poor imaging as a result of machine or materials failure that may occur in the process leading to final imaging production. It is therefore an integral part of the overall quality assurance program in radiology departments.

Some researchers have reported on the various quality control tests in diagnostic radiology. Gholami, Nemati, & Karami, (2015) reported on quality control test of tube voltage and exposure time in conventional radiography. The result of the study indicated that image quality can be affected when the X-ray machine is too old or poorly maintained. Quality control tests on X-ray tube efficiency, reproducibility of dose, time, high voltage, accuracy of kVp, mA, focal spot size and half value layer have been reported by Taha in a paper presented at the tenth Radiation Physics and Protection Conference (2010) in Cairo-Egypt (Taha, 2010). Taha, (2010) reported that, measured output doses were within the international reference's doses and that all the X-ray machines in the study provided accurate and timely diagnosis. Another study reported on total beam filtration, kVp, mAs and linearity tests (Azzoz, Elshahat, & MonemRezk, 2014). Azzoz, et al., found out that implementation of robust quality control program was lacking in diagnostic departments where the study was conducted. It further suggested that creating awareness of radiographers and radiologist about the need for regular quality control tests is necessary for producing good quality images as well as reducing unnecessary radiation dose to patients. Azzoz, et al., (2014) further concluded that optimizing technical factors can lead to significant dose reduction.

The most common quality control tests performed for both patients' dose and image quality evaluation in diagnostic radiology were conducted by (Mana, 2011). Tube peak kilo voltage (kVp) accuracy and repeatability, dose-kVp linearity, dose-mAs linearity, X-ray tube output-kVp relationship, half value layer (HVL), beam alignment and collimation alignment tests were conducted by (Mana, 2011). It was concluded that technical X-ray parameters play important role in reducing patient radiation dose and to produce acceptable image quality (Mana, 2011).

A practical procedure to determine HVL in diagnostic radiology has been reported (Lacerda, Silva, & Oliveira, 2007). HVL is defined as the amount of filtration necessary to reduce the X-ray beam intensity to half its incident magnitude under good geometry conditions. Another researcher used HVL to estimate the quality of filtration of diagnostic X-ray equipment (Akaagerger, Ujah, & Akpa, 2014). All the quality control tests described above relate to the performance of the X-ray generator and could be applicable in both screen-film and digital technology.

2.6 Exposure Indicators

The wider exposure latitude and the post processing algorithm of digital radiography technology have rendered the use of overall optical density as an exposure indicator impossible. The image contrast has no direct relationship to the exposure factors as in screen-film systems. Over or under exposure is no longer manifested as dark or light image but rather as noise levels. As a result, over exposure images may not appear dark except when saturated likewise underexposed images might not appear light. Under

exposed images show more noise which tends to obscure subtle details of anatomical part or pathophysiological processes. However, overexposed images presented with low noise and provide clear visibility of subtle details of pathophysiological processes. Consequently, most radiologists fail to complain on images acquired at higher doses with low noise but reject images acquired at low doses which increases noise levels. To avoid complains from radiologists, radiographers and technologists prefer acquiring images with higher exposure factors which reduces noise levels but unnecessarily increase patient radiation dose. This development leads to gradual increases in radiation dose to patients, a situation known as dose creep (Chin, Robinson, & MCEntee, 2014; Seeram, Davidson, Bushong, & Swan 2016). Since there is a fixed relationship between the exposure and overall optical density, the use of speed or speed class by some digital manufacturers and users resulted in misunderstanding and scientific inaccuracies (AAPM, 2009). It was therefore imperative for digital radiography operators to have feedback regarding the exposure to the detector.

In digital radiography, exposure indicator is only a numerical value that indicates how well a detector has been exposed. It is not directly related to patient dose but could replace signal-to-noise ratio. The exposure indicator is equal to the square of the signal-to-noise ratio. The manufacturer specific EI made it difficult in understanding the importance of this EI in digital radiography. For instance, Fuji systems used S-value which is analogous to speed in screen-film radiography used to determine the receptor exposure in CR. This S-value is inversely proportional to the receptor exposure. Agfa systems coined the term log of median value (I_gM) as a means to measure the

detector exposure. The log of median value has direct logarithmic relationship to the detector exposure. Carestream systems measure the exposure to the detector by means of exposure index which has direct logarithmic relationship to the detector exposure (Don, Whiting, Rutz & Apgar, 2012).

In order to minimize manufacture's specific exposure indicator which tends to create confusion, the International Electroctechnical Commission (IEC) and the American Association of Physicists in Medicine (AAPM) have separately published reports on the need to standardize EI (AAPM Task Group 116, 2009). These standards as recommended by AAPM Task Group 116 are: Indicated equivalent air kerma (K_{IND}), target equivalent air kerma value (K_{TGT}), and the deviation index (DI) which must be incorporated in the digital imaging and communications in medicine (DICOM) header of digital radiography technology.

Indicated equivalent air kerma was defined in that report as an indicator of quantity of radiation that was incident on the regions of the detector for each exposure made. K_{TGT} is the optimum K_{IND} value that should result from any image when the detector is properly exposed. K_{TGT} values were recommended to be established by either the users and/or DR manufacturers and stored as a table within the DR system. DI was also defined as an indicator to determine whether the detector response for specific image K_{IND} agrees with K_{TGT}. The DI is to be reported as DI = 10log [K_{IND}/K_{TGT}] with one significant decimal of precision. The DI is supposed to serve as an indicator for both Radiologist and Radiographers whether correct exposure technique was used to acquire a radiograph or not. When DI indicates 0.0, it means that K_{IND} was equal to K_{TGT} and the exposure was correct.

2.7 Biological Effects of Ionizing Radiation

The mechanisms of biological effects of ionizing radiation are direct and indirect (Kudr, & Heger, 2015; Elgazzar, & Heger, 2006). In the direct mechanism, the ionizing radiation directly imparts its energy to the deoxyribonucleic acid (DNA) of the cells causing damage to the single or double-stranded helical structure. This direct mechanism rarely occurs due to the small size of the DNA. The more occurrence mechanism is the indirect. In this mechanism, the ionizing radiation imparts its energy to the cellular water and produces free radicals. These free radicals can attack the critical target like the DNA of the cells. Since these free radicals can diffuse some distance into the cells, the initial ionization does not have to occur so close to the DNA in order to cause damage. When DNA is attacked either through direct or indirect action, damage is caused to the strands of molecules that make up the double helix structure. Most of this damage consist of breaks in only one of the two strands and is easily repaired by the cell using the opposing strand as a template. However, when double-strand break occurs, the repairing process becomes much more difficult and could lead to mistakes. This may result in mutations or changes to the DNA coding and consequently can lead to cancer or cell death (Beyzadeoglu, Ozyigit, & Cuneyt, 2010).

Biological effects of ionizing radiation can be grouped into deterministic and stochastic effects (Little, Wakeford, Tawn, Bouffler, & de Gonzalez, 2009). Deterministic effect occurs when dose levels exceed a particular threshold. Severity of the deterministic effects increases proportional to radiation dose absorbed. This effect can be skin erythema, necrosis, vomiting, hemorrhage and even death at high dose levels. Stochastic

effects do not have any threshold dose and are probabilistic in nature. Stochastic effects occur as a result of cumulative absorption of radiation over a long period of time. Incidence of stochastic effects increases with the dose received and can cause cancers as well as genetic effects (Aggarwal, 2014).

The assessment of risks of ionizing radiation has been a subject of discussion for some years now. Three theoretical dose-response models have been used to evaluate risk of ionizing radiation exposure. These are linear-no threshold model, linear threshold model and linear quadratic model (Bolus, 2001). The linear-no-threshold (LNT) model suggests that radiation exposure can induce damage no matter how small the dose (Seong et al., 2016). This means that detrimental effects like heritable genetic mutation can occur at any low levels of radiation dose without threshold. This model could estimate radiation risks successfully at high doses. However, current experimental and epidemiological studies do not support this model as estimates for cancer risks at low doses due to conflicting and inconsistent data (Desouky, Ding, & Guangming, 2015). The other challenge with LNT model is that, it does not recognize the role of biological defense in a body and however, assumes that cancer risk occurs in proportionate linear pattern without threshold (Desouky et al., 2015). Notwithstanding these limitations with the model, regulatory authorities in medical radiation protection have accepted this model as the golden standard for radiation risk assessment. This is because the model ensures maximum protection even at the low levels of radiation doses (ICRP, 2007). Linear threshold dose-response model proposed a known threshold below which no effects are seen (Seong et al., 2016). Thus, no radiation risk is expected to occur at dose levels below the threshold point. However, radiation

effects could be observed at the threshold and beyond the threshold, effects increase proportional to the increase in doses. Linear quadratic dose-response model is used for overall human response to radiation, response at low levels of radiation exposure are linearly dependent and then become quadratic at higher doses. This model is mainly used in radiotherapy (Kim et al., 2015).

Biological effects of ionizing radiation have been extensively reported in literature (Betlazav, Middleton, Banati, & Liu, 2016; UNCEAR, 2000). At high radiation dose, detrimental effects of cancer, skin burns, cataracts, and even instant death have been well reported (Little, Wakeford, Tawn, Bouffler, & de Gonzalez, 2009). However, the bone of contention among scientists is the effects of ionizing radiation at low levels (Verdum, Bochud, Gudinchet, Aroua, Schnyder, & Menli, 2008). Some researchers have reported about harmful effects of ionizing radiation at low levels (Pierce & Preston, 2000; UNSCEAR, 2006). The primary effects of exposure to low dose of radiation have been reported as genetic, somatic and in-utero effects (Franco et al., 2016). The genetic effect occurred in the offspring of an individual exposed to radiation. The in-utero effect is often referred to as genetic effect since the effect is only seen after birth. Truly, the in-utero effect is the effect suffered by a developing fetus or embryo. The somatic effect is seen in an individual primarily exposed to radiation. Since cancer is primary effect of radiation exposure, it is also called carcinogenic effect.

Radiation induced cancers remain the most significant effect emanating from exposure to low doses of radiation (Martin, Sutton, West, & Wright, 2009). Some studies have linked cardiovascular diseases to ionizing radiation at low levels (Madan, Benson, Sharma, Julka, & Rath, 2015;

Jaworski, Mariani, Wheeler, & Kaye, 2013). It has been reported that ionizing radiation could affect cardiomyocytes and other cardiac structures to induce cardiomyopathy, valves heart disease and conduction abnormalities (Yusuf, Sami, & Daher, 2011; Nielsen, Offersen, Nielsen, Vaage-Nilsen, & Yusuf, 2017; Donnnellan et al., 2016). Other reports have suggested that there are positive effects of ionizing radiation at low dose levels against spontaneous cancers (Kim et al., 2015; Luckey, & Lawrence, 2006).

Optimization of patient radiation protection therefore becomes a necessary tool in either ionizing radiation at low levels have potential to cause harmful effects or not. If ionizing radiation at low levels as in medical exposures is harmful, optimizing patient radiation protection is very important to mitigate the biological effects. On the other hand, if ionizing radiation at low dose levels have protective mechanism for the body as reported, then again, optimization of radiation dose is still necessary to ensure optimum levels of radiation dose are maintained for the maximum benefit of human population.

2.8 Principles of Radiation Protection

The purpose of radiation protection in diagnostic radiography is to prevent deterministic detrimental tissue effects and to limit the probability of stochastic effects (Grover et al., 2002). In order to control radiation exposure of individuals and the entire population recommendations, directives, ordinances, and laws are used to regulate working and contact with ionizing radiation (Shannoun, Blettner, Schmidberger, & Zeeb, 2008). At the national levels, properly established legal and government framework provide

regulation of facilities and activities that give off radiation, while recommendations and directives are usually established by regional and international bodies.

In the 1950s, the debate on effects of radiation exposure to the public and the patients gathered momentum as a result of atomic bombings of Hiroshima and Nagasaki in 1945 (ICRP 2016). Radiation protection is a professional field that deals with protection of humans and environment from the harmful effects of ionizing radiation. The field evaluates scientific knowledge of adverse health effects from radiation and influences legislation, regulations and working practices for radiation protection. Radiological protection in medicine does not only include protection of patients but also individuals exposed to radiation while caring for patients and volunteers involved in biomedical research. The current international standards for radiation protection are based on ICRP recommendations established in 1977 (ICRP 26, 1977). This recommendation introduced three basic principles of radiation protection which were justification, optimization and dose limit. Since the introduction of the concept of radiation protection, ICRP has been revising the recommendations on systems of radiation protection. In 1990, ICRP revised its recommendations (ICRP 26) and introduced ICRP 60 (ICRP 1991). The latest edition of ICRP recommendations is the ICRP 103, (2007). In all of these revisions, the basic principles have not changed.

Many regional and national bodies have incorporated these basic principles into their directives and national laws. The new directive of European Atomic Community, Directive 2013/59/EURATOM incorporated the ICRP recommendations of radiological protection. In United State of

America, the National Council on Radiation Protection and Measurements (NCRP) is responsible for formulating policies and laws governing the safe use of ionizing radiation. The NCRP also adopted the ICRP recommendations in its report 160 (Thurston, 2010; Kenneth, 2004). Also, Austrian Radiation Protection and Nuclear Safety Authority (ARPANSA, 2014) report title fundamentals for protection against ionizing radiation also placed emphasis on the ICRP basic radiological protection principles.

The three fundamental principles of radiation protection are central to the system of radiological protection and are applicable to the different types of exposure situations (planned, emergency and existing) and the categories of exposure (occupational, public and medical exposures) of patients and the environment (ICRP 103, 2007). Occupational exposure is the exposure incurred by workers as a result of their occupation. Occupational exposures have dose limits to which a worker is supposed not to exceed. All exposures of the public with the exception of medical and occupational exposures are termed as public exposure. Two of the principles, justification and optimization are source related and applicable in all exposure situations (Kenneth, 2004). The use of ionizing radiation is associated with risks to patients (Hall et al., 2008). As a result, all exposures to diagnostic X-rays need to be justified and optimized in terms of benefits and risks.

2.8.1 Justification of practice

Justification of practice is when there is obvious valid clinical indication. It is the first step of patient protection to be observed. There is valid clinical justification when the benefit of exposure far exceeds the risk

involved. It therefore needs risk and benefits assessments of anyone undergoing diagnostic radiography. The principle of justification applies at three levels in medicine according to ICRP 2007. The first level says, the proper use of radiation in medicine is accepted as doing better to society. At the second level, a specified procedure is justified for a group of patients showing relevant symptoms or for a group of individuals at risk for a clinical condition that can be detected and treated. At the third level, the application of a specified procedure to an individual patient is justified if that particular application is judged to do more good than harm to the individual patient. Justification of an examination must rely on professional evaluation of comprehensive patient information which includes prior imaging, laboratory, relevant clinical history and treatment information (Shannoun, Bletter, Schmidberger, & Zeeb, 2008).

2.8.2 Dose limit

The principle of dose limit is individual related and therefore applies only in planned exposure situations. The total dose to any individual from regulated sources in planned exposure situations other than medical exposure of patients should not exceed the appropriate limits recommended by the ICRP. Since medical exposure of ionizing radiation has special considerations, dose limit is not applicable (Do, 2016).

2.8.3 Principles of optimization

The principles of optimization is to reduce patient radiation dose while maintaining the image quality for maximum diagnostic information. It implies that the imaging should be performed using doses that meet ALARA principle, taking into account the social and economic factors. Optimization of

radiological protection for patients in medicine is usually applied at two levels. The first level is design, appropriate selection and construction of equipment and installations. The second level is the daily methods of working (that is the day to day radiological procedures). The main purpose of optimization of protection is to manipulate the protection measures from a source of radiation such that the net benefit is maximized. Optimization of protection in medical exposures does not necessary mean reduction of doses to patient (ICRP 103, 2007). The principle of optimization of radiation protection requires that the likelihood of incurring exposures, the number of people exposed and the magnitude of the exposures should be kept ALARA, taking into account economic and societal factors (ICRP 60, 1991; ARPANSA, 2014). Optimization of patient dose is a process that involves a number of steps which include; image quality assessments, rejection analysis, determination of patient dose, quality control of equipment, implementation of corrective actions and knowledge of both international and local guidance dose levels.

The concept of optimization of patient radiation dose in diagnostic radiology became necessary as many people were exposed to ionizing radiation as well as the emerging evidence of radiation risks associated with low dose levels of ionizing radiation. Increasing public and scientific concerns led to the establishment of national programs in some of the developed countries to evaluate radiation doses from the radiological studies (Martin, 2007). A survey carried out in the UK in the 1980s, indicated a variation in the mean doses from similar radiographic examinations (Martin, 2007). In the United States, similar finding was reported by the National Evaluation of X-ray Trends (NEXT) programme. In Ireland the national radiation dose levels

for four most common performed X-ray examinations (chest, abdomen, pelvis and lumbar spine) indicated lower references dose levels by 40% in comparison to those established by the UK and the Commission of the European Communities (Johnston, & Brennan, 2000; Hart et al., 2002). It has been also reported that standard radiographic examinations have average effective dose variation of a factor above 1000 (0.01-10 msv) (IAEA, 2004; Mettler et al., 2008). Due to these variations in doses more emphasis was placed on optimization of radiological procedures to minimize the risk to patients. The essence of optimization is to recognize the levels of radiographic image quality that is required for effective diagnosis and to determine the imaging technique that could provide good image quality with minimum patient dose. The second aspect of optimization is to review the procedure from time to time to ensure that dose reduction does not negatively affect the clinical diagnosis. The optimization process requires that patient radiation dose and image quality are measured and monitored.

2.9 Optimization in Digital Radiography

In digital radiography, optimizing patient radiation dose has become necessary due to the potential of overexposure. Many optimization strategies have been reported by different researchers (Samei, Dobbins, Lo, & Tornai 2005; Ackom, Inkoom, Sosu, & Schandorf 2017). These studies used the objective parameters such as signal-to-noise ratio (SNR) and contrast-to-noise ratio (CNR) as the strategy for optimizing patient radiation dose. Signal-to-noise ratio has been found to have direct relationship with image quality and high values of SNR could provide corresponding high image quality. The

limitation of these objective optimization techniques is that, there is no correlation between its performance and the clinical performance since it is not conducted under clinical conditions. Other researchers have used the diagnostic performance of imaging systems as a means of optimization strategy (Aldrich, Duran, Dunlop & Mayo, 2006). The study compared the diagnostic performance of CR systems, DR systems and screen-film systems in terms of patient radiation dose and image quality. The results of the study indicated that, patient radiation dose for chest PA in CR was five times higher than the screen-film systems. The basis of this comparison was a little problematic since the AEC used for CR and screen-film were placed differently in the chest region as well as different density of AEC used. While in CR systems the center AEC was used, the lungs field AEC was used in the case of screen film which obviously would increase dose in the center AEC. Another study investigated the effects of phantom orientation and AEC chamber selection on radiation dose and image quality (Manning-Stanley, Ward, & England, 2012). In the study, the phantom was orientated with the outer AEC chambers directed toward the head end while multiple exposures were made and then the exposures were repeated when the phantom has been oriented in opposite direction. It was observed that, 36.8 % reduction in dose was possible in the caudally oriented lateral AEC chambers than the recommended cranially oriented lateral AEC chambers for pelvic examinations.

Another study used radiographic positioning as strategy to optimize lumbar spine examination. It investigated AP and PA projections in relation to effective dose and absorbed organ dose (Davey, & England, 2014). It

concluded that in both effective doses and absorbed organ doses PA projection were lower than the AP projection in all the exposures used. The reason for reduction in organ doses in PA projection was that, the radio sensitivity organs are closer to the anterior surface than the posterior surface and that less radiation beam reached the organs as compared to the AP position. However, PA projection in lumbar spine examination is affected by magnification and distortion.

Exposure indicator has been also used as an optimization tool for pelvic and lumbar spine examination (Seeram, Davidson, Bushong, & Swan, 2016). The study was to determine the minimum dose to anthropomorphic phantom without degrading the image quality. Seeram, et al., (2016) found linear correlation between ESD and mAs as well as an inverse relationship between ESD and EI. The study then observed that optimizing exposure indicator could be linked to optimizing patient radiation dose indirectly.

In all these optimization strategies, the principal objective was to reduce patient radiation dose without compromising image quality. However, there was no attempt to improve image quality. This implies that due to post processing capabilities of digital imaging systems image quality is not a major challenge as compared with patient radiation dose. Therefore, any optimization strategy in digital radiography must focus on radiation dose reduction rather than improving image quality. None of the strategies discussed has been found to be more superior to the other and that research in optimization of digital radiography systems are still ongoing. The main challenges confronted in optimizing strategy are the difference in body

thickness in clinical practice and the different diagnostic task requirement encountered in clinical conditions.

2.10 Patient Radiation Dosimetry

Patient radiation dose is basically determined by ESD or dose-area product (DAP). ESD and DAP could provide good means of audit, monitoring and compare radiation doses from different radiological examinations (George et al., 2004).

2.10.1 Entrance skin dose

There are two categories of doses to patients that are very important in diagnostic radiology. These are ESD and Effective dose. Entrance skin dose values are used as monitoring diagnostic reference levels for the purpose of optimizing patient radiation dose (Rubai et al., 2018). Entrance skin dose is the dose to skin at the point where X-ray beam enters the body and includes both the incident air kerma and radiation backscatter from the tissue. Entrance skin dose has been recommended as the most reliable dosimetric quantity for patient radiation dose in simple radiographic examinations (IAEA 2004). This is because ESD fits perfectly into all the three basic conditions set out by IAEA (IAEA, 2004). Thus, dosimetric quantity for patient dose estimation should be simple to measure, permits direct measurement on patients during examinations and must be representative of the dose received by the patient (IAEA 2004). Again, the Commission of the European Communities in the document quality criteria for the most common radiographic images also recommended the use of ESD for the estimation of patient radiation dose (EC

1996). ESD also allows for easy comparison with other published diagnostic reference levels (Ofori, Antwi, Scutt, & Warfd, 2013).

Entrance skin dose can be estimated by direct or indirect methods using human patients or phantoms (Alghoul, Abdalla & Abubakar, 2017). The direct measurement uses thermoluminescent dosimeter (TLD) which is placed on the skin of the patient. The main challenge with thermoluminescent dosimeters is that there is a minimum absorbed dose of 0.1 mGy to produce reasonable accurate results (Ogundare, Uche, & Balogun, 2004). Despite this challenge, some patient dose surveys have been published using direct method (Abdelhalim, 2010). Patient radiation dose for chest (PA) was estimated using TLD in Ethiopia (Mulubrihan, & Atnafu, (2001). ESD estimation for seven radiographic examinations (chest PA, Abdomen AP, Pelvis AP, Lumbar AP, Skull AP, Knee AP, and Hand AP) were performed using TLD in Nigeria (Jibiri & Olowookere, 2016).

The indirect method of measurement uses computational approach either by mathematical formula or dedicated software such as Monte Carlo Simulations, CALDOSE_X5 etc. In Ghana, patient doses were estimated for thorax/chest (PA/RLAT), pelvis (AP), cervical spine (AP/LAT), thoracic spine (AP/LAT) and lumbar spine (AP) using same CALDOSE_X5 programme (Ofori, Gordon, Akrobortu, Ampene, & Darko, 2014). In these measurements the tube output was first measured with an appropriate dosimeter. The use of mathematical methods for estimating the patient radiation dose was first published by chaney et al in 1981 (Owolabi, & Ogundare 2005). The computational method for estimating ESD permits dose survey to be carried out on larger number of examinations with less cost than using TLDs. Again,

assessments of low dose examinations which may deliver doses below the sensitivity level of TLDs and DAP meters are also possible (Owolabi, & Ogundare, 2005). This explains why many researchers and national surveys are done using indirect method. Some few studies using both methodologies have been published (George et al., 2004).

Patient dose surveys have been widely published in literature with various degrees of variations when compared with international and regional reference levels like IAEA and ICRP. In Ghana, dose estimated for pelvic and skull examinations showed these variations (Ofori, Antwi, Scutt, & Ward, 2012). Studies conducted in Saudi Arabia for estimation of patient dose for seven radiographic examinations (skull PA, kidney ureter and bladder (KUB) AP/LAT, ankle, AP/LAT, foot AP/ oblique (OBL) and LAT/OBL, Hip AP/LAT and sinuses paranasal AP) also showed variations in dose when compared with international reference standards (Abdelhalim, 2010). Patient radiation dose survey in Serbia and Montenegro for cervical spine (AP/LAT), pelvis (AP), thoracic spine (AP), lumbar spine (AP/LAT) chest (PA/LAT), and skull (PA/LAT) recorded variations (Ciraj, Markovic, & Kosutic, 2004). Another study in Saudi Arabia which estimated patient dose for six commonly performed examinations (chest PA, skull PA, abdomen AP, cervical spine AP, pelvis AP, and foot PA) also recorded variations. In this study effective dose was also calculated from ESD (Taha, 2014).

Variations in the ESD may be due to differences in patient sizes, radiographic technique used by different radiographers, radiographic equipment, film type, chemicals and processing conditions. Assessment of patient dose regularly is a vital tool for dose reduction in diagnostic

radiography. Patient dose surveys in UK since the 1980s have significantly contributed to reduction in patient dose (Hart, Hillier, & Wall, 2009).

2.10.2 Effective dose

Effective dose (ED) is very essential in diagnostic radiology since it relates to the risk of stochastic effect. It combines a set of organ or tissue equivalent doses into one single quantity. For the estimation of radiation risks to patient, effective dose is the best dosimetric quantity. It accounts for the absorbed doses, relative radio-sensitivities of the organs exposed in the patient and thus better quantifies the patient radiation risks (Martin, 2006; Ofori, Akrobortu, Ampene, & Darko, 2014). Effective dose can be calculated from ESD to the various organs using conversion factors published by the International Commission on Radiation Units and Measurements (ICRU, 2005) or ICRP (ICRP, 1982). Effective dose is calculated by multiplying the organs equivalent dose (H_T) by organ weighting factors (W_T) and summed up as shown in equation 2.1 (ICRP103)

$$ED = \sum W_T W_R D_{T,R} \qquad 2.1$$

where $D_{T,R}$ is the average absorbed dose to tissue from radiation of type R; W_R is the radiation weighting factor. The value of W_R is 1 for X-rays and W_T is the organ weighting factor (UNSCEAR 2000; Sharifat et al., 2009).

2.10.3 Organ equivalent dose

The organ equivalent doses (H_T) are expressed in terms of absorbed doses to soft tissue, muscles and water. (ICRP 103) define H_T as shown in equation 2.2

$$HT = \sum W_R \, D_{T,R} \qquad 2.2$$

where $D_{T,R}$ is the average absorbed dose to tissue from radiation of type R; W_R is the radiation weighting factor.

Absorbed dose was also defined by ICRP as the amount of energy deposited in a medium per unit mass. Absorbed dose is often equal to the Air kerma for the same medium in diagnostic radiation (Ciraj et al., 2003; ICRP, 103). Dose-area product is the product of dose in air (Air kerma) within the X-ray beam and the beam area. It is therefore a measure of all the radiation that enters the patient. It can be measured by using an ionization chamber fitted to the X-ray tube (Martin, 2007). It is recommended for complex examinations as in fluoroscopy (IAEA 2004).

2.11 Diagnostic Reference Levels

Another powerful tool in optimization of patient radiation protection is the establishment of diagnostic reference levels (DRLs). DRLs were introduced in diagnostic radiology based on the ICRP recommendation (ICRP 73 (3)). Establishment of DRLs became mandatory in European countries with passage of directive 97/43/Euratom. It was introduced by the European Union as standard to reduce patient radiation dose (Sharifat, & Oyeleke, 2009). DRLs is defined as a dose level set for standard procedures and for groups of standard sized patients or standard phantom ESD per radiography.

The purpose of establishing DRLs is to help avoid unnecessary high dose to patient and minimize variation in patient dose for similar examinations in different radiographic facilities. The principles behind the operation of DRLs are; estimate the patient dose, compare DRLs values with international standards and perform any corrective action(s) should the DRLs levels are

significantly higher than the internationally recommended. Diagnostic references levels have been established for certain examinations after wide national dose surveys in terms of either ESD or DAP. By convention, DRLs is determined using the third quartile distribution of patient doses. The mean dose of an average patient should not be more than the proposed or established DRLs. Investigations into further optimization procedures must be initiated when the patient mean dose exceeds that of established DRLs.

The National Radiological Protection Board (NRPB) in UK had reported significant reduction in patient radiation doses since the introduction of optimization protocols with national and local DRLs (Johnston & Brennan, 2000; Hart, Hillier & Wall, 2002; George et al., 2004). It is imperative that every country establishes its own diagnostic reference levels that are appropriate for their own radiographic techniques and practices for effective optimization of patient radiation protection (Tung, Tsai & Lo, 2001).

2.12 Image Quality Assessment

In medical radiology, images are produced for the purpose of diagnosis and treatment. Good radiographic image must therefore be able to fulfill these tasks. The definition of quality of radiographic images becomes useless if not linked with task (Barrett et al., 2004). Therefore, radiographic image is said to be of good quality when it contains necessary diagnostic information needed to accomplish its intended purpose (ICRU 1996). Image quality assessments evaluate how best an image fulfils its intended purposes. The quality of image could be assessed by subjective or objective methods (Tapioraara, 2006). In practice the subjective methods consume time, expensive, and inconvenient

than the objective assessment (Wang, Sheikh & Simoncelli 2004). However, the objective evaluation has not been well linked to clinical image quality assessments. Notwithstanding, the objective assessments could play vital role in diagnostic radiology. It could provide means to monitor and adjust image quality. It could be used to optimize algorithms and parameter settings of image systems (Wang, Sheikh & Simoncelli, 2004).

The objective assessments of image quality evaluate the physical characteristics of the image system such as contrast, spatial resolution, and noise (Curningham, 2000). The measurements of these characteristics are done with the help of contrast-detail phantoms or real human beings. The combined effects of spatial resolution and contrast resolution define image details that could be observed (Tapioraara, 2006). Contrast, sharpness (spatial resolution) and noise have been identified as the basic factors that affect image quality. These factors could be evaluated by modulation transfer function (MTF) and the wiener spectrum (Doi, 2006). The MTF represents the spatial frequency response of imaging systems such as screen-film and the geometric unsharpness as a result of the focal point of an X-ray tube. Modulation transfer function could be deduced from the one-dimensional Fourier transform of the line spread function (LSF) or from two dimensional Fourier transform of the point spread function (PSF) of imaging systems. The wiener spectrum represents the spatial frequency content of noise. It could be determined from the Fourier analysis of noise patterns obtained from uniform exposure of X-rays to imaging systems.

The major source of noise in images in diagnostic radiography is the quantum noise (quantum mottle) (Doi, 2006). Modulation transfer function,

noise equivalent number of quanta (NEQ) and detective quantum efficiency have been evaluated in photostimulable phosphor luminescence imaging systems to quantify image quality (Sakurai et al., 2010). Detective quantum efficiency (DQE) combines MTF, noise and exposure levels. It is a vital tool to describe the overall performance of digital radiographic system (Moy, 2000). However, it is very difficult to measure in clinical practice. The DQE can be used to compare the total image of two radiographic systems. It is a quantity that describes the overall capability of the system to use the information of the incoming photon fluency distribution for the formation of the image.

Over the years researchers have tried to establish the true relationship between physical image quality measurements and the clinical usefulness. However, the relationship between the results of physical measurements and clinical performance is not completely established (Wagner et al., 2001). Some researchers have reported that improvement in physical measurements such as contrast, noise and sharpness could lead to improvement of image quality which might provide more useful diagnostic information which could lead to good clinical performance (Ween & Jacobsen, 2015). It is argued that, radiographic image quality is enhanced when anatomical structures on the images can be easily visualized and recognized. The visibility is optimal if the density is sufficient, its noise is minimal and contrast is maximal. De-Crop et al., found positive correlation between physical image quality and the clinical assessments (De-Crop et al., 2012). Sakurai et al., made similar observation (Sakurai et al., 20100).

Subjective methods (observer performance) provide a good measure of the clinical image quality of imaging systems. The challenge associated with these methods is the influence by the observer. Its efficacy is limited by the performance of the observer. The recommendation by Commission of European Communities (CEC) on quality criteria for assessment of image quality usually employs the subjective approach (CEC, 1996). The subjective methods include; receiver operating characteristics (ROC) for detection of signal, Visual grading analysis (VGA) and Image criteria score (IC) for visibility of anatomical structures (Tingberg, 2000). Combination of VGA and IC methods allow comparison of the visibility of selected image criteria between the images acquired from different tube voltages (Vodovatov et al., 2017). The methods are very simple to use and reliable. It has been found to be clinically useful because, the evaluation of image quality is based on the visualization of clinically important structures that could be selected and defined using established standards. Also, the ratings performed by the observer takes into consideration all the contributions of the technical components of the imaging chain in reproducing image structures.

2.13 Visual Grading Analysis

Visual grading analysis (VGA) allows part or the entire image to be evaluated visually. In VGA, the visibility of a defined anatomical structure is either compared with reference image (relative grading) or no reference image is required (absolute grading). Visual grading analysis studies could be used to evaluate anatomical or pathological structures and physical quality parameters. The reason being that, the ability to detect pathology correlates positively with

accurate anatomical presentation (Ludewig, Richter, & Frame, 2010). Visual grading analysis was first introduced by Bath and Mansson (Bath & Mansson, 2007) and has been widely used by some researchers (Ina, Akintomide, Edim, Nzotta, & Egbe, 2013; De-Crop et al., 2012). Visual grading analysis was used to evaluate image quality based on EC image quality criteria for pelvic radiography images (EC, 1996) in Nigeria Teaching hospitals (Ina, Akintomide, Edim, Nzotta, & Egbe, 2013). Ina et al., 2013 reported 68% compliance rate in terms of EC criteria for image quality. De-Crop et al., (2012) also evaluated image quality in chest radiography using visual grading analysis technique based on CEC criteria (CEC, 1996).

2.14 Image Criteria Scoring

In image criteria scoring (ICS) assessment, an observer is required to express their opinion on how well a particular criterion is fulfilled and score likewise. ICS score is then calculated as the ratio of the number of fulfilled criteria to the overall number of criteria assessed (Ludewig, Richter, & Frame, 2010). Clinical evaluation of image quality for intravenous urography based on the EC image quality criteria (EC, 1996) using ICS has been reported, which found image quality in Sudan hospitals to be 65.9% compliance with EC image quality criteria (Loaz, Yousef, & Sulieman, 2015). Loaz, et al., (2015) also found image criteria scoring as a valuable tool in evaluating image quality and recommended for its daily use in diagnostic radiology departments.

2.15 Receiver Operating Characteristics Analysis

Receiver operating characteristics (ROC) analysis is employed in clinical radiology to evaluate the accuracy of imaging examinations (Eng, 2005). This method could allow radiologists to evaluate both sensitivity and specificity of imaging systems (Obuchowski, 2005). Receiver operating characterlistics analysis measurement is accepted as best methodology for quantification and reporting of diagnostic performance. However, the statistical approach to ROC construction is complex and time consuming which makes it daily use in clinical radiology limited (Victor, 2000). The indicator of diagnostic performance in ROC analysis is the area under the curve (AUC). The AUC in practice represents the average accuracy of the diagnostic test. The AUC may be interpreted as the average sensitivity over the entire range of possible specificity or the average specificity over the entire range of possible sensitivity (Eng, 2005). ROC curve is basically a plot of trade- off between sensitivity and specificity. The ROC curve could also be considered as a factor that best describes clinical image quality.

2.16 Gaps in Literature

The literature search has revealed the following gaps in the optimization of patient radiation protection in diagnostic radiography examinations:

1. In digital radiography, one of the challenges recognized during literature review was the lack of an immediate visual feedback to radiographers and technologists regarding over or under exposures. Existing literature on this challenge is very limited.

2. In digital radiography, sparse literature exists on EI. The measurement of patient radiation dose is still same as in the conventional screen-film radiography. Since each manufacturer reports EI differently, there is the need for more research to ensure that the manufacturers' reporting system actually corresponds to the exposure reaching the detector. Again, since the EI is only directly related to image quality but not the patient dose, it would be helpful to research into the relationship between the patient dose and EI and how best patient dose could be estimated from the EI as a means for easy prediction of patient radiation dose in digital radiography. Literature on how to estimate patient dose from EI are scanty.
3. The transition from screen-film to digital radiography has been rapid over the years. However, most existing established standards such as DRLs and image quality criteria are still based on the screen-film technology. Since digital detectors have different sensitivity to X-ray as compared to screen-film systems, it is important to establish these standards for digital radiography in order to properly optimize patient radiation dose. Existing literature for DRLs based on digital radiography is very limited and non- existing in Ghana.
4. Digital radiography has the potential to reduce patient's radiation dose. However, its wider dynamic latitude could also present an opportunity for unnecessary dose to patient. Limited literature exists in subjective assessment of dose-image quality in lumbar spine AP and lumbar spine LAT to determine the optimum exposure parameters for these examinations.

2.17 Chapter Summary

This chapter reviews literature related to the area of study. Three (3) radiographic systems (screen-film, computed and direct digital systems) were discussed. Conventional screen-film has limited dynamic range which increases repeat examinations. However, in digital radiography (CR and DDR) repeat examinations are very rare due to the wider dynamic range. Digital radiography are compatible with PACS.

Exposure indicator is only a numerical value which indicates how much a detector is exposed. It is not directly related to patient dose but could replace signal-to-noise ratio. The manufacturer specific EI systems made it difficult in understanding the importance of this EI. In order to minimize manufacturer's specific EI, IEC and AAPM have made recommendations on the need to standardize EI.

The mechanisms of biological effects of ionizing radiation are direct and indirect. The direct mechanism rarely occurs due to the small size of DNA while the indirect mechanism occurs frequently. Biological effects of ionizing radiation are grouped into deterministic and stochastic effects. These effects could be cancer, skin burns, cataracts, and hereditary.

The purpose of radiation protection in diagnostic radiography is to prevent detrimental tissue effects and to limit the probability of stochastic effects. Three fundamental principles of radiation protection that are applicable to different types of exposure situations (planned, emergency and existing) and the categories of exposure (occupational, public and medical) are justification, optimization and dose limit. Justification and optimization are source related and applicable in all exposure situations. However, since

medical exposure of ionizing radiation has special considerations, dose limit is not applicable. Patient dose is basically determined by ESD or DAP. ESD and DAP could provide good means of audit, monitoring and compare radiation doses from different radiological examinations. Two important categories of doses to patients in diagnostic radiology are ESD and Effective dose.

CHAPTER THREE

RESEARCH METHODS

3.0 Introduction

Properly designed research methods are essential in obtaining maximum information that is reliable and acceptable to answer research questions. This chapter describes the detailed methodology and materials used to obtain the results for this work. It covers research design, study area, population, sampling procedures, data collection instruments, data collection procedures, data processing and analysis, and chapter summary.

3.1 Research Design

Research design is a blueprint or conceptual framework within which research is conducted. It comprises outline of data collection, measurement, and analysis. Depending on the type of evidence needed to answer the research question, different research designs can be selected.

Research design can be descriptive, explanatory, correlational, and experimental (Creswell, 2003). Correlational research design (case control, observational, semi-experimental) was selected for this study to achieve the set objectives. Correlational research design deals with the measurement of two or more variables to determine or estimate the extent to which the values of the variables relate or change in identifiable manner. In this study design, the researcher did not manipulate any of the independent variables. Observational correlational design was used to measure both dependent and independent variables in order to achieve the objectives of the study. Dependent variables measured were ESD, EI and image quality assessment

while the independent variables measured were Q, V, age, sex, weight, height, body part thickness, focus to detector distance (FDD), focus to skin distance (FSD).

Selection of a particular research design usually depends on the strength and limitations of the research as well as the information being sought for. The strength of this correlational design is that, it investigates the relationship between two variables as well as the interaction among the variables. It also permits the use of larger data than the experimental design. However, correlational design is fundamentally limited in proving causation and therefore significant correlation between variables must be interpreted with caution. The correlational research, thus only proves an existence of relationships but does not provide information as to why the relationship exists.

3.2 Study Area

The country was divided into three main zones (coastal zone, middle zone, and northern zone). The coastal zone comprised of Greater Accra Region, Volta Region, Oti Region, Western Region, Western North Region and Central Region. The middle zone included Ashanti Region, Eastern Region, Ahafo Region, and Bono East. The Northern zone included Bono Region, Upper East Region, Upper West Region, Savanna Region, Northern Region and North East Region. The estimation of patient entrance skin dose aspect of this study was conducted in four (4) regional and one (1) teaching hospitals selected throughout the zones in Ghana. Two (2) hospitals were each selected from coastal and northern zones while one hospital was selected from

the middle zone. This was done because, the volume of work would have made it practically difficult to include all the radiographic facilities in Ghana in this single study. The selected facilities were all referral hospitals in Ghana and therefore performed large numbers of radiological examinations in a year. Therefore, study results from these facilities would be a good representative of the country. The five radiographic facilities that were selected were Sunyani Regional hospital, Tamale Teaching hospital, Koforidua Regional hospital, Effia Nkwanta Regional hospital, and Greater Accra Regional hospital. The identity of these hospitals were coded into HP1, HP2, HP3, HP4, and HP5 respectively to avoid disclosure of results of the study center. HP3 was selected for the dose-image quality optimization phase of this research work. This was because HP3 recorded highest ESD [mGy] for chest PA and lumbar spine LAT examinations after the patient ESD [mGy] survey.

3.3 Population

The selected population for the study were adult patients of 18 years and above with justified radiographic request from a registered medical practitioner to undergo any of the selected examinations (chest PA, abdomen AP, lumbar spine AP, lumbar spine LAT, cervical spine AP, cervical spine LAT, skull AP and skull LAT). Patients who could not be positioned according to the standard procedure of the examination type were excluded from the study. Also, patients under 18 years were not part of this study. The study involved two hundred and ninety (290) females and one hundred and sixty (160) males for the entrance skin dose survey. The average age, weight

and height of the study population were 50 ± 14 years, 69 ± 8 kg, 162 ± 9 cm respectively.

3.4 Sampling

Selection of radiographic facilities was done using purposive sampling while participants for the patient radiation dose assessment were selected using convenience sampling. Purposive sampling is a non probability sampling technique used for identification and selection of necessary information source to achieve set objectives of a study (Palinkas, Horwitz, Green, Wisdom, Duan & Hoagwood, 2015). Criterion purposive sampling, where participants or respondents are selected based on criteria was used for this section of the study. The criteria used for the selection of radiographic facilities were that the facility must be a regional hospital and a referral center, it must have CR X-ray systems and it must have qualified radiographer(s).

Convenience sampling (availability sampling) is also non-probability technique used to create sample as per ease of access, readiness to be part of the sample, availability at a given time (Bhat, 2018). This sampling technique was used to recruit participants into the section where patient radiation dose was estimated. The choice of this sampling was influenced by the fact that the dynamics of participants cannot influence the results of the entrance skin dose estimated. Convenience sampling technique is uncomplicated, economical and quick technique to collect data as compared to simple random sampling, stratified sampling, or systematic sampling (Bhat, 2018). The sampling size for the entrance skin dose estimation was four hundred and fifty (450). Ten people were recruited for each of the nine considered radiographic

examinations at each hospital and therefore ninety (90) participants were recruited for each of the five hospitals in Ghana.

3.5 Data Collection Instruments

Four data collection instruments were developed to collect required data.

The following categories of data collection instruments were developed;

1. Data collection instrument for quality control test.
2. Data collection instrument for entrance skin dose estimation.
3. Data collection instruments for the acquisition of phantom images for chest PA, lumbar spine AP and Lumbar spine LAT phantom dose assessment.
4. Data collection instrument for phantom image quality assessment.

3.5.1 Data collection instrument for quality control test

In order to assess the performance of all the X-ray equipment used for the entrance skin dose assessment, this data collection instrument was developed. It was used to collect data on kVp accuracy, kVp reproducibility, X-ray tube output, exposure linearity, exposure reproducibility and timer accuracy. This data instrument indicated selected exposure parameters (Q, V, and time). These parameters were selected from the control console of the X-ray machine. It also indicated the measured parameters (V, dose, dose rate, HVL, and time) which were measured using Raysafe X2 dosimeter.

3.5.2 Data collection instrument for entrance skin dose assessment

In order to estimate ESD to patients, data collection instrument shown in Appendix A was developed. This instrument was developed to collect data on selected exposure factors (Q, V,) for radiographic examinations, patient habitus (weight, height, age, sex and the thickness of the body part being examined), FDD and FSD.

3.5.3 Data collection instrument for acquisition of anthropomorphic phantom images for lumbar spine AP, lumbar spine LAT, chest PA and phantom dose assessment

This data collection instrument shown in Appendices B – D were developed to collect data required to estimate ESD of the anthropomorphic phantom, related EI and phantom images for dose-image quality optimization in order to determine the optimal exposure factors. The data sheet contained the following items;

1. Selected exposure factors (voltage, quantity of charge,)
2. Exposure indicator
3. Focus dectator distance.
4. Focus skin distance.
5. Estimated phantom ESD.
6. Visual grading analysis score.

3.5.4 Data collection instrument for phantom image quality assessment

To evaluate the image quality acquired from the anthropomorphic phantom, this data collection instrument was developed to collect data required to assess the image quality for chest PA, lumbar spine AP, and lumbar spine LAT. The image quality criteria used to develop this data instrument was the European

guidelines on quality criteria for diagnostic radiographic images established in 1996 (EC, 1996). The image quality assessment was based on visualization of these anatomical structures' criteria and scored as follows;

1 Clearly confident that the criterion is fulfilled (5)

2 Somewhat confident that the criterion is fulfilled (4)

3 Indecisive whether criterion is fulfilled or not (3)

4 Somewhat confident that the criterion is not fulfilled (2)

5 Clearly confident that the criterion is not fulfilled (1)

This image quality assessment is known as visual grading analysis score (VGAS) which can be reference VGAS or absolute VGAS (Tingberg, 2000). Reference VGAS is performed when test images are scored in comparison with a standard reference image while in an absolute VGAS, the scoring of test images is not in comparison with a reference image. An absolute value is assigned to the criterion depending on the extent of its visibility. This type of VGAS was used for this work. This type of VGAS provided simplified presentation of the results. However, the average score including all structures could hide useful information in a criterion (Amen, Tingberg, Besjakov &Mattson, 2004).

The image quality criteria and scoring systems were combined into single data collection instrument for chest PA, lumbar spine AP, and lumbar spine LAT assessment (Appendices E– G).

3.6 Image Quality Anatomical Criteria for Chest PA

The following anatomical criteria, based on the European Commission guidelines on quality criteria for diagnostic radiographic images (EC, 1996) were contained in the instrument (Appendix E).

1. Visualization of the spine through the heart shadow.
2. Visually sharp reproduction of the trachea and proximal bronchi.
3. Visually sharp reproduction of the diaphragm.
4. Visually sharp reproduction of borders of the heart.
5. Reproduction of the whole rib cage above the diaphragm.
6. Visually sharp reproduction of the lateral costopherenic angles.

3.7 Image Quality Anatomical Criteria for Lumbar Spine AP

The following image quality criteria are contained in this instrument (EC 1996);

1. Reproduction of the sacro-iliac joints.
2. Visually sharp reproduction of the pedicles.
3. Reproduction of the transverse process.
4. Reproduction of the spinous process.
5. Reproduction of the intervertebral spaces.
6. Reproduction of the adjacent soft tissues, particularly the psoas shadow.

The data collection instrument is shown in Appendix F.

3.8 Image Quality Anatomical Criteria for Lumbar Spine LAT

1. Reproduction of the pedicles.
2. Reproduction of the intervertebral foramina.
3. Visualization of the spinous process.
4. Visually sharp reproduction of the intervertebral spaces.
5. Visually sharp reproduction of the cortex and trabecular structures.

The data collection sheet is shown in Appendix G. EC, (1996) defined the degree of visibility for the anatomical structures as follows;

1. Visually sharp reproduction: anatomical details are clearly defined, details are clear.
2. Reproduction: details of anatomical structures are visible but not necessarily clearly defined, detail emerging.
3. Visualization: anatomical features are detectable but details are not fully reproduced, features are just visible.

3.9 Data Collection Procedures

This section presents detailed information on how the data were collected. It covers X-ray equipment, quality control test, estimation of entrance skin dose, anthropomorphic phantom image acquisition and dose assessment for chest PA, lumbar spine AP, and lumbar spine LAT, image quality assessment, and dose- image quality optimization.

3.10 X-Ray Equipment

The X-ray equipment used at HP1, HP2, and HP3 were CR systems, general radiographic floor mounted systems from Shimadzu. The equipment

at HP1, HP2 and HP3 were RADSPEED MF type with model number UD150LC-40E. These equipment were installed between 2012 and 2014. The maximum kVp was 150 and the maximum mAs was 500. The X-ray equipment at HP4 was CR systems from Philips Medical Systems (DMC GmbH, Hamburg, Germany). The model number was SN11000366 with maximum kVp of 150 and maximum mAs of 400. This equipment was installed in 2012. The X-ray equipment at HP5 was direct digital radiography systems from General Electric with model number XR656 PLUS (Discovery). This system was installed in 2016 with maximum kVp of 150 and maximum mAs of 500.

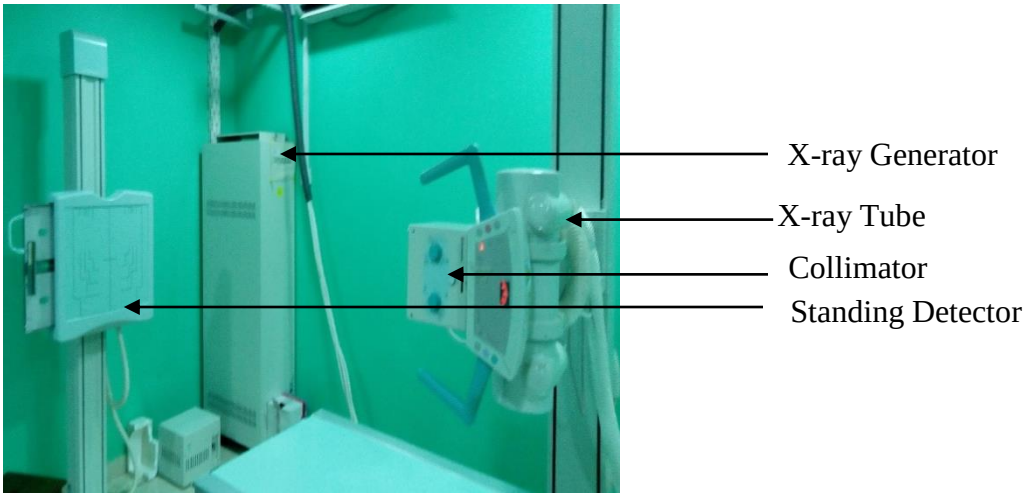

Figure 3.1: Image of X-Ray Equipment used at HP3

The equipment shown in Figure 3.1 was one of the X-ray equipment used for this study. It has a high frequency generator and its exposure time ranges from 0.001 – 10 S.

3.11 Quality Control Tests on X-ray Generator Performance

The American Society for Quality defines quality control (QC) as "the observation techniques and activities used to fulfil requirement for quality" (Jones et al., 2015). AAPM (Task group 151 Report), also defined QC in medical imaging as "as series of regular (often annual) detailed evaluations of a piece of medical imaging equipment by qualified medical physicist" (Jones et al., 2015).

The purpose of QC is to identify error (s) in the imaging chain that affect image quality clinically or increase patient radiation dose significantly (AAPM report 74, 2002). In this work, six quality control parameters were performed. These included kVp accuracy, kVp reproducibility, timer accuracy, exposure linearity, exposure reproducibility and radiation tube output. These parameters relate to X-ray equipment generator's performance which can affect radiation output when their values fall outside the recommended tolerances.

All measurements were done using RaySafe X2 (3.10R01f) radiation dosimeter manufactured and calibrated by Unfors RaySafe AB in Sweden. This instrument provides simultaneous readings for kVp, dose, dose rate, HVL, time, and total filtration. It consists of base unit, sensors, and the X2 viewing computer software. The Raysafe X2 has three sensors namely;

1. Radio frequency (R/F) for radiography and fluoroscopy measurements.
2. Mammography (MAM) for mammography measurements.
3. Computed tomography for CT applications.

The R/F sensor for radiography and fluoroscopy measurements was used for measurements in this work. Using the R/F sensor for measurements,

the R/F sensor was connected to the base unit and the sensor was centered in the X-ray field with the cross hair towards the X-ray source. The angle of the sensor in the horizontal plane of the field has no impact on the measurement results. This is because Raysafe X2 sensor is based on compensated silicon diode array and prevents heel effects of the measurement due to technological advancement of the sensor. The X-ray field was collimated to 10 cm x10 cm to avoid unnecessary backscatter. The FSD of 100 cm was used in all the quality control measurements as reported in literature (Akpochafor et al., 2016: Godfry, Adeyemo, & Sadiq, 2015).Figure 3.2 shows the experimental setup of the RaySafe X2 dosimeter.

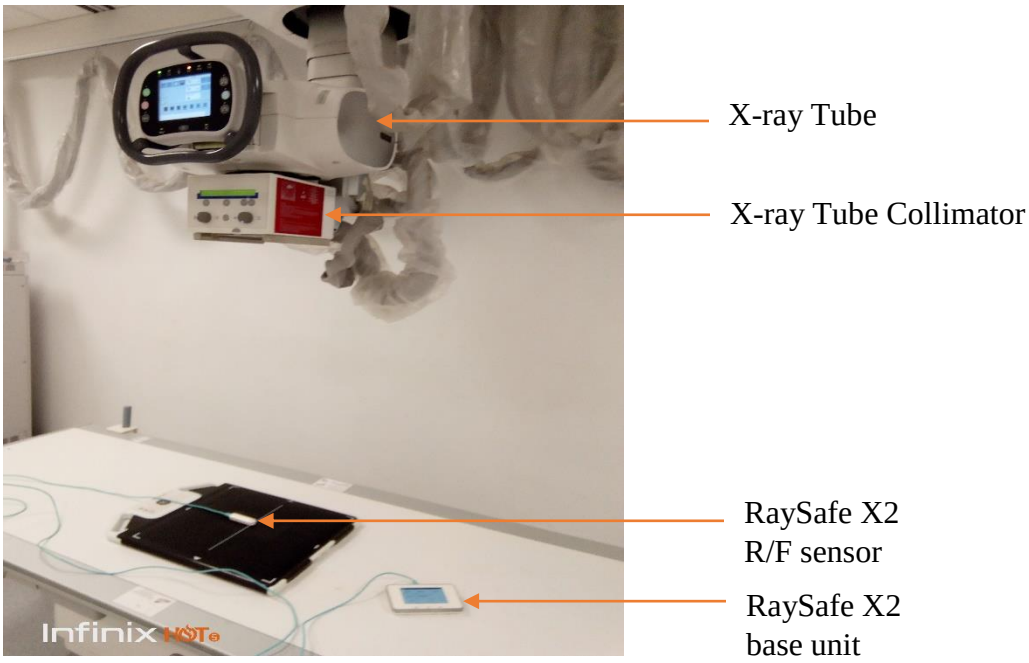

Figure 3.2: Setup of RaySafe X2 Dosimeter at HP5 for QC Tests

3.11.1 kVp reproducibility

To determine kVp reproducibility, the kVp was varied from 50 to 100 kVp at step increments of 10 (50, 60, 70, 80, 90, 100) while mAs of 4, 6.30, 12.5, 18, 20, and 25 respectively were selected. Three exposures for each set

of parameters were made and the average kVp was recorded. kVp reproducibility was determined using equation 3.1 which has been used by Godfry, Adeyemo, & Sadiq, (2015) and Khosh nazar, Hejazi, Mokhtarian & Mooshi, (2013).

$$\text{kVp Reproducibility} = \left(\frac{\text{kVp}_{max} - \text{kVp}_{min}}{\text{kVp}_{max} + \text{kVp}_{min}} \right) \times 100\% \qquad 3.1$$

where kVp_{max} and kVp_{min} are selected kVp and measured kVp respectively. The result of kVp reproducibility is presented in Table 4.2.

3.11.2 kVp accuracy

kVp accuracy was performed to detect how selected kVp deviates from the measured kVp. kVp was varied from 50 to 110 at step increments of 10 (50, 60, 70, 80, 90, 100, and 110) while the mAs was kept constant at 4 for all the kVps. Three exposures were made for each kVp at constant mAs and the results were recorded. kVp accuracy was calculated using equation 3.2 (Godfry, Adeyemo, & Sadiq, 2015: Khoshnazar, Hejazi, Mokhtarian & Mooshi, 2013).

$$\text{kVp Accuracy} = \left(\frac{\text{kVp}_{max} - \text{kVp}_{min}}{\text{kVp}_{min}} \right) \times 100\% \qquad 3.2$$

3.11.3 Exposure linearity

Exposure linearity means that sequential increase in mAs should produce the same sequential increase in exposure dose. This measurement was done to verify the deviation in exposure dose when mAs was varied. This was determined by keeping the kVp constant at 70 kVp while mAs varied from 4, 8, 12.5, and 16. Three exposures were performed for each set of the exposure factors. Dose for each exposure was recorded and the average estimated. The

ratio of radiation output to Q [mGy/mAs] were also determined. The exposure linearity was therefore calculated using equation 3.3 (Godfrey, Adeyemo, & Sadiq, 2015: Khoshnazar, Hejazi, Mokhtarian & Mooshi, 2013).

$$\text{Exposure Linearity} = \left(\frac{\frac{\text{mGy}_{\max}}{\text{mAs}} - \frac{\text{mGy}_{\min}}{\text{mAs}}}{\frac{\text{mGy}}{\text{mAs}}\text{Average}} \right) \div 2 \times 100\% \qquad 3.3$$

3.11.4 Exposure reproducibility

Exposure reproducibility implies that the radiation intensity emitted by the X-ray tube is always the same whenever that same set of technical factors are used for any radiological examination. This measurement was done to determine the variation in exposure when technical factors are altered. To determine the exposure reproducibility, kVp was varied from 60 to 100 at step increments of 10 (60, 70, 80, 90, and 100). The mAs was also varied from 6.30, 12.5, 18, 20, and 25 respectively. Three exposures were made for each set of technical factors and the doses [mGy] were recorded using RaySafe X2 dosimeter. Deviation of exposure reproducibility was calculated using equation 3.4 (Godfrey et al., 2015: Khoshnazar et al., 2013).

$$\text{Exposure Reproducibility} = \left(\frac{\text{mGy}_{\max} - \text{mGy}_{\min}}{\text{mGy}_{\max} + \text{mGy}_{\min}} \right) \div 2 \times 100\% \qquad 3.4$$

3.11.5 Timer accuracy

Timer accuracy was determined at constant kVp of 70 kVp and mAs was varied from 4, 8, 12.5,16, 20 and 25. The time (in ms) was selected from 8, 16, 25, 32, 40, and 50, respectively. Three exposures were performed for each of the selected parameters. Time (in ms) was then recorded for each of the exposure and each average time was then estimated. Timer accuracy was

then calculated using equation 3.5 (Godfrey et al., 2015: Khoshnazar et al., 2013).

$$\text{Timer Accuracy} = \left(\frac{\text{Measured Time} - \text{Selected Time}}{\text{Selected Time}} \right) \times 100\% \qquad 3.5$$

3.12 Radiation Tube Output [µGy/mAs] Measurements

X-ray tube output is the measure of radiation dose [µGy] per the product of tube current and the exposure time. This was initially recorded in [µGy/mAs] and was converted to [mGy/mAs] during the estimation of the entrance skin dose. To determine the tube output, a fixed Q of 4 mAs was selected and applied voltage was varied from 50 to 110 kVp at step increments of 10 (50, 60, 70, 80, 90, 100, 110 kVp). Three exposures were made for each set of technique factors and dose [µGy] were recorded using Raysafe X2 dosimeter. The average dose was then divided by the quantity of charge Q [mAs] to obtain tube output [µGy/mAs] for the selected technique factors. A graph of tube output [µGy/mAs] was ploted against the squre of the applied voltage [kVp^2] in order to determine the value of tube output for each selected applied voltage. A correlational equation describing the relationship between the square of applied volatge and tube output was derived and used to estimate output for each V of the X-ray machine. The square of applied voltage was used instead of applied voltage because the former produced best correlation with higher R^2 than the latter and has been used by some researchers (Kothan & Tungjai, 2011). The radiation tube output was determined for each of the six (6) study centers with same exposure factors as described above

3.13 Entrance Skin Dose Calculation

Entrance skin dose is a dosimetric property which is monitored for the purposes of optimizing radiation exposure to patient. It is a measure of the amount of radiation that enters the surface of irradiated body part. Entrance skin dose of nine (9) radiographic examinations were estimated in this work (chest PA, lumbar spine AP, lumbar spine LAT, pelvis AP, abdomen AP, skull AP, skull LAT, cervical spine AP, and cervical spine LAT).

To estimate the entrance skin dose for these radiographic examinations, patient habitus (age, weight, height and sex) were recorded. The weight was obtained by using seca weighing scale while the height was measured using five meter tape measure. Exposure parameters (V, Q), FDD, FSD and the thickness of body part to be examined were also measured and recorded. These technical factors were selected during the radiographic examinations by radiographers. The ESD was estimated using equation 3.6.

$$\mathrm{ESD}[\mathrm{mGy}] = \text{Tube output}\left[\frac{\mathrm{mGy}}{\mathrm{mAs}}\right] \times \mathrm{Q} \times \left(\frac{\mathrm{FDD}}{\mathrm{FSD}}\right)^2 \times \mathrm{BSF} \qquad 3.6$$

This approach and equation 3.6 have been used by many researchers to estimate ESD for the purpose of optimizing radiation dose (Ofori, Antwi, Scutt, & Ward, 2012: Taha, Al- Ghorabie, Kufbi, & Saib, 2015). The first component of equation 3.6, which is the tube output differ from one X-ray equipment to another. Therefore, the radiation output/mAs [mGy/mAs] for each X-ray equipment involved in this study was calculated as shown in chapter four. For this reason, equation 3.6 was modified according to the radiation tube output/mAs for each X-ray equipment as shown in equations 3.7- 3.11.

Technical parameters used to estimate ESDs [mGy] for each radiographic examination at HP1 are shown in Table 3.1.

Table 3.1: Technical Parameters used for ESD Estimation at HP1

Examinations/ Projections	Selected Voltage [kVp] Average (SD)	Selected Quantity of charge [mAs] Average (SD)	FDD [cm]	FSD [cm] Average (SD)
Chest PA	101.6 ± 1.2	2.8 ± 0.9	150	126.5 ± 2.6
Lumbar spine AP	96.0 ± 8.9	25.8 ± 3.5	100	76.7 ± 1.5
Lumbar spine LAT	96.2 ± 9.0	30.3 ± 5.5	100	74.8 ± 1.5
Cervical spine AP	71.3 ± 2.3	6.5 ± 0.3	100	88.5 ± 1.1
Cervical spine LAT	72.5 ± 2.7	6.5 ± 0.4	100	85.5 ± 1.2
Skull PA	78.6 ± 4.5	12.5 ± 4.5	100	81.4 ± 1.9
Skull LAT	78.4 ± 0.9	20.7 ± 4.4	100	78.2 ± 3.3
Pelvis AP	85.0 ± 4.7	21.4 ± 4.5	100	78.0 ± 1.4
Abdomen AP	90.0 ± 10.2	25.6 ± 6.7	100	78.6 ± 1.9

Note; SD is the standard deviation

The ESD [mGy] for each radiographic examination was estimated using equation 3.7

$$\mathrm{ESD}[\mathrm{mGy}] = 0.007V^2 - 4.5522 \times Q \times \left(\frac{\mathrm{FDD}}{\mathrm{FSD}}\right)^2 \times \mathrm{BSF} \qquad 3.7$$

where BSF is the backscatter factor, BSF of 1.37 recommended by IAEA was used for all calculations in this research work (IAEA, 1996), Q is the quantity of charge [mAs] and V is the applied voltage [kVp].

FDD is the focus detector distance and FSD is the focus skin distance. FDD of 150 cm was used for chest PA while 100 cm was used for remaining eight (8) examinations at HP1.

The technical parameters used to estimate ESDs [mGy] at HP2 are shown in Table 3.2.

Table 3.2: Technical Parameters used for ESD Estimation at HP2

Examinations/ Projections	Selected Voltage [kVp] Average (SD)	Selected Quantity of Charge [mAs] Average (SD)	FDD [cm]	FSD [cm] Average (SD)
Chest PA	80.5 ± 12.1	7.8 ± 3.3	200	176.4 ± 3.0
Lumbar spine AP	74.4 ± 2.4	25.5 ± 4.4	100	76.5 ± 4.3
Lumbar spine LAT	79.3 ± 1.6	32.6 ± 4.6	100	74.2 ± 4.2
Cervical spine AP	58.5 ± 0.9	8.2 ± 1.9	100	87.5 ± 1.2
Cervical spine LAT	58.5 ± 0.9	8.2 ± 1.9	100	85.8 ± 0.8
Skull PA	70.0 ± 0	10.8 ± 3.4	100	81.0 ± 1.7
Skull LAT	69.3 ± 1.0	16.8 ± 3.4	100	83.0 ± 1.7
Pelvis AP	73.9 ± 3.5	24.5 ± 3.7	100	74.4 ± 3.1
Abdomen AP	74.3 ± 2.3	22.0 ± 3.9	100	74.5 ± 1.9

The ESD [mGy] for each radiographic examination at HP2 was estimated using equation 3.8.

$$\mathrm{ESD}[\mathrm{mGy}] = 0.0084\mathrm{V}^2 - 0.7464[\mu\mathrm{Gy}] \times \mathrm{Q} \times \left(\frac{\mathrm{FDD}}{\mathrm{FSD}}\right)^2 \times \mathrm{BSF} \qquad 3.8$$

FDD of 200 cm was used for chest PA while 100 [cm] was used for remaining eight (8) radiographic examinations. These technical factors were selected during radiographic examinations by the radiographers.

The technical parameters used to estimate ESDs [mGy] at HP3 are shown in Table 3.3

Table 3.3: Technical Parameters used for ESD Estimation at HP3

Examinations/ Projections	Selected Voltage [kVp] Average (SD)	Selected Quantity of charge [mAs] Average (SD)	FDD [cm]	FSD [cm] Average (SD)
Chest PA	73.4 ± 2.2	23.5 ± 2.5	180	156.6 ± 2.3
Lumbar spine AP	74.3 ± 1.1	27.8 ± 4.7	100	76.9 ± 2.7
Lumbar spine LAT	74.2 ± 0.8	56.9 ± 4.7	100	74.1 ± 2.6
Cervical spine AP	71.4 ± 1.2	14.6 ± 2.2	100	87.8 ± 1.3
Cervical spine LAT	71.0 ± 1.1	14.6 ± 1.6	100	86.0 ± 1.3
Skull PA	71.7 ± 0.7	20.4 ± 0.9	100	80.2 ± 2.3
Skull LAT	71.7 ± 0.7	19.4 ± 0.9	100	80.0 ± 2.0
Pelvis AP	72.2 ± 2.1	21.7 ± 2.6	100	79.3 ± 1.6
Abdomen AP	73.4 ± 1.4	25.5 ± 3.8	100	76.9 ± 1.8

The ESDs [mGy] for each radiographic examination at HP3 was estimated using equation 3.9.

$$ESD[mGy] = 0.0087V^2 - 4.4438[\mu Gy] \times Q \times \left(\frac{FDD}{FSD}\right)^2 \times BSF \qquad 3.9$$

FDD of 180 cm was used for chest PA while 100 cm was used for remaining eight examinations

The technical parameters used to estimate each ESDs [mGy] at HP4 are shown in Table 3.4.

Table 3.4: Technical Parameters used for ESD Estimation at HP4

Examinations/ Projections	Selected voltage [kVp] Average (SD)	Selected Quantity of charge [mAs] Average (SD)	FDD [cm]	FSD [cm] Average (SD)
Chest PA	118.6 ± 8.3	1.8 ± 0.20	180	157.1 ± 2.1
Lumbar spine AP	79.7 ± 6.0	9.7 ± 5.8	100	76.1 ± 4.1
Lumbar spine LAT	95.1 ± 8.9	10.9 ± 4.3	100	73.0 ± 4.7
Cervical spine AP	70.0 ± 0	5.8 ± 1.3	100	87.8 ± 1.4
Cervical spine LAT	74.3 ± 3.8	7.0 ± 1.5	100	85.8 ± 1.4
Skull PA	70.8 ± 1.9	15.6 ± 1.4	100	85.0 ± 2.9
Skull LAT	70.0 ± 0	15.5 ± 2.2	100	83.0 ± 3.0
Pelvis AP	76.2 ± 2.2	6.8 ± 2.2	100	78.0 ± 2.6
Abdomen AP	79.6 ± 3.7	9.3 ±2.1	100	77.8 ± 2.2

The ESD for each radiographic examination at HP4 was estimated using equation 3.10.

$$ESD[mGy] = 0.0093V^2 + 11.395[\mu Gy] \times Q \times \left(\frac{FDD}{FSD}\right)^2 \times BSF \qquad 3.10$$

At this radiographic center, FDD of 180 cm was used for chest PA while 100 cm was used for remaining eight examinations.

The technical parameters used to estimate each ESDs [mGy] at HP5 are shown in Table 3.5.

Table 3.5: Technical Parameters used for ESD Estimation at HP5

Examinations/ Projections	Voltage [kVp] Average (SD)	Quantity of charge [mAs] Average (SD)	FDD [cm]	FSD [cm] Average (SD)
Chest PA	120.0 ± 0	1.4 ± 0.6	180	158.0 ± 2.0
Lumbar spine AP	80.0 ± 0	19.9 ± 4.3	120	96.8 ± 1.7
Lumbar spine LAT	90.0 ± 0	31.5 ± 13.7	120	93.6 ± 1.6
Cervical spine AP	75.5 ± 2.7	5.3 ± 2.1	120	109.0 ± 1.0
Cervical spine LAT	78.5 ± 2.3	4.3 ± 0.5	120	107.0 ± 1.0
Skull PA	75 .0 ± 0	10.9 ± 4.5	120	103.8 ± 2.0
Skull LAT	70.0 ± 0	5.3 ± 2.0	120	102.0 ± 1.7
Pelvis AP	80.0 ± 0	12.3 ± 7.8	120	96.9 ± 1.9
Abdomen AP	80.0 ± 0	13.5 ± 7.7	120	97.1 ± 2.5

The ESDs [mGy] for each radiographic examination at HP5 was estimated using equation 3.11.

$$\mathrm{ESD[mGy]} = 0.0052\mathrm{kVp}^2 - 1.4204[\mu\mathrm{Gy}] \times \mathrm{mAs} \times \left(\frac{\mathrm{FDD}}{\mathrm{FSD}}\right)^2 \times \mathrm{BSF} \qquad 3.11$$

At this radiographic center, FDD of 180 cm was used for chest PA while 120 cm was used for remaining eight examinations.

3.14 Rando Anthropomorphic Phantom

Anthropomorphic phantoms are manufactured to simulate physical and attenuation characteristics of human body using tissue-equivalent materials (Winslow FJ, Hyer, D.E., Fisher, R.F., Tien, CJ, and Hintenlang, D.E (2009).

It has been used in radiology for the assessment of absorbed dose, image quality assessment and simulation of image procedures.

Two models of the anthropomorphic phantoms commercially available are male and female models. The male model represents height of 175cm and 73.5 kg while the female is 163 cm and 54 kg. The female model manufactured by Phantom Laboratory Salem, New York with model RAN100 was used in this work for dose-image optimization to determine the optimal exposure factors (mAs, kVp and its related EIs) for chest PA, lumbar spine AP and lumbar spine LAT. This phase of the study took place at HP3 where doses of 1.77 [mGy] and 4.64 [mGy] were recorded for chest PA, and lumbar spine LAT respectively during ESD survey.

The phantom is transected-horizontally into 2.5 cm slices thick. Each slice has holes which is filled with bone-equivalent, soft-tissue equivalent, or lung tissue-equivalent pins that can be replaced by thermoluminescent dosimeter (TLD) holder pins. Figure 3.3 shows image of female rando anthropomorphic phantom used for the image-quality control optimization.

Figure 3.3: Image Showing Female Anthropomorphic Phantom without Head

3.15 Acquisition of Phantom Images – Chest PA

Thirty-six (36) test images and one reference image were obtained for the chest PA examination using the female rando anthropomorphic phantom.This section of the study was conducted at HP3. Random numbers were assigned to these images acquired on different exposure techniques. Post processing algorithm was not applied to any of the images since it was difficult to guarantee the same level of post processing.

The phantom was positioned in PA projection with FDD of 150 cm. The X-ray beam was focused at the inferior border of the scapula and collimated to the region of interest. A Fuji detector (ST. Imaging plate) with dimension of 35 cm x 43 cm was used with Fuji readout. The ESD to the chest of the phantom were estimated using the same methodology as described in the patient ESD estimation. The reference image was taken with 73 kVp and 25 mAs which was obtained as an average exposure parameter for chest PA at HP3 during the patient ESD survey of this study. The exposure indicator on each of the images were recorded. Figure 3.4 shows chest PA projection of the anthropomorphic phantom, while Table 3.6 shows the exposure, factors used for the acquisition of chest PA images

Figure 3.4: Image Showing Chest PA Positioning

Table 3.6: Exposure Parameters used for Acquisition of Phantom Chest PA Images

Image No	Quantity of charge [mAs]	Voltage [kVp]	Image No	Quantity of charge [mAs]	Voltage [kVp]
32	1.6	70	8	1.6	100
10	2.0	70	1	2.0	100
3	2.5	70	14	2.5	100
20	3.20	70	21	3.20	100
15	3.6	70	36	3.6	100
22	4.0	70	5	4.0	100
11	1.6	80	16	1.6	110
33	2.0	80	35	2.0	110
19	2.5	80	23	2.5	110
7	3.20	80	27	3.2	110
12	3.6	80	24	3.6	110
18	4.0	80	9	4.0	110
25	1.6	90	31	1.6	120
28	2.0	90	17	2.0	120
6	2.5	90	26	2.5	120
13	3.20	90	4	3.2	120
29	3.6	90	34	3.6	120
2	4.0	90	30	4.0	120
Reference image	25	73			

3.16 Model Equation of EI, Q, and V for Chest PA

The model equation was developed using values in Table 3.7. EI values were recorded from the anthropomorphic phantom images. The values of 1/EI, mAs and kVp were imported into MATLAB program version R2018b (9, 5, 0, 944444) where the values of 1/EI, mAs and kVp were plotted as shown in Figure 4.32. The relationship between 1/EI, voltage, quantity of charge were derived in the form of equation of 1/EI as function of voltage and quantity of charge as shown in equation 4.14.

Table 3.7: Chest PA Exposure Factors and Inverse EI

Q [mAs]	V [kVp]	EI	1/EI x10^{-4}
1.6	70	6638	1.51
2.0	70	6195	1.61
2.5	70	5396	1.85
3.20	70	4809	2.10
3.6	70	4189	2.38
4.0	70	3909	2.55
1.6	80	4921	2.03
2.0	80	4000	2.50
2.5	80	3105	3.22
3.20	80	2524	3.96
3.6	80	2198	4.54
4.0	80	2099	4.76
1.6	90	3733	2.67
2.0	90	2898	3.45
2.5	90	2148	4.65
3.20	90	1787	5.59
3.6	90	1521	6.57
4.0	90	1419	7.04
1.6	100	2767	3.61
2.0	100	2355	4.24
2.5	100	1706	5.86
3.20	100	1387	7.20
3.6	100	1154	8.66
4.0	100	565	17.69
1.6	110	2466	4.05
2.0	110	2099	4.76
2.5	110	1486	6.73
3.2	110	1236	8.09
3.6	110	1005	9.95
4.0	110	938	10.66
1.6	120	1871	5.34
2.0	120	1556	6.42
2.5	120	1127	8.87
3.2	120	938	10.66
3.6	120	798	12.53
4.0	120	711	14.06

3.17 Acquisition of Phantom Images – Lumbar Spine AP

Forty-four (44) test images and one reference image were obtained for the optimization of lumbar spine AP examination. The phantom was positioned in supine position on the radiographic table and the X- ray beam was directed perpendicularly. The detector and the X-ray beam were centered at the iliac crests joint of the phantom to include all the vertebrae of the lumbar region. A 35 cm x 43 cm dimension of Fuji detector (ST. Imaging plate) was used but the X- ray beam was collimated to only the region of interest. A focus to detector distance of 100 cm was used for all the images acquired. The images acquired were not subjected to post processing as in the case of chest PA. Entrance skin dose to the phantom was also estimated as described under the section entrance skin dose. The detectors were then readout and the associated EI were recorded. The reference image was acquired using 74 kVp and 28 mAs which was recorded as average exposure parameter for lumbar spine AP at the HP3. Figure 3.5 shows radiographic positioning of the rando anthropomorphic phantom for lumbar spine AP images while the exposure parameters used for the acquisition of lumbar spine AP images are shown in Table 3.8.

Figure 3.5: Image Showing Lumbar Spine AP Positioning

Table 3.8: Exposure Parameters used for Acquisition of Phantom Lumbar Spine AP Images

Image No	Q [mAs]	V [kVp]	Image No	Q [mAs]	V [kVp]
13	16	70	24	16	90
22	18	70	25	18	90
2	20	70	23	20	90
42	22	70	52	22	90
4	25	70	14	25	90
40	28	70	53	28	90
5	32	70	16	32	90
10	36	70	12	36	90
27	40	70	29	40	90
7	45	70	31	45	90
42	50	70	44	50	90
26	16	80	15	16	100
28	18	80	17	18	100
3	20	80	19	20	100
50	22	80	54	22	100
1	25	80	30	25	100
51	28	80	55	28	100
36	32	80	9	32	100
33	36	80	34	36	100
18	40	80	6	40	100
32	45	80	8	45	100
41	50	80	39	50	100
Reference image	28	74			

3.18 Acquisition of Phantom Images – Lumbar Spine LAT

Forty-four (44) test and one reference images of lumbar spine LAT were acquired from the phantom. The reference image was acquired from 74 kVp and 56 mAs exposure factors which were an average exposure factor for lumbar spine LAT at HP3. FDD of 100 cm was used to acquire all the images.

No post processing was applied to the images since it was difficult to ensure uniform processing. The phantom was positioned in the lateral position and the X-ray beam was centered at the iliac crest level to ensure that all the vertebrae were included. Random numbers were assigned to each image for easy identification. The collimation was restricted to only the region of interest. The ESD to the phantom was also estimated using previously described method in section 3.13. The detector was then readout and the EI on each image was recorded. The exposure factors used for the acquisition of the lumbar spine LAT images are shown in Table 3. 9.

Table 3.9: Exposure Parameters used for Acquisition of Phantom Lumbar Spine LAT Images

Image No	Q [mAs]	V[kVp]	Image No	Q[mAs]	V [kVp]
2	16	70	23	16	90
26	18	70	21	18	90
28	20	70	17	20	90
44	22	70	42	22	90
4	25	70	14	25	90
46	28	70	41	28	90
5	32	70	16	32	90
10	36	70	12	36	90
27	40	70	29	40	90
7	45	70	31	45	90
42	50	70	44	50	90
3	16	80	19	16	100
24	18	80	15	18	100
38	20	80	20	20	100
45	22	80	40	22	100
1	25	80	30	25	100
43	28	80	37	28	100
36	32	80	9	32	100
33	36	80	34	36	100
18	40	80	6	40	100
32	45	80	8	45	100
41	50	80	39	50	100
Reference image	56	74			

3.19 Clinical Assessments of Phantom Images

Three senior radiographers were selected to evaluate the image quality for all the examinations. In all, 123 test images were assessed by the observers in comparison with the reference image of each examination. The observers were educated on the process of visual grading analysis before the assessment. The observers were blinded from the exposure factors to avoid bias.

To avoid influence of fatigue on the results of the assessment, the observers were given the freedom to evaluate the images at their own convenience. The soft images were assessed on the CR review monitor because HP3 has no PACS. The monitor was not calibrated during the study and the room and monitor ambient lighting were not measured due to constraint of equipment. However, this challenge did not affect the assessment of image quality since the facility was still using same conditions for their image assessments quality.

The observers evaluated each image independently and scored the anatomical structures on a five points scale (1, 2, 3, 4, 5) with 5 being highest ranked and 1 as lowest ranked. When anatomical structure was scored 5, meant that the observer was clearly confident that the structure clearly fulfilled clinical requirement, 4 meant the observer was somewhat confident that the structure met clinical requirement, 3 meant the observer was indecisive whether the criterion was fulfilled or not, 2 meant the observer was somewhat confident that the criterion was fulfilled and 1 meant that the observer was clearly confident that the structure did not meet clinical requirement. This type of assessment gives better clinical information than the objective methods since clinical practice depends on subjective interpretation of images, however

the subjective assessment depends on observer's clinical knowledge and experience.

Six (6) anatomical structures were evaluated in chest PA examination, for each of 36 images, while five (5) anatomical structures were evaluated in lumbar spine AP and lumbar spine LAT examinations for each of 89 images. The overall image quality was estimated using the visual grading analysis score (VGAS) as shown in equation 3.12 which has been used by some researchers (Moore, Wood, Beavis, & Saunderson, 2013; Oliveira et al., 2013).

$$\text{VGAS} = \frac{\sum_{i=1}^{I}\sum_{s=1}^{S}\sum_{o=1}^{O} Gi.s.o}{I \times S \times O} \qquad 3.12$$

where $Gi.s.o$ is the grading (1, 2, 3, 4, 5) given by observer O for image I and structures, I is the number of images, S is the number of anatomical structures graded, and O is the number of evaluators.

3.20 Data Analysis

All data obtained were imported into Microsft Excel (2013) for processing and analysis. Data clearing option was used to either delete or confirm double data. Having ensured the accuracy of the data, analysis was carried out using Microsft Excel graphical tool to plot all the necessary graphs. Where necessary, equations were added to the graphs using Excel "add trend". Correlation between parameters were checked using correlation factor R^2 from Excel (2013). MATLAB program version R2018b (9, 5, 0, 944444) was used to plot kVp, mAs, VGAs, and dose to help obtain the optimal values for chest PA, lumbar spine AP and lumbar spine LAT. Mathematical model relating EI,

V and Q was developed with MATLAB program version R2018b (9, 5, 0, 944444).

3.21 Ethical Clearance Approval

Two ethics approval were obtained for carrying out this research work. The first one was obtained from Institutional Review Board Secretariat of University of Cape Coast as the host institution of this research. The ethics approval was UCCIRB/CANS/2017/06. The second ethical approval was obtained from Ghana Health Service Ethics Review Committee in order to use the hospitals selected for this research. The ethical clearance approval number was GHS/RDD/ERC/Admin/APP19/003. Beside these ethical clearance approvals all the hospitals involved in this research work approved for the use of their facilities.

3.22 Chapter Summary

This chapter discusses the methods and materials used to obtain the results. Observational correlational study design was to measure both dependent and independent variables. Dependent variables measured were ESD, EI and image quality assessment while independent variables were applied voltage, quantity of charge, age, weight, height, body part thickness, FDD and FSD. The country was divided into three zones (costal, middle, and northern) where two (2) hospitals were selected from each of the costal and northern zone while one (1) hospital was selected from the middle zone for the ESD estimation.

The selected population for the study were adult patients of 18 years and above with justified radiographic request from a registered medical practitioner to undergo any of the selected examinations. The study involved two hundred and ninety (290) females and one hundred and sixty (160) males for the entrance skin dose survey. The average age, weight and height of the study population were 50 ± 14 years, 69 ± 8 kg, 162 ± 9 cm respectively.

Four (4) data correction instruments were developed to collect data on quality control tests, ESD estimation, acquisition of phantom images and image quality assessment for chest PA, lumbar spine AP and lumbar spine LAT. The anatomical criteria for image quality assessment were adopted from European Commission guidelines on quality criteria for diagnostic radiographic images.

Six (6) quality control parameters were performed. These included kVp accuracy, kVp reproducibility, timer accuracy, exposure linearity, exposure reproducibility and radiation tube output. Exposure parameters (V, Q), FDD, FSD and the thickness of body part to be examined were also measured and recorded. The ESD was estimated using equation using mathematical formula.

Three senior radiographers were selected to evaluate the image quality for all the examinations. Six (6) anatomical structures were evaluated in chest PA examination, for each of the 36 images, while five (5) anatomical structures were evaluated in lumbar spine AP and lumbar spine LAT examinations for each of the 89 images. The overall image quality was estimated using the visual grading analysis score.

CHAPTER FOUR

RESULTS AND DISSCUSION

4.0 Introduction

This chapter presents the results and discussion on X-ray tube output modelling equations, quality control test, entrance skin dose, dose-image quality optimization for chest PA, lumbar spine AP, lumbar spine LAT, optimal exposure factors with associated exposure indicator, modelling equation for exposure indicator and optimization strategy flow chart.

4.1 X-ray Tube Output Measurements

The results of measured V, V deviation, radiation tube output [µGy] and tube output [µGy/mAs] for the five X-ray equipment used for this study are presented in Table 4.1. The X-ray equipment at HP5 was DDR systems and its characteristics were different from those at HP1, HP2, HP3 and HP4 which were CR. Therefore, the comparison was made between HP1, HP2, HP3, HP4 and HP5.

Table 4.1: X-Ray Equipment Tube Output Results at 4 mAs

Institution	Selected V [kVp]	Measured V[kVp]	V deviation [kVp]	Dosimeter readings [µGy]	Tube output [µGy/mAs]	Total filtration [mm Al]
HP1	50	47.6	2.4	50.57	12.64	-
	60	57.8	2.2	83.62	20.91	4.1
	70	66.7	3.3	120.03	30.01	3.9
	80	76.5	3.5	160.47	40.12	3.8
	90	86.1	3.9	205.77	51.44	3.7
	100	96.5	3.5	254.97	63.74	3.8
	110	106.9	3.1	323.56	80.89	3.7
HP2	50	45.7	4.3	76.39	19.09	-
	60	58.7	1.3	118.86	29.71	3.1
	70	67.7	2.3	164.33	41.08	3.0
	80	77.7	2.6	214.13	53.53	3.0
	90	87.0	3.0	269.96	67.49	2.9
	100	96.8	3.2	330.50	82.62	2.9
	110	107.6	2.4	402.31	100.53	2.9
HP3	50	47.6	2.4	76.82	19.23	-
	60	58.1	1.9	121.41	30.41	3.1
	70	70.3	-0.3	154.35	38.64	3.0
	80	83.7	-3.7	182.54	45.05	2.9
	90	90.4	-0.4	246.41	61.66	3.0
	100	97.2	2.8	335.82	83.94	2.9
	110	106.7	3.3	419.10	104.85	2.9
HP4	50	48.5	1.5	192.11	48.02	-
	60	59.3	0.7	145.14	36.27	2.9
	70	69.0	1.0	203.60	50.90	2.8
	81	80.0	1.0	277.52	69.37	2.7
	90	89.4	0.6	343.31	85.82	2.6
	102	101.3	0.7	439.01	109.75	2.7
	109	108.2	0.8	496.10	124.02	2.7
HP5	50	49.2	0.8	42.40	10.60	-
	60	59.6	0.4	68.83	17.20	3.8
	70	68.9	1.1	97.23	24.30	3.8
	80	79.3	0.7	128.90	32.22	3.6
	90	89.9	0.1	166.40	41.60	3.4
	100	100.1	-0.1	202.30	50.57	3.3
	110	110.1	-0.1	241.10	60.27	3.3

where the dash (-) in Table 4.1 means that total filtration was not measured.

The X-ray equipment at HP4 does not allow for selection of 80, 100 and 110 but rather 81, 102 and 109 kVp, respectively. Negative values in voltage deviation indicates that the measured voltage values were higher than the selected voltage values. This occurred at HP3 for 70, 80, 90 kVp and HP5 for 100 and 110 kVp. The voltage deviations of HP4 were lower than HP1, HP2 and HP3. The minimum and maximum deviations were 0.6 kVp and 1.5 kVp, respectively. HP1 had the highest voltage deviation with 2.4 as minimum and 3.9 kVp as maximum. These variations in the measured voltage contributed to the variations in tube output of each X-ray equipment. HP5 had the lowest voltage deviations with the minimum of -0.1 kVp and maximum of 1.1 kVp.

To estimate ESD, the tube output for each X-ray equipment was determined and the results are presented in Figures 4.1 to 4.5. Tube output increases linearly and is proportional to square of voltage in Figures 4.1 to 4.5. This means that when voltage is doubled, tube output increases by a factor of four, hence voltage affects radiation dose significantly. A study conducted on estimation of X-ray output using mathematical model made similar observation on the relationship of voltage and tube output (Kothan & Tungjai., 2011). In Another study in which ten X-ray equipments' tube output were investigated at different FDD (100 cm and 60 cm) also made similar observation (Sezdi, 2011: Kothan & Tungjai, 2011).

Figure 4.1 illustrates the relationship between X-ray tube output [µGy/mAs] and the square of voltage [kVp²] for X-ray equipment at HP1

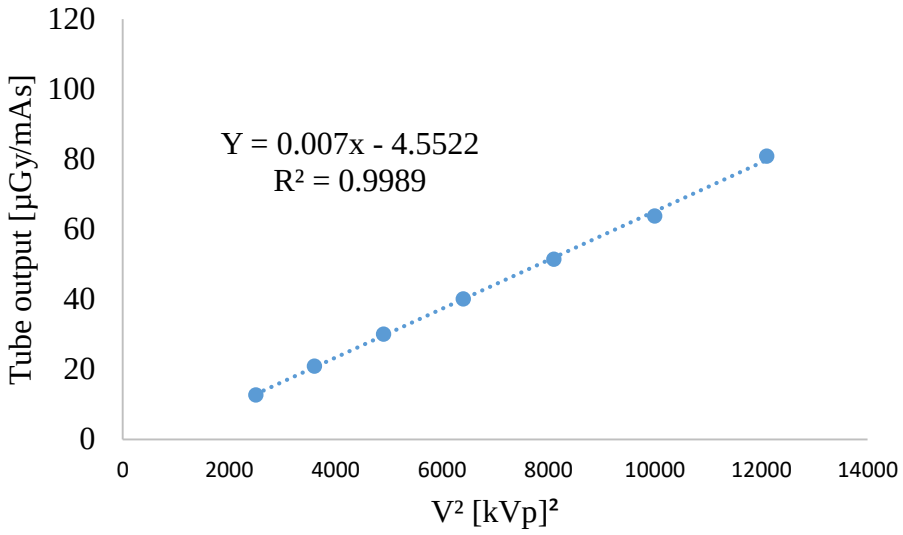

Figure 4.1: Relationship between Tube Output and V² at HP1.

The minimum and maximum tube output were 12.64 and 80.89 [µGy/mAs] occurring at 50 and 110 kVp, respectively. Equation 4.1 describes the relationship between tube output and the square of voltage with a correlation factor of $R^2 = 0.9989$:

$$Y = 0.007X - 4.5522 \qquad 4.1$$

where Y is tube output and X is V². Equation 4.1 was used to estimate radiation tube output for each volatge that was used to produce radiographic examination during ESD at HP1.

The relationship between X-ray tube output and square of the volatge for the X-ray equipment at HP2 is shown in Figure 4.2.

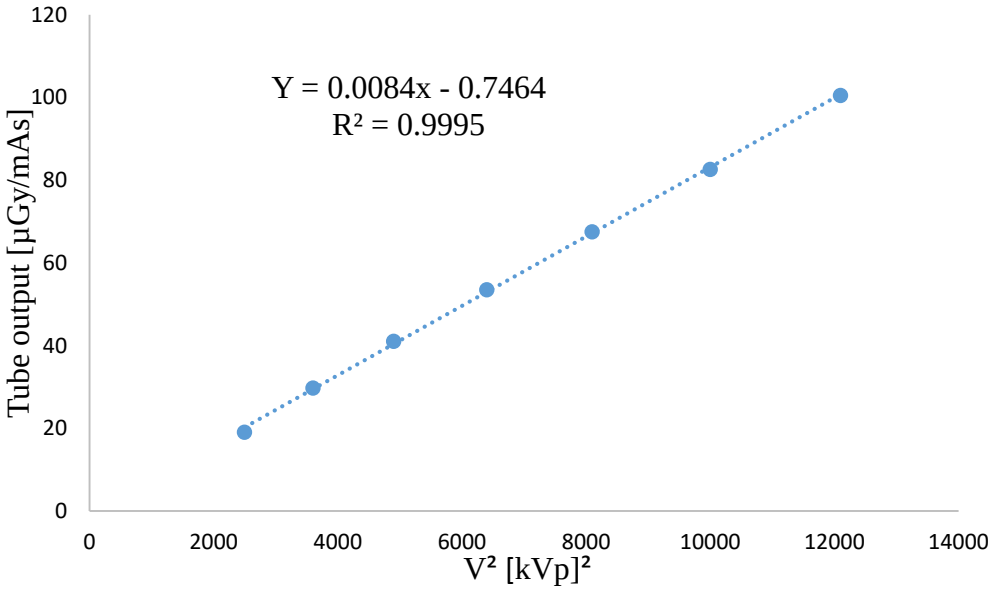

Figure 4.2: Relationship between Tube Output and V^2 at HP2.

The minimum and maximum tube output were 19.09 and 100.53 [µGy/mAs]. They occurred at 50 and 110 kVp, respectively. This means that as V increases, tube output also increases and thus patient radiation dose equally increases. The equation 4.2 describes the tube output for the X-ray equipment at HP2 with correlation factor of $R^2 = 0.9995$:

$$Y = 0.0084X - 0.7464 \qquad 4.2$$

where Y is tube output and X is V^2. Equation 4.2 was used to estimate radiation tube output for each voltage that was used to produce radiographic examination during ESD at HP2.

Relationship between X-ray tube output and the square of voltage for the X-ray equipment at HP3 is shown in Figure 4.3.

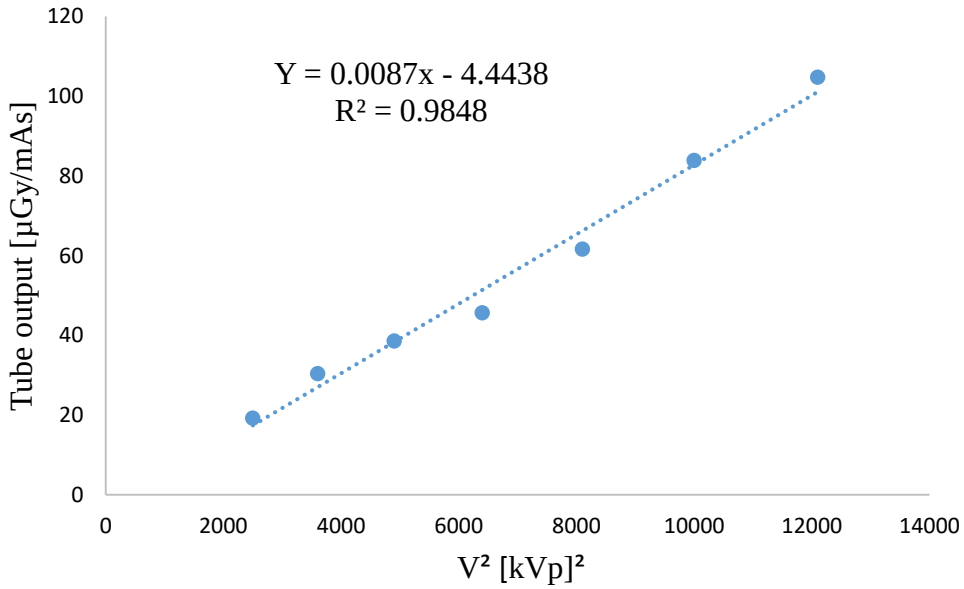

Figure 4.3: Relationship between Tube Output and V² at HP3.

The minimum and maximum tube output for this X-ray equipment were 19.2 and 104.8 [µGy/mAs] which occurred at 50 and 110 kVp, respectively. Equation 4.3 describes the tube output for the X-ray equipment at HP3 with correlation factor of $R^2 = 0.9848$:

$$Y = 0.007X - 4.4438 \qquad 4.3$$

where Y is the tube output and X is V².

Although Figure 4.3 shows a linear relationship between tube output and sqaure of voltage, significant points deviated slightly from the actual straight line. These deviations could be as a result of voltage fluctuations on the power supply line to this radiographic facility. As shown in Figures 4.1 and 4.2, the number of X-ray photons generated in the tube directly depend on the applied voltage and therefore fluctuations due to applied voltage may cause inconsistent output values. It is therefore important that, radiographic facilities ensure constant and stable supply of power to the facility.

Relationship between X-ray tube output and square of voltage for the X-ray equipment at HP4 is shown in Figure 4.4.

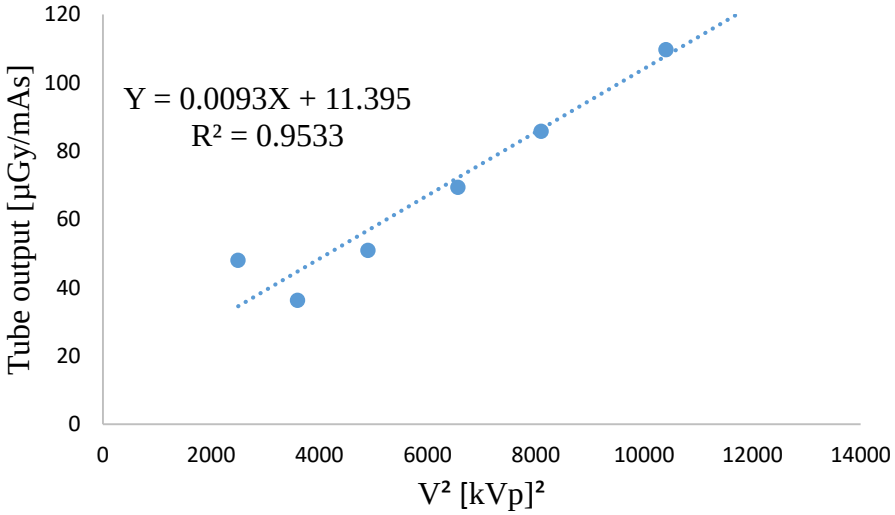

Figure 4.4: Relationship between Tube Output and V^2 at HP4.

The minimum and maximum tube output for this equipment were 48.0 and 124.0 [µGy/mAs] and they occurred at 50 and 109 kVp, respectively. Equation 4.4 describes the tube output for the X-ray equipment at HP4 with correlation factor of $R^2 = 0.9533$:

$$Y = 0.0093X + 11.395 \qquad 4.4$$

where Y is tube output and X is V^2. In Figure 4.4, some of the data deviated slightly from the fitting line, similar to Figure 4.3. Similarly, fluctuations in the power supply line may have caused these deviated values.

Relationship between X-ray tube output and V^2 for the X-ray equipment at HP5 is shown in Figure 4.5.

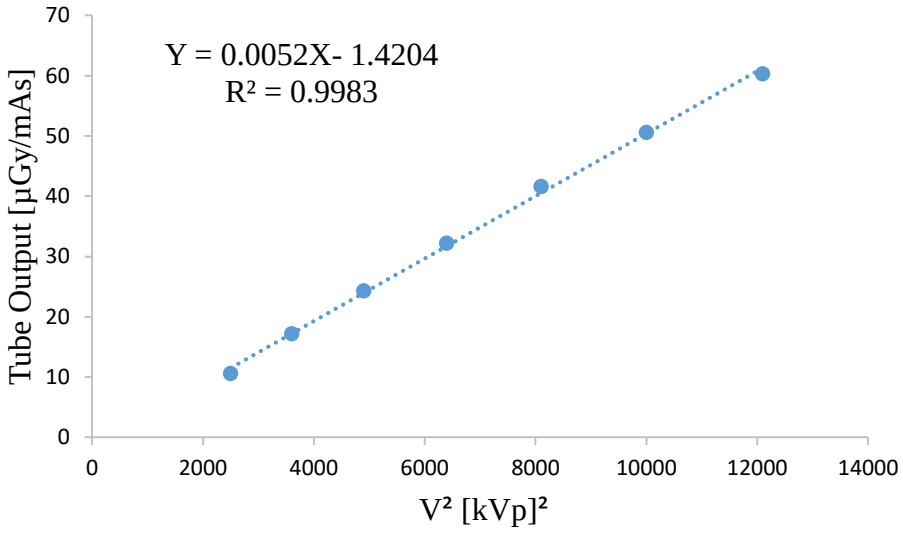

Figure 4.5: Relationship between Tube Output and V^2 at HP5.

The minimum and maximum tube output for this X-ray equipment were 10.6 and 60.3 [µGy/mAs] which occurred at 50 and 110 kVp, respectively. Equation 4.5 describes the tube output for the X-ray equipment at HP5 with correlation factor of $R^2 = 0.9983$:

$$Y = 0.0052X - 1.4204 \qquad 4.5$$

where Y is tube output and X is V^2.

Generally, all X-ray equipment output has linear relationship to the square of applied volatge and that the efficiency of an X-ray tube production is greater at the higher applied voltage values. The X-ray energies and penetrability depend on the voltage applied to the tube (Sungita, Mdoe, & Msaki (2006). In diagnostic radiography, applied voltage has effect on patient skin dose, image quality and EI values and therefore needed to be selected carefully. High values of applied voltage will increase Compton scattering which degrades image contrast and adversely affect image quality (Martin, 2007). However, lower voltage values increase image contrast due to

photoelectric absorption and increase patient radiation dose (Huda, 2014). Selection of tube voltage for particular examination must be done to achieve balance between image quality and patient radiation dose, a task that has been a challenge in diagnostic radiography since its introduction. Inappropriate selection of tube voltage would lead to overexposure of patients and poor image quality which impede retrieval of diagnostic information that adversely affects patients' care.

X-ray tube output could be influenced by a number of factors and therefore each X-ray equipment has different values of the output. To evaluate the factors that influence tube output, a comparison of tube output for the X-ray equipment at HP1, HP2, HP3, HP4 and HP5 at 90 kVp was done and the results are presented in Figure 4.6.

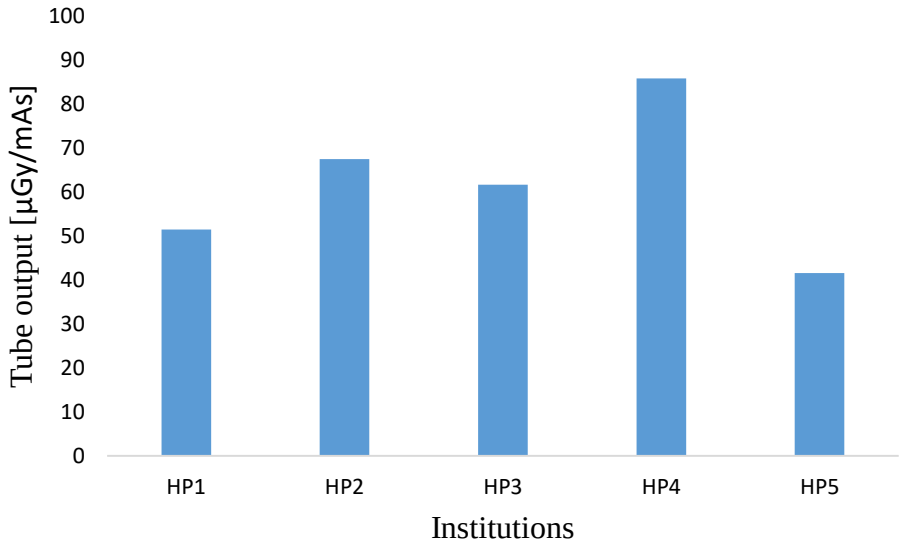

Figure 4.6: Comparison of Tube Output among HP1, HP2, HP3, HP4 and HP5 at 90 kVp

Comparison of the tube output at 90 kVp showed variations among the X-ray equipment. The comparison showed that HP4 generated highest tube output of

85.82 and HP5 had the lowest tube output of 41.6 at 90 kVp. The percentage difference between the highest and the lowest tube output/mAs was 51.5 %.

Reasons for this variation could be multifactorial. Variations in applied volatge output can contribute to the variations in tube output since applied voltage has quadratic effect on the tube output (Figures 4.1 to 4.5). Applied voltage output deviation from the selected values of X-ray equipment at HP4 was lower than HP1, HP2 and HP3. The minimum and maximum applied voltage deviations of X-ray equipment at HP4 were 0.6 kVp and 1.5 kVp, respectively. However, the DDR system at HP5 has the lowest applied voltage deviation among all the X-ray equipment with minimum and maximum deviations of -0.1 kVp and 1.1 kVp, respectively. HP1 has very high applied voltage output deviation with 2.2 kVp as minimum and 3.9 kVp as maximum (Table 4.1). This may explain why HP1 has the lowest tube output among all the CR systems. However, between HP3 and HP2 the observation was different. The applied voltage deviations at HP3 were lower than HP2 (Table 4.1). However, the output for HP3 was lower (61.66 µGy/mAs) than HP2 (67.49 µGy/mAs) with variation of 8.6 %. This implies that other factors such as time of exposure, filtration, and difference in equipment rather than applied voltage can influence the tube output.

Timer accuracy for HP3 was 1.6 % while that of HP2 was 2.1 % at $t \geq 10$ ms (Table 4.2). This means that HP3 has shorter exposure time than HP2 which may explain why HP2 has higher output than HP3. Time of exposure affects output dose, the longer the exposure time, the higher the output dose. Also, HP4 had higher timer accuracy of 4.1 % than all the CR systems, which

means that it has longer exposure time than all the equipment and hence the highest tube output.

Another interesting factor that could contribute to output variations is the difference in equipment from different manufactures. HP1, HP2 and HP3 were manufactured by same company (Shimadzu) while equipment at HP4 was from a different manufacturer (Philips). Although, there were also differences in output dose between HP1, HP2, and HP3 which all came from same manufacturer, the output dose difference between HP4 and the three others were high indicating that different manufacturer's effect should not be ignored. Also, the equipment at HP5 was DDR from a different manufacturer (General Electric) and has the lowest applied voltage deviations, lowest tube ouput, lowest timer accuracy which suggested that different X-ray modalities produce different tube output.

Other researchers have made similar observations in tube output variations among different X-ray equipment (Gholami, Nemati and Karami, 2015). Seven (7) X-ray equipment were investigated by Gholami, et al., 2015. The results indicated tube output variations of about 36.65 % - 133.20 % and kVp deviations of 0.1 to 27.52 %. Gholami, et al., (2015) observed that the highest output was recorded from the oldest X-ray equipment installed in 1982 and the lowest dose was recorded from X-ray equipment installed in 2000. It was then concluded that advancement in the age of an equipment increases its radiation output (Gholami, et al., 2015). However, this conclusion could not be authenticated in this current study. In the current study, X-ray equipment at HP4 which recorded the highest output was installed in 2012, same year as the X-ray equipment at HP2 and HP1. Therefore, the difference in output could

not be attributed to age of the equipment. There are divergent views among researchers on how age affects a tube's radiation output. A study conducted on dose optimization for quality control tests on X-ray equipment reported that X-ray tube output decreases with age of X-ray equipment (Sezdi, 2011) contrary to the study conducted by Gholami et al., (2015).

Another study conducted by Jibiri and Olwooke, (2016) showed no effect of ageing on the variations of the tube output. In that study, ten (10) X-ray equipment were investigated but only three (3) of them had the installation date. The output were 0.3859 [mGy/mAs], 0.2902 [mGy/mAs] and 0.4555 [mGy/mAs] for the equipment installed in 2013, 2011 and 2007, respectively. The output for equipment installed in 2011 should have been higher than that installed in 2013 if aging of X-ray equipment plays significant role in increasing the output (Jibiri & Olwooke, 2016). Sezdi (2011) reported that tube filtration could also affect tube output of X-ray equipment (Sezdi, 2011). Tube filtration removes lower energy X-rays from the X-ray spectrum which otherwise would have caused unnecessary radiation dose to patients as well as degradation of the image quality.

4.2 Quality Control Results

Table 4.2 presents the results of quality control tests for all the five different X-ray equipment at various radiographic centers.

Table 4.2: Results of Quality Control Tests of X-Ray Equipment at HP1, HP2, HP3, HP4 and HP5

Quality control test	Results					Acceptable Range %	Remarks
	HP1 %	HP2 %	HP3 %	HP4 %	HP5 %		
kVp Accuracy	4.2	3.4	4.0	1.3	0.6	± 5	All equipment pass
kVp reproducibility	2.1	1.7	4.6	0.6	0.4	± 5	All equipment pass
Exposure linearity	7.4	5.5	2.9	0.2	1.3	± 10	All equipment pass
Exposure reproducibility	0.3	0.2	0.2	0.1	0.1	± 5	All equipment pass
Timer/mS Accuracy $t \leq 10$ ms	$t \leq 10$ 7.5	$t \leq 10$ 7.5	$t \leq 10$ 8.8	$t \leq 10$ 8.8	$t \leq 10$ 2.4	$t \leq 10$ ± 20	All equipment pass
$t \geq 10$ ms	$t \geq 10$ ms, 2.1	$t \geq 10$ ms, 2.1	$t \geq 10$ ms, 1.3	$t \geq 10$ ms, 4.1	$t \geq 10$ ms, 0.3	$t \geq 10$ ms, ± 5	

The results presented in Table 4.2 indicated that all X-ray equipment used for this study passed generator performance tests. Although all equipment passed the QC tests, there were variations in the performance of these X-ray generators. Again, the X-ray equipment at HP5 has lower values of kVp accuracy (0.6%), kVp reproducibility (0.4%), exposure linearity (1.3%) and exposure reproducibility (0.1 %) than all the equipment. The X-ray equipment at HP1 has the lowest generator performance in terms of kVp accuracy and exposure linearity.

Some studies have reported failure in QC tests of X-ray equipment. A study conducted by Khoshnazar, et al., (2013) on QC of radiography equipment in Golestan province of Iran found that 29.5 % of the equipment had kVp accuracy out of the acceptable range, 16.7 % had exposure reproducibility out of the acceptable range. It was also found 39 % of the equipment unsatisfactory on exposure linearity and 37 % showed bad timer accuracy. The conclusion was that, there was the need to perform QC test more regularly and suggested six to twelve months interval especially as X-ray equipment are aging. Regular QC tests would ensure high image quality, reduce patient radiation dose and reduce repeat examinations (Khoshnazar, et al., 2013).

Another study conducted by Oluwafisuye et al., (2010) on QC and environmental assessment of equipment used in diagnostic radiology found three X-ray equipment out of five investigated with an unacceptable result on kVp accuracy, and kVp consistency (Oluwafisoye et al., 2010). In Ghana, QC tests are periodically conducted by NRA for renewal of license. However, other professionals like servicing engineers and radiographers also perform some QC tests. Performing QC tests on X-ray equipment once within three years as the case in most diagnostic radiography departments in Ghana would not achieve the maximum benefits from QC.

4.3 Entrance Skin Dose [mGy]

Entrance skin dose survey was conducted for nine (9) radiographic examinations in five (5) diagnostic facilities. The results are presented in Table 4.3 which shows average and standard deviations of ESDs for each

radiological examination. The results demonstrated differences in ESD for all considered examinations. For chest PA, HP3 recorded the highest ESD with an average of 1.77 ± 0.25 mGy while HP5 recorded the lowest ESD with an average of 0.19 ± 0.07 mGy. The radiographic examination with highest ESD was lumbar spine LAT of 4.64 ± 0.89 mGy at HP3.

Table 4.3: ESD [mGy] of Nine Radiological Examinations at HP1, HP2 HP3, HP4 and HP5

Examination/ Projections	HP1 ESD [mGy] Average (SD)	HP2 ESD [mGy] Average (SD)	HP3 ESD [mGy] Average (SD)	HP4 ESD [mGy] Average (SD	HP5 ESD [mGy] Average (SD)
Chest PA	0.37± 0.14	0.67 ± 0.16	1.77 ± 0.25	0.30 ± 0.09	0.19 ± 0.07
Lumbar spine AP	3.57± 0.71	2.80 ± 0.78	2.77 ± 0.60	1.90 ± 1.86	1.35 ± 0.33
Lumbar spine LAT	4.42± 0.96	4.32 ± 1.04	4.64 ± 0.89	2.84 ± 1.78	2.63 ± 1.01
Cervical spine AP	0.35± 0.03	0.42 ± 0.07	1.04 ± 0.19	0.33 ± 0.04	0.25 ± 0.09
Cervical spine LAT	0.39± 0.05	0.42 ± 0.09	1.07 ± 0.16	0.37 ± 0.05	0.23 ± 0.04
Skull PA	2.13± 0.20	1.43 ± 0.35	1.73 ± 0.17	1.03 ± 0.17	0.56 ± 0.25
Skull LAT	1.96 ± 0.1	1.33 ± 0.29	1.66 ± 0.16	0.99 ± 0.15	0.51 ± 0.23
Pelvis AP	2.16± 0.49	2.74 ± 0.43	1.95 ± 0,37	1.03 ± 0.39	0.83 ± 0.50
Abdomen AP	3.57± 1.55	2.34 ± 0.23	2.46 ± 0.48	1.48 ± 0.31	0.92 ± 0.57

Figure 4.7 illustrates a comparison of the ESD of individual examinations among the participating hospitals. It could be seen that HP5 recorded the lowest ESD in all the radiographic examinations while HP4 also recorded second lowest ESD in all the examinations. It must be noted that, the X-ray equipment at HP5 was direct digital radiography operated with

AEC. The X-ray equipment at HP4 was CR operated with AEC while the X-ray equipment at HP1, HP2, and HP3 were CR operated without AEC. Direct digital radiography has been found to produce lower patient radiation dose as compared to CR due to the higher sensitivity of its detectors to radiation (Aldrich, Duran, Dunlop, & Mayo, 2006: Compagnone et al., 2006). Aldrich, et al., 2006 compared patient doses in CR, film- screen and direct digital radiography and found that CR doses in chest PA were five times higher than in screen-film. AEC helps to regulate the amount of radiation that reaches detector and thus control patient radiation dose.

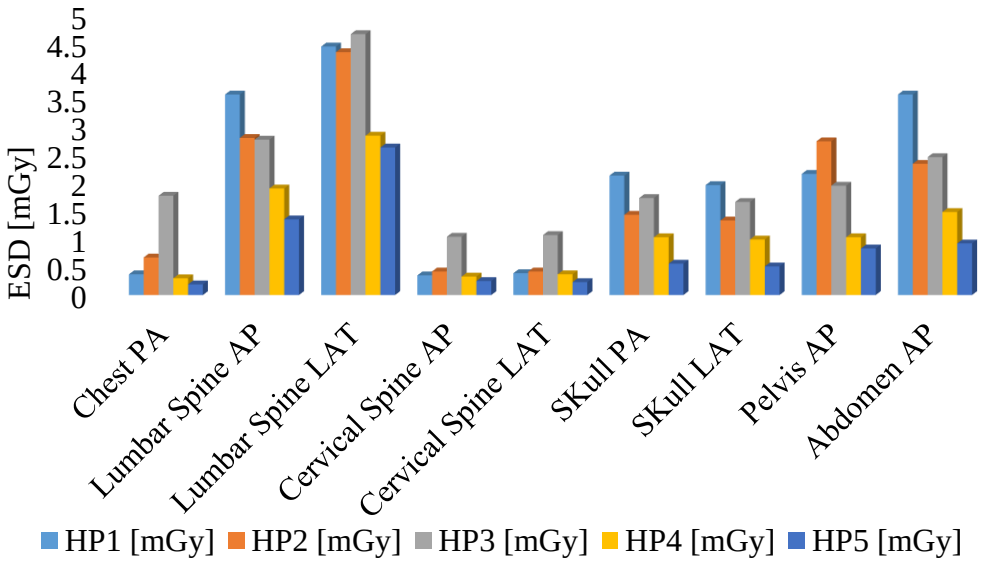

Figure 4.7: Comparison of ESDs between Hospitals HP1, HP2, HP3, HP4 and HP5.

The percentage differences in ESD for chest examinations between HP1 and HP2 was 81% while there was 375.7% variation between HP1 and HP3. When HP2 and HP3 were compared, a variation of 162.7% was observed. Lumbar spine LAT also recorded varying doses of 4.44, 4.33 and 6.08 mGy at HP1, HP2, and HP3 respectively. The causes of these variations

could be as a result of differences in X-ray machine output, technical exposure parameters (kVp, and mAs), patient thickness, focus detector distance and lack of proper quality control. In a study conducted by Yacoob and Hariwan (2016), similar observations were made in the causes of variations in ESD. The high ESD obtained at HP3 for chest PA examination was largely due to the selected exposure factors. Low V (73.4 kVp ± 2.2) with high Q (23.5 mAs ± 2.5) technique was used in the case of HP3 while HP1, HP4 and HP5 used high V with low Q technique (Tables 3.1, 3.4 and 3.5). The use of low V with high Q has been associated with increasing patient radiation dose as compared to the use of higher V with low Q (Aliasgharzadeh, Mihandoost, Masoumbeigi, Salimian, & Mohseni, 2015). Comparison between the current study and other published studies shows variations in ESD as shown in Table 4.4. For chest PA, the current study recorded highest average ESD of 0.66 ± 0.60 mGy higher than the other studies (Alameen et al., 2016; George et al., 2004; Matsumota et al., 2003). The high ESD of chest PA of this study was largely due to higher ESD at HP3 (1.77 ± 0.25 mGy).

Variations in ESD between radiographic centers are common in the practice of diagnostic radiography which have been reported by many investigators (Martin, 2007; Hart & Wall, 2002; Johnston & Brennan, 2002). One of the basic means to deal with patient dose variations in diagnostic radiography is through regular audit of patient radiation dose with purposes of optimizing the radiation dose. The practice of periodically auditing patient radiation dose is not formalized in Ghana which might contribute to these variations in patient radiation doses. Optimization of patient radiation dose in

diagnostic radiography is very necessary due to the potential radiogenic risks associated with medical exposure to ionizing radiation.

Table 4.4 shows comparison of calculated ESD [mGy] of this work with (Alameen et al., 2016, Matsumota et al., 2003 and George et al., 2004,).

Table 4.4: Comparison of Calculated ESD [mGy] with Alameen et al., 2016; Matsumota et al., 2003 and George et al., 2004

Examinations /Projections	Current study ESD [mGy]	Alameen et al., 2016 ESD [mGy]	Matsumota et al., 2003 ESD [mGy]	George et al., 2004 ESD [mGy]
Chest PA	0.66 ± 0.60	0.29	0.24	0.2
Lumbar spine AP	2.47 ± 0.8	2.72	3.95	6.7
Lumbar spine LAT	3.77 ± 0.9	4.01	10.32	20
Cervical spine AP	0.47 ± 0.3	-	-	1.3
Cervical spine LAT	0.49 ± 0.3	-	-	0.8
Skull PA	1.37 ± 0.6	2.11	-	-
Skull LAT	1.29 ± 0.5	1.29	-	1.8
Pelvis	1.74 ± 0.8	1.53	2.06	4.3
Abdomen	2.15 ±0.9	-	2.44	5.3

Note: Dash (-) means that, those radiographic examinations were not investigated.

The result of this comparison indicated differences between the current study and the previous studies (Alameen, Badrey, Abdullateaf & Ahmed, 2016; George, Eatough, Frain, Mountford, Oxtoby, & Koller, 2004; Matsumoto, Ota, Inone, Ogata, Yamanoto & Johkoh 2003). Entrance skin dose of 10.32 mGy in lumber spine LAT examination was recorded by one study (Matsumota, et

al., 2016) as against 3.77 ± 0.9 mGy in this current work and 4.01 mGy was recorded by Alameen et al., (2016).

4.4 Dose-Image Quality Optimization of Chest PA

Results on ESD, EI, inverse EI, image quality score (VGAS) and mAs of the phantom studies at 100 kVp are presented in Table 4.5. The results for 70 kVp, 80 kVp, 90 kVp, 110 kVp and 120 kVp are presented in appendix D. The highest and the lowest ESD [mGy] obtained were 0.594 mGy at 4.0 mAs and 0.237 mGy at 1.6 mAs respectively. Exposure indicator of 2767 at 1.6 mAs was obtained as the highest while 850 was obtained as the lowest EI at 4.0 mAs.

Table 4.5: Phantom Results for Chest PA at 100 kVp

mAs	ESD [mGy]	EI	Inverse EI	VGAS
1.6	0.237	2767	0.000361	0.765
2.0	0.297	2355	0.000425	0.831
2.5	0.371	1706	0.000586	0.833
3.2	0.475	1387	0.000721	0.835
3.6	0.535	1154	0.000867	0.840
4.0	0.594	565	0.0011	0.841

A graphical representation showing relationship between ESD [mGy] and mAs, for chest PA is presented in Figure 4.8.

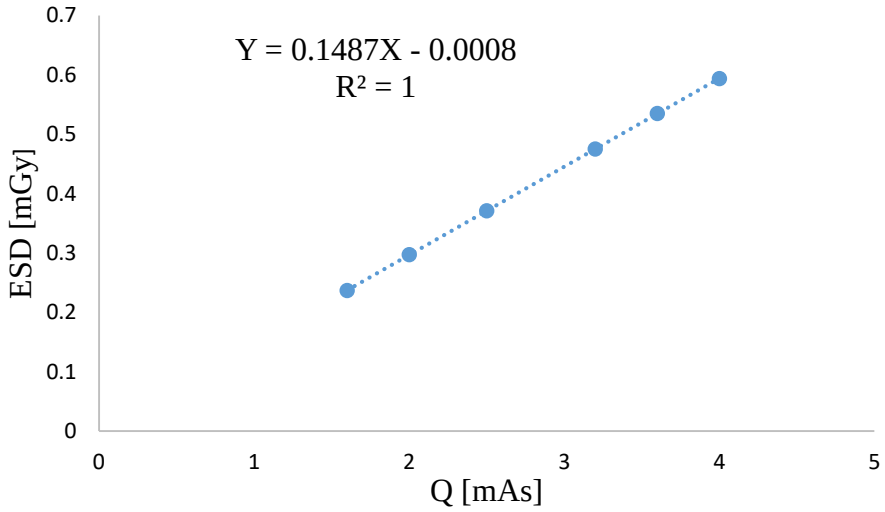

Figure 4.8: Relationship between ESD and Q at 100 kVp for Chest PA.

From Figure 4.8, as the Q increases, the ESD linearly increases as well. The minimum and maximum ESD were 0.237 and 0.594 mGy and were obtained at mAs of 1.6 and 4 respectively. There was a positive linear relationship between ESD and quantity of charge with $R^2 = 1$. The linear relationship between ESD and quantity of charge was true for all the applied voltage (70, 80, 90, 110, 120 kVp) investigated in this study. This means that as Q increases, ESD also increases proportionately in chest PA examinations. Equation 4.6 describes this relationship at 100 kVp with $R^2 = 1$:

$$Y = 0.1487X - 0.0008 \qquad 4.6$$

where Y represents ESD and X represents quantity of charge.

In CR systems mAs plays a significant role in radiographic image acquisition. The number of photons generated by an X-ray tube is determined by the value of Q. Higher Q increases patient radiation dose while lower Q appears as noise on radiographic images which sometimes cannot be processed using post processing algorithm and therefore requires retake. Retake examinations cause

overexposure. The selection of mAs for chest PA must be balanced with patient radiation dose and image quality.

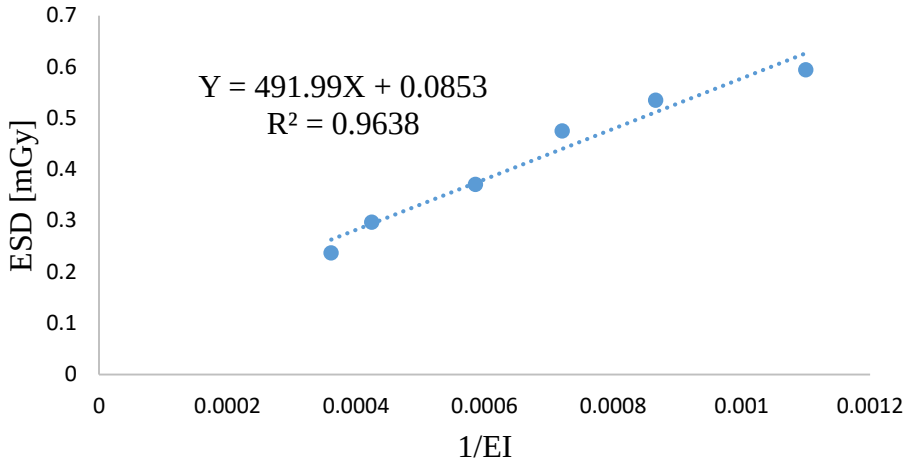

Figure 4.9: Relationship between ESD and 1/EI at 100 kVp for Chest PA

From Figure 4.9, ESD increases linearly with inverse EI for Fuji CR detector. This means that, high EIs correspond to low ESDs while low EIs indicate higher ESD as shown. Again, this relationship is true for all values of the applied voltage investigated in this study for chest PA. Equation 4.7 describes this linear relationship at 100 kVp.

$$Y = 491.99X + 0.0853 \qquad 4.7$$

where Y represents ESD and X is inverse of exposure indicator. The correlation factor of this equation was $R^2 = 0.9638$.

Exposure indicator was introduced in CR systems to serve as feedback to radiographers and technologists regarding the exposure to the detector. It describes image quality without any known relationship to ESD. However, equation 4.7 would be very useful in estimating ESD from EI for chest PA examination when performed at FFD of 150 cm, on average body thickness of

23 cm. Equation 4.7 can be easily implemented since EI values are readily available on each image.

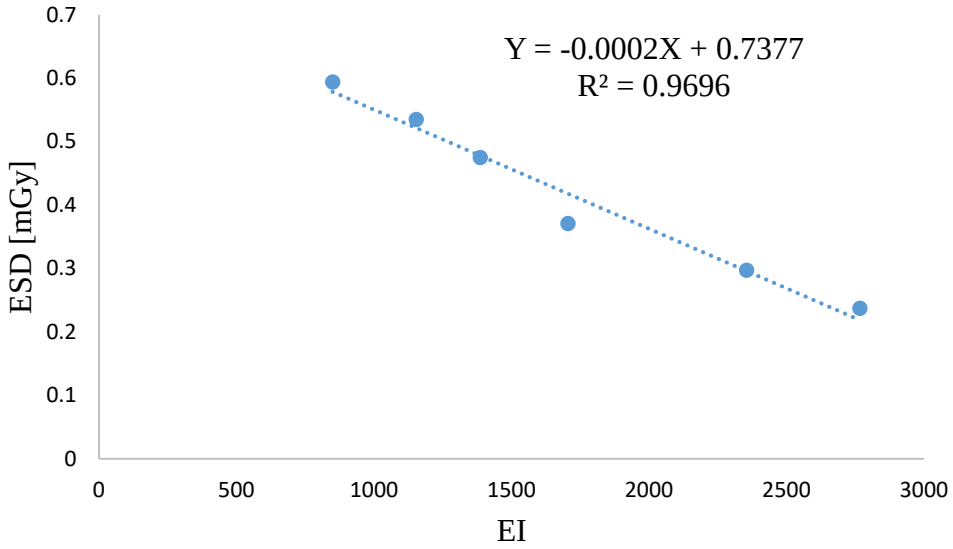

Figure 4.10: Relationship between ESD and EI at 100 kVp for Chest PA.

Figure 4.10 shows that ESD increases as EI decreases with a negative slope. The essence of Figure 4.10 is that, though it is the inverse EI that has direct relationship with ESD, it is rather the actual EIs that are indicated on the images and therefore, the relationship of the actual EI and ESD must be well understood in other to optimize its use. To avoid this confusion, it would have been better if Fuji technology had used the algorithm that would display inverse EI which has positive direct relationship rather than the actual EI. Notwithstanding this challenge, radiographers and technologists must abreast themselves with the relationship between EI and ESD to help reduce patient radiation dose.

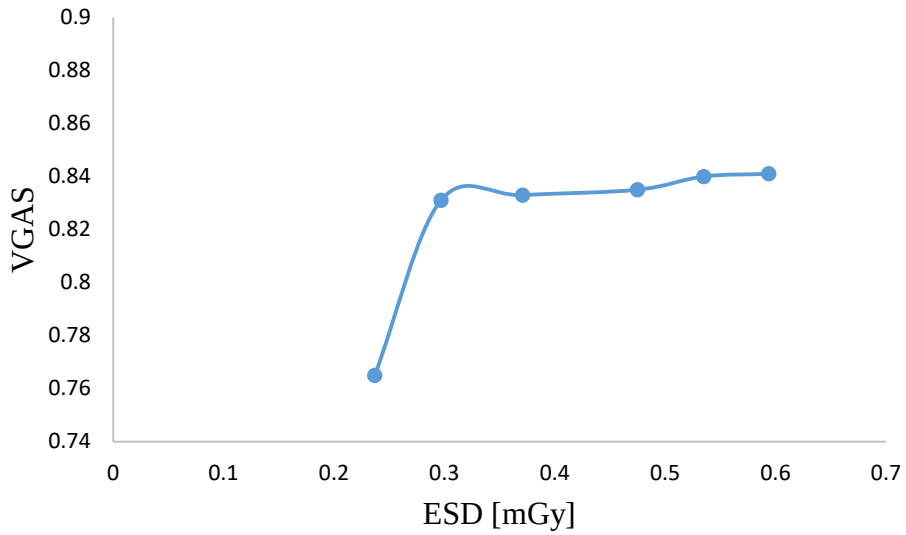

Figure 4.11: Relationship between VGAS and ESD at 100 kVp for Chest PA.

Figure 4.11 compares the relationship between image quality in the form of VGAS and ESD. Image quality increases with ESD [mGy], from 0.765 to 0.841. The highest image quality was obtained at 0.841 which corresponds to 0.594 mGy and lowest image quality was obtained at 0.765 which also correspond to 0.237 mGy.

In diagnostic radiography, image quality and patient radiation dose are the two most important parameters that must be considered whenever performing any examination. Acceptable image quality improves patient diagnosis and management within reasonable time. The main factors that influences image quality and ESD are the applied voltage and quantity of charge, although other factors such as filtration, collimation, focus-source to detector distance, thickness of the body and positioning could influence patient radiation dose and image quality (England et al., 2015). In this regard, any optimization protocols in radiography must be balanced by image quality and ESD.

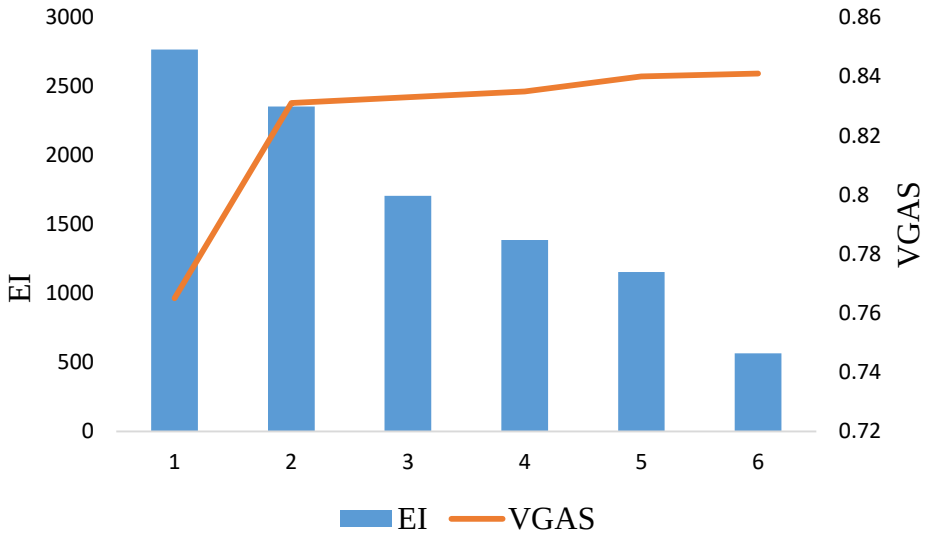

Figure 4.12: Comparison of VGAS and EI at 100 kVp for Chest PA.

Figure 4.12 compares VGAS and EI and shows that image quality increases as the EI decreases. High image quality of 0.841 corresponding to EI of 565 and the low image quality of 0.765 corresponding to EI of 2767 were obtained for the chest PA examination. In CR systems, decrease in EI values means that more radiation is getting to the detector. In CR systems, image quality increases with increasing radiation dose until the saturation limit of the detector is reached. On the other hand, low radiations reaching the detector degrade the image quality with a lot of noise. Noise on radiographic images mask out subtle structures and pathological process leading to poor diagnosis. Figure 4.13 shows a chest PA radiograph acquired on optimal exposure parameters from anthropomorphic phantom.

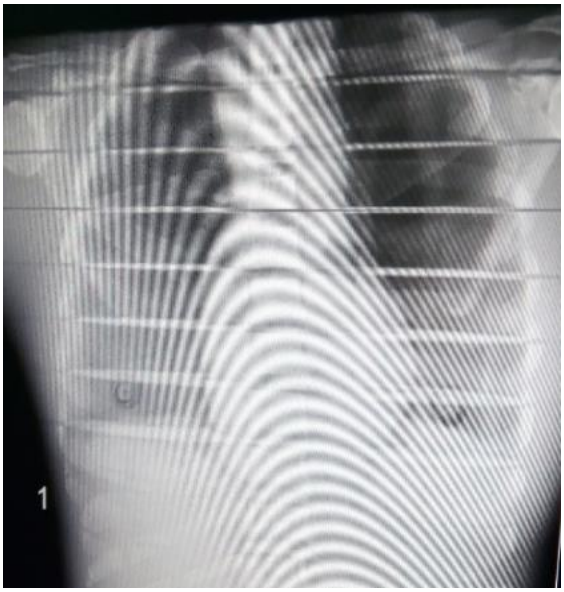

Figure 4.13: Image Showing Chest PA Acquired from Rando Female Anthropomorphic Phantom at 100 kVp, 2 mAs, ESD = 0.297, EI = 2355.

Figure 4.14 shows combination of ESD, VGAS and kVp for chest PA from anthropomorphic phantom studies. Figure 4.14 was developed for determination of optimal exposure parameters for chest PA examinations.

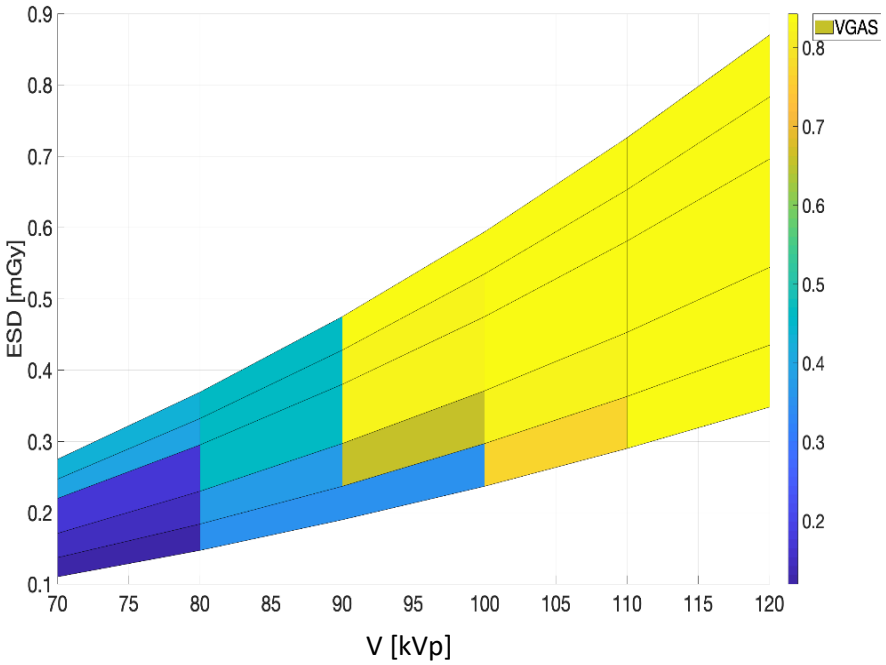

Figure 4.14: Applied Voltage, ESD and VGAS Comparison for Chest PA. Deep Blue is Very Low VGAs, Sea Blue is Low VGAs, Light Yellow is High VGAs and Deep Yellow is Very High VGAs.

From Figure 4.14, deep blue, sea blue, light yellow and deep yellow regions show very low, low, high and very high values of VGAs, respectively. At 70 kVp, there were very low values of VGAS for all values of ESD [mGy] as indicated in the deep blue region. At 80 kVp, low VGAS values were recorded for all values of ESD [mGy] as indicated by the sea blue region. At 90 kVp and 100 kVp higher VGAS values were obtained from 0.297 mGy and above while higher values of VGAS were obtained for all values of ESD [mGy] at 110 and 120 kVp as indicated by the yellow region. Applied voltage and Q combinations to obtain acceptable image quality is shown in Figure 4.15.

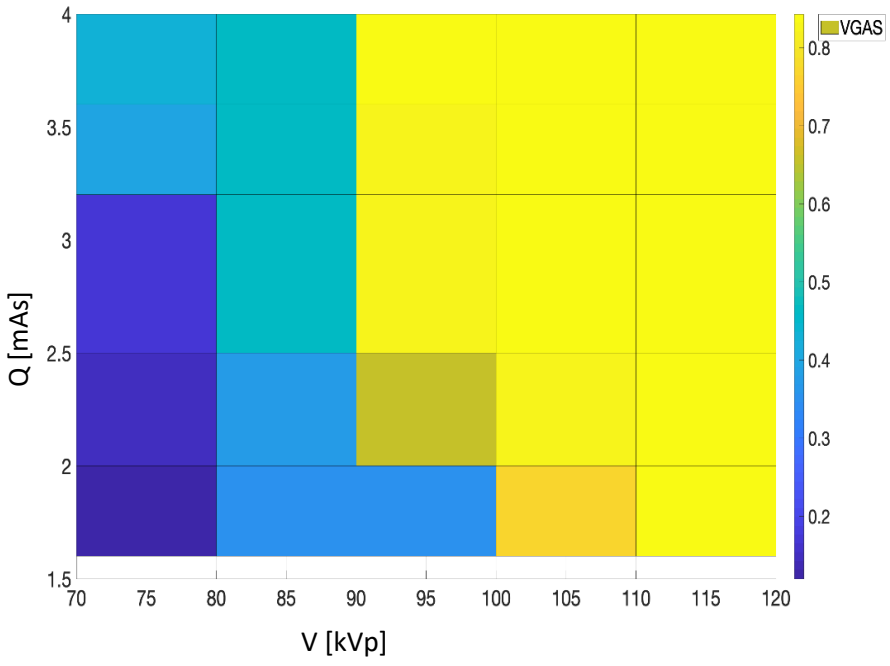

Figure 4.15: Applied Voltage and Q Combinations to Obtain Acceptable VGAS for Chest PA. Deep Blue is Very Low VGAs, Sea Blue is Low VGAs, Light Yellow is High VGAs and Deep Yellow is Very High VGAs.

Again, the deep blue, sea blue and yellow represent very low, low and higher VGAS respectively. All the values of mAs (1.6 – 4.0 mAs) at 70 kVp recorded very low values of VGAS as indicated in the deep blue region. At 80 kVp, all the combinations of Q produced low values of VGAS as indicated by the sea blue region. At 90 kVp higher values of VGAS were recorded from 2.5 mAs and higher values of VGAS were recorded from 2.0 mAs at 100 kVp. For 110 and 120 kVp higher values of VGAS were recorded for all values of Q.

Radiation dose to patient undergoing chest PA examination is comparatively low. However, due to the large number of chest examinations its collective dose contribution to the population is significant (Veldkamp, Kroft & Geleijns, 2009) and therefore, its optimization is very necessary.

Dose-image quality optimization for chest PA was based on clinical visualization of anatomical structures and assessment of ESD to anthropomorphic phantoms. Image quality at 70 kVp for all the values of mAs were very poor indicated by low values of VGAs. The image quality at 80 kVp for all values of mAs (1.6 - 4.0) were relatively better than that of 70 kVp but could not achieve the clinical requirement. The poor image quality at low kVps (70 and 80) could be attributed to the fact that visualization of ribs increases at low kVp and this could obscure the lungs markings. Also, visual reproduction of spine through the heart would be very poor at low kVps. Lungs vascular markings would be poorly reproduced since the ribcage will substantially attenuate the primary beam. In order to compensate for these shortcomings at low kVps, high mAs must be used. This practice would unnecessarily increase patient radiation dose and shorten tube life span due to tube overload.

Image quality at 90 kVp with mAs of 2.5 recorded high VGAS of 0.830 and ESD of 0.297 mGy. The highest image quality of 0.840 was obtained at 120 kVp with 4.0 mAs (Appendix 2). The difference between the image quality score of 0.830 and 0.840 was 1.1 % and the difference in ESD for same image quality was 64.6%. This means that diagnostic information that could be obtained from these two images might not differ. The low percentage difference in image quality score is an indication that, in CR systems image quality does not increase significantly after the detector had received enough dose for acceptable image quality. Overexposure of 64.6 % could be possible in CR chest PA examinations for the technical parameters investigated. However, higher overexposure than 64.6% is possible when technical factors selected are wider from those investigated. Similar observations have been made by (Lorusso et al 2015). Lorusso, et al., 2015 compared image quality at 120 kVp, 140 kVp and 150 kVp and the conclusion was that, there was no difference in image quality for these values of V and thus ESD reduction of 72% was possible in chest PA examinations.

From Figures 4.14 and 4.15, optimal exposure factors for chest PA examinations for body thickness of 23 cm would be 90 kVp, 2.5 mAs, 100 kVp 2.0 mAs and 110 kVp, 1.6 mAs with ESD of 0.297 mGy. A study conducted by Doyle et al, 2005 partly agreed with this current study. Chest PA examination was optimized using SNR to assess image quality and concluded that optimal SNR was obtained at 90 and 100kVp. However, Q was not optimized and therefore no optimal values for Q was reported as in this current study (Doyle, Martin & Gently, 2005).

The average ESD of chest PA examination for HP3 (study center for this work) was 1.88 mGy while the optimized ESD from this work was 0.29 mGy (Tables 4.8 & 4.9). This means that ESD reduction of 84.5% was achieved after dose-image quality optimization. Another study achieved ESD reduction of 77% after dose-image quality optimization in chest PA examination (Korir, 2010). Another study that optimized chest PA examination in terms of SNR indicated that Q affects noise more than V, thus it was possible to reduce V from 120 to 100 kVp without losing diagnostic information and achieved 44% reduction in patient radiation dose (Sun, Lin, Tyan, Hoong, 2012). The large possibility of dose reduction in chest PA examinations confirmed that overexposure of patient in CR systems is more obvious and that proper optimization protocols should be established by the radiographic facilities.

4.5 Dose-Image Quality Optimization of Lumbar Spine AP

Results on ESD, EI, inverse EI and Q of the anthropomorphic phantom studies at 70 kVp are presented in Table 4.6. The results for 80 kVp, 90 kVp, and 100 kVp are presented in Appendix B.

Table 4.6: Phantom Results for Lumbar Spine AP at 70 kVp

Quantity of charge [mAs]	ESD [mGy]	EI	Inverse EI	VGAS
16	1.411	592	0.001689	0.601
18	1.586	527	0.001897	0.634
20	1.762	515	0.001472	0.745
22	1.941	679	0.001897	0.847
25	2.203	527	0.001769	0.846
28	2.467	565	0.002444	0.846
32	2.819	409	0.003533	0.848
36	3.172	283	0.003968	0.848
40	3.524	252	0.003968	0.845
45	3.965	225	0.004444	0.849
50	4.406	241	0.004149	0.852

The highest ESD, EI and VGAS obtained were 4.406 mGy, 679, and 0.855 respectively. The lowest ESD, EI and VGAS were 1.411 mGy, 225 and 0.545 respectively.

Lumbar spine AP examinations are the second most frequently performed radiographic examinations after chest radiography (Korir et al., 2010; Wambani et al., 2015). The dose received by patients undergoing lumbar spine examinations are however higher than chest examinations according to published literature (Wambani et al., 2015; Minaei, Firouzi & Khosravi, 2014). For this reason, optimizing exposure factors for lumbar spine AP examinations is very crucial in patient radiation protection in diagnostic radiography.

The relationship between ESD and quantity of charge at 70 kVp for lumbar spine AP is shown in Figure 4.16

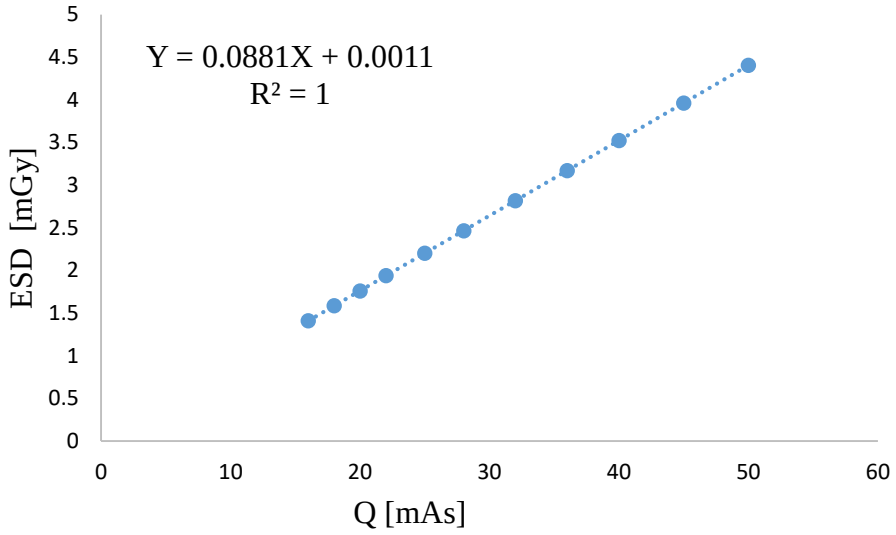

Figure 4.16: Relationship between ESD and Q for Lumbar Spine AP at 70 kVp.

Figure 4.16, shows positive linear relationship between ESD and quantity of charge for lumbar spine AP examination with strong positive correlation factor of $R^2 = 1$. This means that when mAs is doubled ESD will also double. This observation was consistent with similar findings by Seeram et al (Seeram et al., 2016). Quantity of charge is one of the most important exposure factors in lumbar spine AP examinations. Due to high tissue thickness around the lumbar region, more Q are required to produce acceptable radiographs for lumbar spine examination and this explains why ESD is higher in lumbar spine AP examinations. Selection of Q for lumbar spine AP examinations must be carefully done to avoid overexposure of the patient. Equation 4.8 describes this linear relationship at 70 kVp for lumbar spine AP:

$$Y = 0.0881 + 0.0011 \qquad 4.8$$

where Y represents ESD and X represents Q.

Each lumbar spine AP image has its EI value indicating the amount of radiation dose to the detector. Figure 4.17 shows relationship between ESD and inverse of EI for the lumbar spine AP examination.

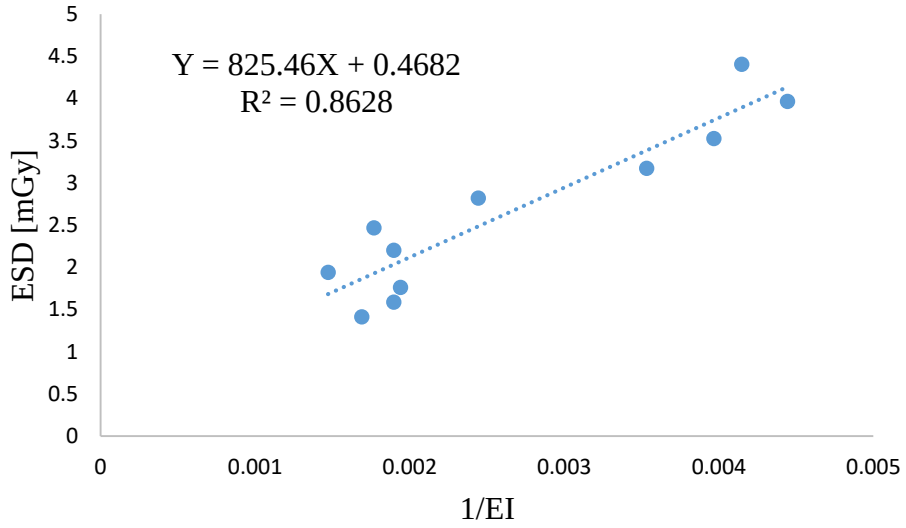

Figure 4.17: Relationship between ESD and 1/EI for Lumbar Spine AP at 70 kVp

Figure 4.17 shows direct linear relationship between ESD and inverse of EI with positive slope of 825.46 and correlation factor of $R^2 = 0.8628$. Thus confirming the inverse relationship between EI and ESD. In a study conducted by (Seeram et al., (2016) on optimizing the EI as dose management strategy in CR for pelvic and lumbar spine examinations, they found similar relationship between ESD and inverse EI. The equation 4.9 describes this relationship:

$$Y = 825.46X + 0.4682 \qquad 4.9$$

where Y = ESD [mGy] and X= inverse of EI.

Figure 4.18 shows relationship between ESD and the EI values for lumbar spine AP examination.

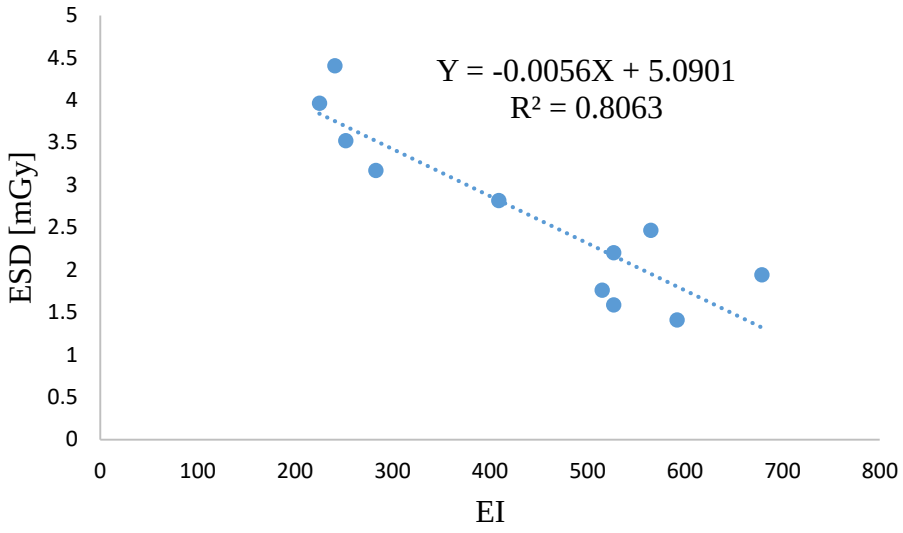

Figure 4.18: Relationship between ESD and EI for Lumbar Spine AP at 70 kVp

Figure 4.18 shows that as ESD increases, the EI decreases and that there was an inverse relationship existing between ESD and EI with correlation factor of $R^2 = 0.8063$. The equation 4.10 describes this relationship and shows a negative slope of 0.0056 confirming the inverse relationship between ESD and EI.

$$Y = -0.0056X + 5.0901 \qquad 4.10$$

where Y = ESD and X = exposure indicator (EI).

EI values have no direct relationship with patient radiation dose, but are an indication of how the detector is being exposed and therefore, deductions from that show how patients are also exposed. Lower values of EI indicated that more radiation dose is reaching the detector while higher EI values indicated that less radiation dose is reaching the detector. This could provide an assumption on either the patients are over exposed or under exposed. Equations 4.9 and 4.10 would be useful in relating EI values to the ESD for radiographers and technologists to have better idea of ESD to patients in lumbar spine AP examination.

The relationship between image quality and ESD was also investigated and the result is shown in Figure 4.19.

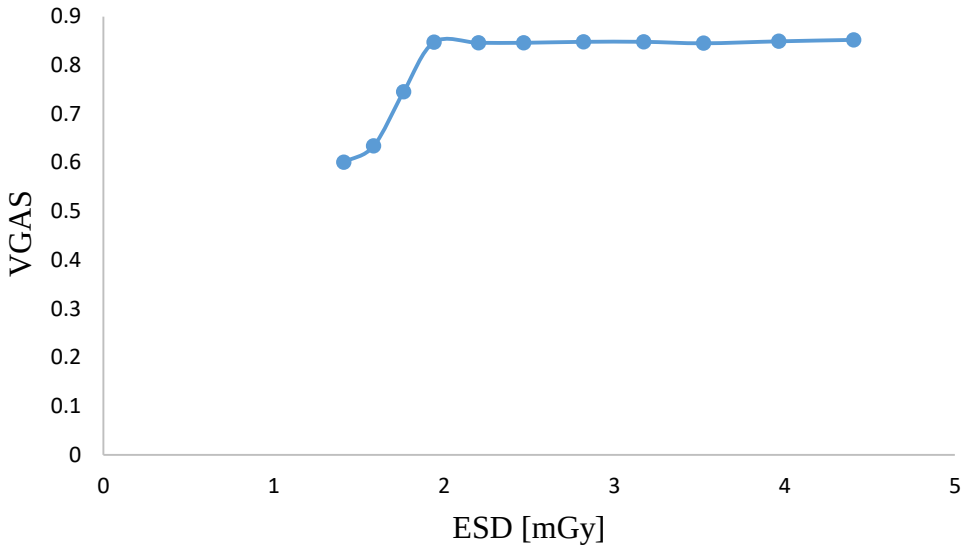

Figure 4.19: Relationship between VGAS and ESD for Lumbar Spine AP at 70 kVp.

Image quality increases with ESD from 0.601 at 1.411 mGy to 0.852 at 4.406 mGy. However, there was no significant variations from 0.847 at 1.941 mGy to 0.852 at 4.406 mGy. From Figure 4.19, Image quality increases as ESD increase until VGAS of 0.847 and 1.94 mGy. Between 1.94 mGy and 4.4 mGy image quality gradually increased to the maximum of 0.852. The image quality score between 1.94 mGy and 4.406 mGy (0.847 – 0.852) varies by 0. 58 %. In terms of visibility of diagnostic information there was no obvious difference between these two-image quality scores. This means that, in CR technology, when sufficient dose for producing acceptable image quality is reached, there is no significant change in image quality with increase in radiation dose for lumbar spine AP examination.

EI and image quality were compared to understand how image quality relates to EI in diagnostic radiograph of lumbar spine AP examinations as shown in Figure 4.20.

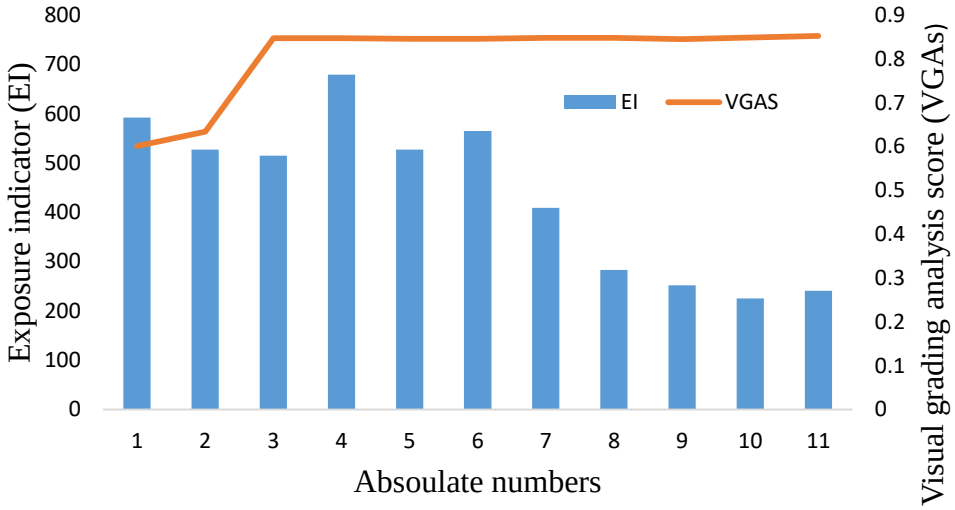

Figure 4.20: Comparison between VGAS and EI for Lumbar Spine AP at 70 kVp.

The comparison between image quality and EI generally shows that image quality increases with decrease in EI for lumbar spine AP examination. This is because in CR systems image quality improves with increasing radiation dose to the detector. However, due to inverse relationship between EI and dose to the detector, EI values would decrease as more radiation reach the detector.

To obtain the optimal V with acceptable ESD from all the investigated values of V for lumbar spine AP examination, Figure 4.21 was developed.

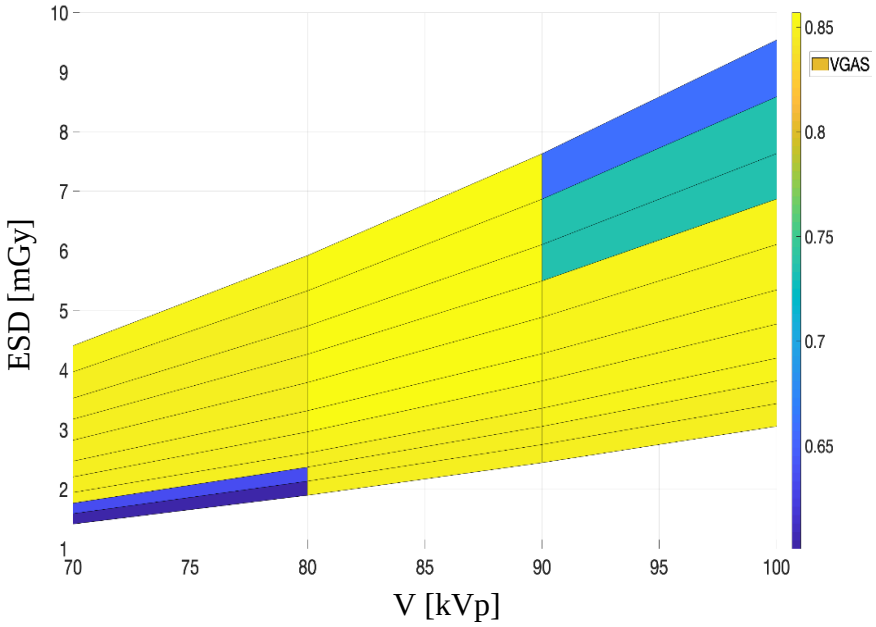

Figure 4.21: V, ESD and VGAS Comparison for Lumbar Spine AP. Deep Blue is Very Low VGAs, Sea Blue is Low VGAs, Light Yellow is High VGAs and Deep Yellow is Very High VGAs

Figure 4.21 shows a relationship between ESD, V and VGAS for lumbar spine AP. The deep blue, sea blue, light blue, and yellow colours represent very low, low, high and very high VGAS respectively. At 70 kVp, very low and low VGAS were recorded from 1.411 mGy up to 1.7941 mGy while very high VGAS were recorded from 1.941 mGy. All values of ESD at 80 kVp recorded very high values of VGAS. At 90 and 100 kVp very high VGAS were recorded up to 4.88 mGy, and low VGAS occurred from 5.341 mGy. In order to determine acceptable optimal exposure factors without degrading the image quality, the effect of V and Q on image quality was modelled as shown in Figure 4.22.

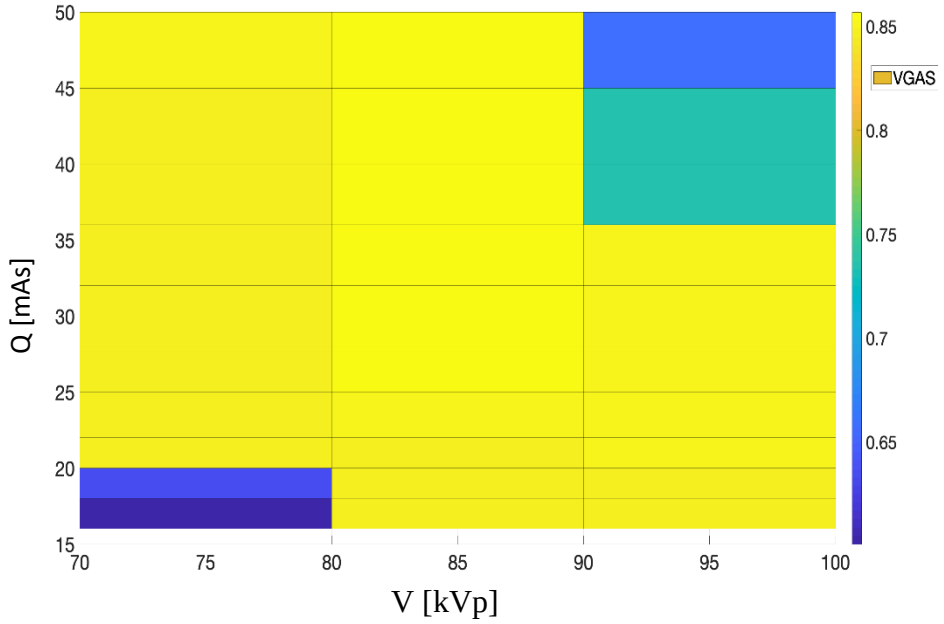

Figure 4.22: V, Q Combinations to Obtain Acceptable VGAS for Lumbar Spine AP. Deep Blue is Very Low VGAS, Sea Blue is Low VGAS, Light Yellow is High VGAs and Deep Yellow is Very High VGAS

From Figure 4.22, the deep blue, sea blue, light blue, and yellow colours represent very low, low, high and very high VGAS respectively. At 70 kVp, very low and low values of VGAS were recorded from 16 to 20 mAs. At 80 kVp, all the combinations of mAs produced very high values of VGAS. At 90 and 100 kVp very high values of VGAS were recorded from 16 to 35 mAs. However, VGAS values decreased beyond 35 mAs.

From Figure 4.22, the highest image quality was recorded at 4.88 mGy with VGAS of 0.852. The image quality score then decreased from 0.736 to 0.656 with increasing ESD from 5.327 to 9.537 mGy respectively. This may be as a result of poor absorption of photons by the detector as higher energy reaches it, or as the saturation limit of the detector is being reached. Attenuation of X-ray decreases as its energy increases because it less interacts

with the medium at higher energy levels which might account for poor image quality at higher ESD values.

At 70 kVp and 22 mAs, the VGAS recorded was 0.847 while the highest VGAS was 0.852 at 100 kVp and 25 mAs. The ESD at VGAS of 0.847 was 1.941 mGy while the ESD [mGy] for the highest VGAS was 4.88 mGy. The wider range in ESD of 60% (1.941 – 4.882 mGy) with small change in image quality (0.58%) means that, ESD of 1.941 mGy could produce image quality with same diagnostic information as that of 4.882 mGy. Therefore, exposure factors that produced ESD of 1.941 mGy could be accepted as optimal parameters that would produce an acceptable image quality for maximum diagnostic information with minimum dose in line with ALARA principle. 70 kVp and 22 mAs were then accepted as optimal exposure factors for standard body size lumbar spine AP examinations in CR diagnostic radiography. From Figure 4.22, there were no low values of VGAS at 80, 90, and 100 kVp for all the mAs investigated. Therefore, it could be possible that below 16 mAs sufficient image quality could be obtained at 80, 90 and 100 kVp.

90 kVp and 40 mAs that generated ESD of 4.882 mGy could produce acceptable image quality for diagnosis but may not be recommended in terms of patient radiation safety. Again, it would not be necessary to use 100 kVp for lumbar spine AP on 16 mAs upwards, since dose of 1.941 mGy is enough to produce acceptable image quality for lumbar spine AP. Applied voltage must be carefully combined with appropriate Q in order to achieve reasonable radiation dose. The wider ESD range with insignificant change in image quality is an obvious indication that 60% overexposure of patients is possible

in diagnostic radiography examinations of lumbar spine AP if proper optimization protocol is not instituted. The selection of exposure factors for the examination is very critical in ensuring patient radiation safety. Inappropriate selection of these exposure factors could adversely affect image quality and patient radiation dose (Akpochafor et al., 2016).

In comparison of the optimal exposure factors (70 kVp, 22 mAs) with the study center's average exposure factors (74 kVp, 28 mAs), patient radiation dose reduction of 29.3 % was achieved.

Different studies have published different exposure factors for lumbar spine AP examinations (Naji, Jaafar, Ali, & Al-Ani, 2017: Massoud & Diab 2014: Ofori et al., 2014). These studies reported kVp ranges from 60 kVp to 95 kVp with varying mAs from 10 to 120 mAs. Another study conducted by Korir et al.,2010 which optimized lumbar spine AP by comparing film-screen speed of 200 and 400 reported an optimal exposure factors of 73 kVp and 21 mAs. Reduction of 72% in patient radiation dose was achieved by changing from 200 speed screen-film to 400 speed screen-film (Korir et al., 2010). Another study carried out by (Naji et al., 2017) observed that, 70 kVp has higher energy to provide more penetrability for X-ray photons and provides optimum contrast when range of kVps (50 – 110 kVp) were compared using aluminum step wedge. The anthropomorphic phantom image acquired on the optimal exposure factors (70 kVp, 22 mAs) is shown in Figure 4.23.

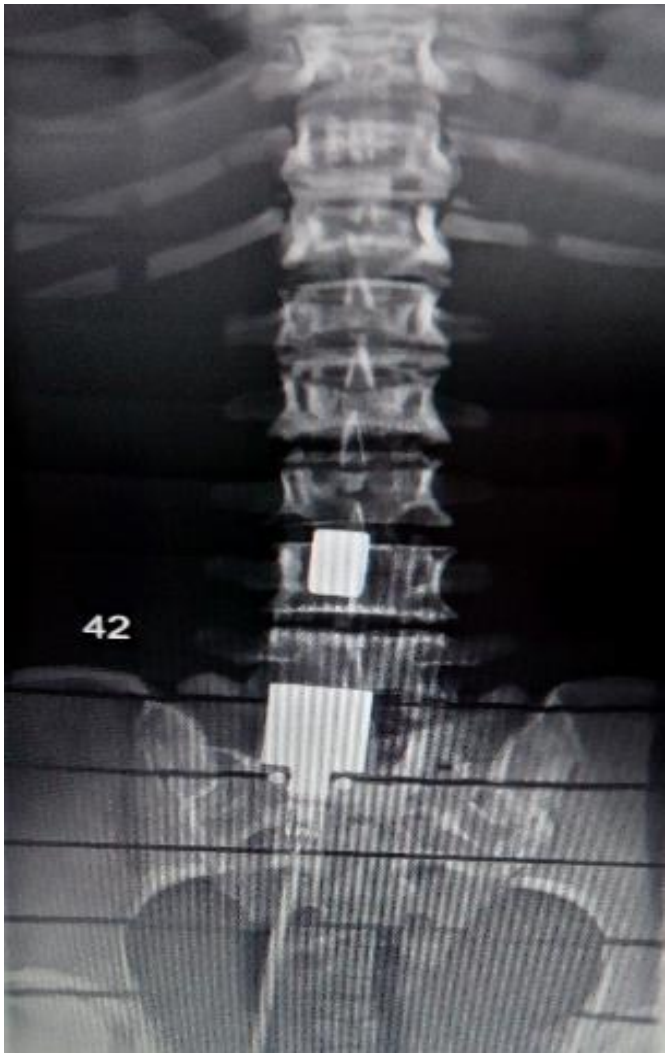

Figure 4.23: Image Showing Lumbar Spine AP Acquired from Rando Female Anthropomorphic Phantom at 70 kVp, 22 mAs, ESD = 1.94 mGy, EI = 679.

4.6 Dose-Image Quality Optimization of Lumbar Spine LAT

Results on EI, inverse EI and Q of the phantom studies at 80 kVp are presented in Table 4.7. The results for 70 kVp, 90 kVp, and 100 kVp are presented in Appendix C.

Table 4.7: Phantom Results for Lumbar Spine LAT at 80 kVp

mAs	ESD (mGy)	EI	Inverse EI	VGAS
16	2.050	2099	0.0004764	0.565
18	2.307	2148	0.0004655	0.575
20	2.563	2005	0.0004987	0.652
22	2.820	1236	0.0008096	0.682
25	3.204	1005	0.0009951	0.853
28	3.589	1236	0.0008096	0.855
32	4.101	695	0.0014388	0.857
36	4.614	711	0.0014064	0.860
40	5.127	649	0.0015408	0.865
45	5.768	679	0.0014727	0.865
50	6.409	504	0.0019841	0.865

The highest ESD, EI and VGAS obtained were 6.409 mGy, 2148, and 0.865 respectively. The lowest ESD, EI and VGAS were 2.050 mGy, 504 and 0.565 respectively. To investigate how mAs varies with ESD for lumbar spine LAT examination, a plot of ESD against mAs was obtained as shown in Figure 4.24.

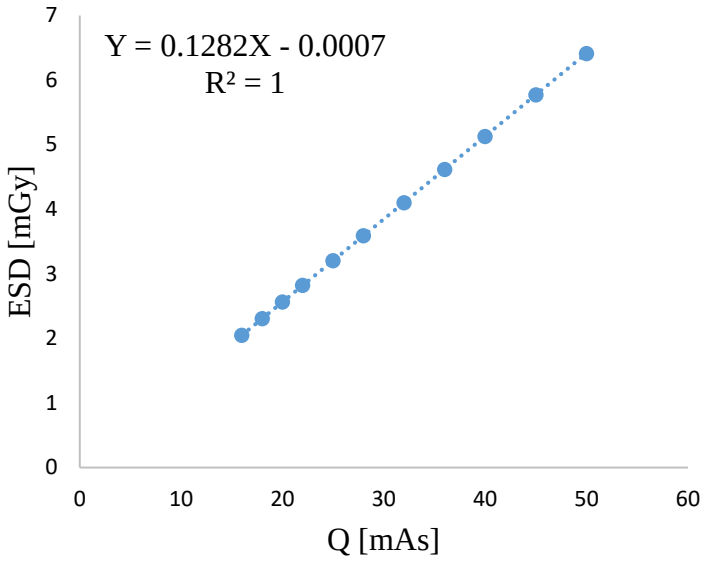

Figure 4.24: Relationship between ESD and Q for Lumbar Spine LAT at 80 kVp.

Figure 4.24 shows that as Q increases, ESD also increases proportionately and therefore there was a direct linear relationship between Q and ESD for lumbar spine LAT examinations. Equation 4.11 describes this linear relationship for lumbar spine LAT with strong correlational factor of $R^2 = 1$.

$$Y = 0.1282X - 0.0007 \qquad 4.11$$

where Y represents ESD, and X represents Q.

This means that selection of mAs for this examination plays an important role regarding patient radiation dose. Overexposure or underexposure of patients would significantly depend on the value of Q that would be selected. For this reason, optimizing Q to obtain optimal values for lumbar spine examination should be considered as an important tool to avoid overexposure of patients who undergo lumbar spine examinations. Radiation dose to patients undergoing lumbar spine LAT examination is relatively higher than chest PA and lumbar spine AP due to larger tissue thickness and that Q

selection should be done properly to ensure that optimal diagnostic information can be obtained. Inappropriate selection of Q colud influence the quality of diagnostic information being sought for and delays treatment of the patient. Knowledge of how Q relates to patient radiation dose is therefore useful to be able to determine appropriate Q that could achieve an acceptable image.

A plot of ESD against inverse EI was obtained as shown in Figure 4.25 to further investigate the inverse relation between EI and ESD for lumbar spine LAT examination.

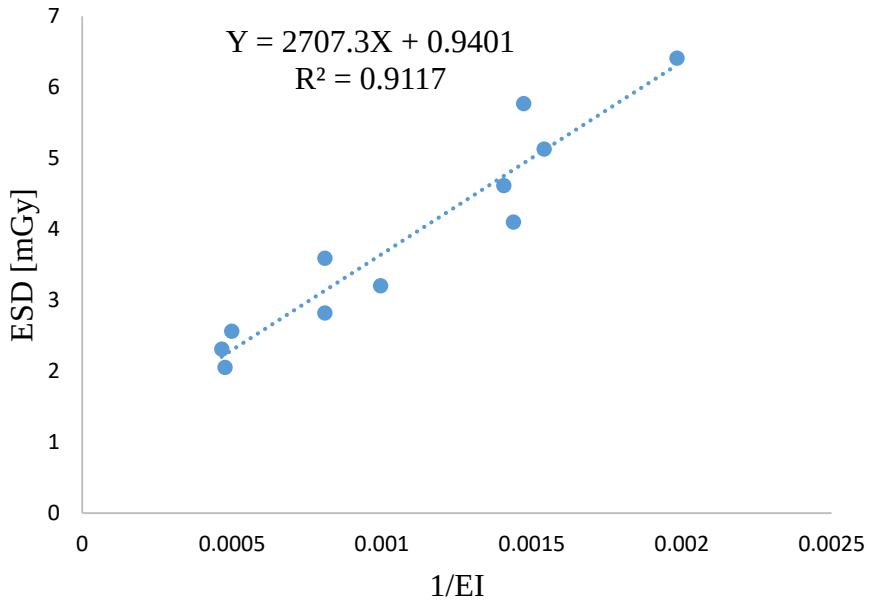

Figure 4.25: Relationship between ESD and 1/EI for Lumbar Spine LAT at 80 kVp.

From Figure 4.25, as ESD increases, the inverse EI directly increases and thus confirming the inverse relationship between ESD and EI. There was a positive slope of 2707.3 with correlational factor of $R^2 = 0.9117$. Equation 4.12 describes this relationship:

$$Y = 2707.3X + 0.9401 \qquad 4.12$$

where Y = ESD and X= 1/EI.

Optimizing EI values could be a useful tool for radiation protection in diagnostic radiography because it relates to both patient radiation and image quality. Thus optimizing EI values would indirectly optimize the factors that mainly affect image quality and patient radiation dose (V, Q). This is why properly understanding the EI values is very important in diagnostic radiography examination of lumbar spine LAT.

To investigate the relationship between ESD and EI, a plot of ESD against EI was obtained as shown in Figure 4.26.

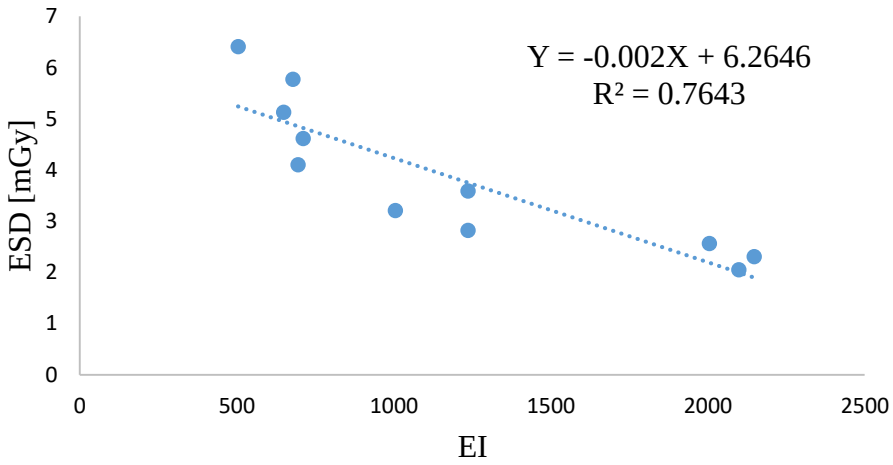

Figure 4.26: Relationship between ESD and EI for Lumbar Spine LAT at 80 kVp.

From Figure 4.26, as ESD increases, EI decreases with a negative slope of 0.002. This means that there is inverse relationship between EI and ESD. The equation 4.13 describes this relationship and the correlational factor was $R^2 = 0.7643$:

$$Y = -0.002X + 6.2646 \qquad 4.13$$

where Y = ESD, and X = EI.

The significance of EI is that it provides feedback to radiographers and technologists regarding the extent of exposure to the detector, without direct information for patient radiation dose. The relationship between EI and ESD would now help radiographers and technologists to understand how patients are being exposed by looking at the EI values. Higher EI values means low ESD to patient while low values of EI indicates higher ESD to patients and thus whether patients are being overexposed or underexposed could be easily deduced from the relationship between EI and ESD. Equation 4.13 could play a useful role in estimating ESD from EI for lumbar spine LAT examinations in order to properly optimize exposure factors to avoid unnecessary radiation dose to patients. It must be however emphasized that equation 4.13 is only limited to X-ray equipment at HP3 where the study was carried out. Notwithstanding, equation 4.13 could be generated for each individual X-ray equipment.

To validate the relationship between image quality and ESD, a plot of VGAS against ESD was obtained as shown in Figure 4.27.

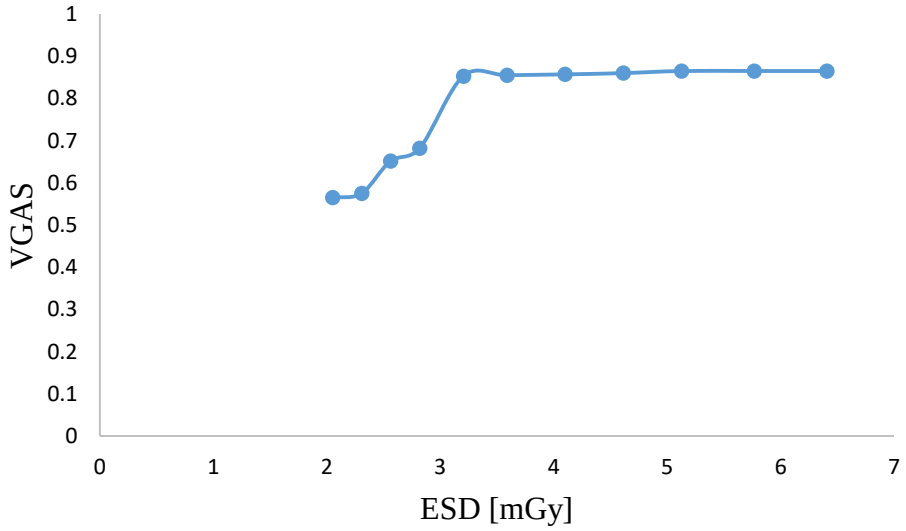

Figure 4.27: Relationship between VGAS and ESD for Lumbar spine LAT at 80 kVp.

Image quality increases with ESD from 0.565 at 2.050 mGy to 0.865 at 6.409 mGy. However, there was no significant variation from 0.853 at 3.204 mGy to 0.865 at 6.409 mGy. The image quality score between 3.204 mGy and 6.409 mGy (0.853 – 0.865) varies by 1.38 %. In terms of visibility of diagnostic information, there was no obvious difference between these two-image quality scores. This means that, in CR technology, when sufficient dose for producing acceptable image quality is reached, there is no significant change in image quality with increasing radiation dose for lumbar spine LAT examination. Image quality is very important in optimization protocols since poor image quality could delay patient treatment and unnecessarily increase patient radiation dose as well as increase in cost to the facility due to repeat of examinations. Image quality could be influenced by selection of V and Q and thus selection of these exposure factors ensure that both image quality and patient radiation dose are acceptable.

Figure 4.28 compares image quality and EI in order to establish the relationship between these two parameters.

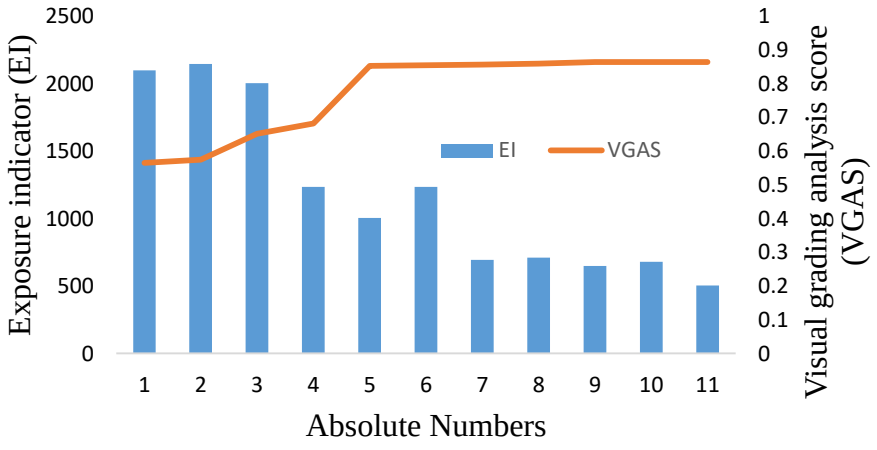

Figure 4.28: Comparison between VGAS and EI for Lumbar Spine LAT at 80 kVp.

Generally, image quality increases with decrease in EI. However, there are little deviations from the general observation in Figure 4.28. For instance, EI at point 6 was supposed to be smaller than the EI at point 5 but that did not occur. This means that EI values could be influenced by other factors which introduced this inconsistency in values.

One of these significant factors is collimation of the radiation field. In CR systems, the image processor algorithm use exposure data recognizer (EDR) in auto mode to recognize irradiated part of the image and sample that into histogram for the generation of EI. Therefore, collimation of field significantly influences the value of EI. Barker also found that collimation of radiation field has significant influence on the values of EI (Barker, 2012).

To deduce the optimal exposure factors for lumbar spine LAT examination, ESD [mGy], image quality and Q were compared as shown in Figure 4.29.

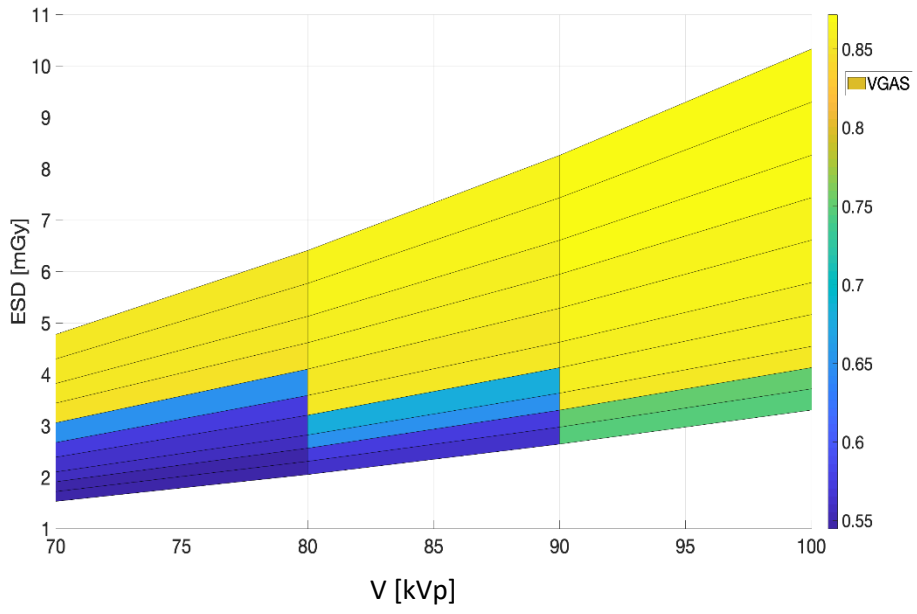

Figure 4.29: V, ESD and VGAS Comparison for Lumbar Spine LAT. Deep Blue is Very Low VGAs, Sea Blue is Low VGAs, Light Yellow is High VGAs and Deep Yellow is Very High VGAs.

The deep blue, sea blue, light green, and yellow colors represent very low, low, high and very high VGAS values respectively. At 70 kVp, very low and low VGAS were recorded from 1.52 mGy up to 3.0 mGy while very high VGAS were recorded from above 3.0 mGy. At 80 kVp, very low and low VGAS were recorded from 2.050 to 2.820 mGy while very high values of VGAS were recorded from 3.20 mGy. At 90 and 100 kVp high VGAS were recorded up to 2.0 mGy, then high VGAS was recorded from 3.30 up to 10.327 mGy.

The effect of V and Q on image quality was investigated as shown in Figure 4.30.

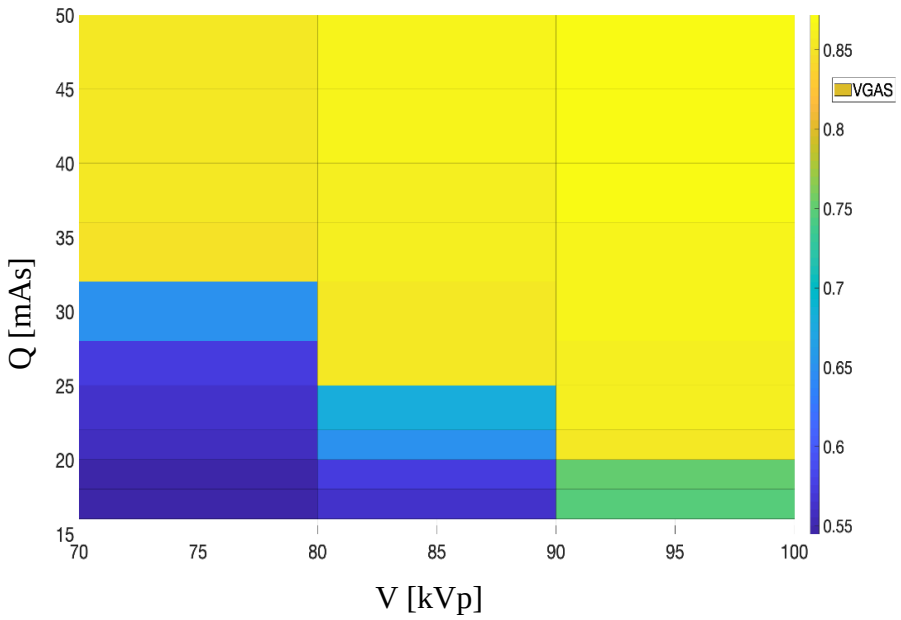

Figure 4.30: V, Q Combinations to Obtain Acceptable VGAS for Lumbar Spine LAT. Deep Blue is Very Low VGAs, Sea Blue is Low VGAs, Light Yellow is High VGAs and Deep Yellow is Very High VGAs.

The deep blue, sea blue, light green, and yellow colors represent very low, low, high and very high VGAS, respectively. At 70 kVp, very low and low values of VGAS were recorded from 16 to 32 mAs and high VGAS from

32 mAs to 50 mAs. At 80 kVp, very low and low VGAS was recorded from 16 mAs to 22 mAs and very high values of VGAS started from 25 mAs to 50 mAs. At 90 and 100 kVp very high values of VGAS were recorded from 22 mAs to 50 mAs.

From Figures 4.29 and 4.30, optimal exposure factors were found to be 80 and 90 kVp on 25 and 20 mAs, respectively. These exposure factors were found to produce high image quality score of 0.853 with acceptable ESD of 3.20 mGy. Dose reduction of 38.2% was achieved when these optimized values were compared to the average values of the study center (74 kVp, 56 mAs, and 5.34 mGy). The difference between image quality of the optimal exposure factors of 0.853 and the highest image quality score of 0.871 was 2.0%. In terms of visibility for diagnostic information there was no obvious difference between these two image quality scores. The ESD [mGy] difference between these same image quality scores was 60%. This means that in lumbar spine LAT examinations, there is possibility of 60% over exposure of patients. Therefore, in optimizing radiographic procedures, patient dose assessment must remain paramount.

Published literature on optimization of lumbar spine LAT is very limited. However, a few that were found made similar observations as the current study. In a study that optimized lumbar spine LAT using different radiographic positioning reported the optimal factors to be 80 kVp and 32 mAs with dose reduction of 83 % (Al- Qaroot, Bashar, Hogg, Peter, Twiste & Howard 2014). Another study that used different film-screen speed (200 and 400) to optimize lumbar spine LAT examination reported the optimal

exposure factors to be 80 kVp and 21 mAs with the screen-film speed of 400 (Korir, Wambani, & Ochieng, 2010).

Challenges such as unaccessibility to radiologist to be part of image quality assessment, and the scattered nature of the study areas were challenges encountered during the research. However, these challenges did not affect the results of this work.

Figure 4.31 shows lumbar spine LAT radiograph from anthropomorphic phantom that was acquired on the optimal exposure factors of 90 kVp and 20 mAs.

Figure 4.31: Image Showing Lumbar Spine LAT Acquired from Rando Female Anthropomorphic Phantom at 90 kVp, 20 mAs.

4.7 Optimal Exposure Factors for Chest PA, Lumbar Spine AP and Lumbar Spine LAT

Having compared the ESD, image quality in terms of VGAS and the EI, the exposure factors in terms of V and Q for chest PA, lumbar spine AP and lumbar spine LAT selected as optimal exposure factors are shown in Table 4.8.

Table 4.8: Optimal Exposure Factors and their Associated ESD and EI for Chest PA, Lumbar Spine AP, and Lumbar Spine LAT.

Examination	V [kVp]	Q[mAs]	ESD [mGy]	EI
Chest PA	90	2.5	0.29	2323 - 2355
	100	2.0	0.29	
	110	1.6	0.29	
Lumbar spine AP	70	22	1.97	348 -363
Lumbar spine LAT	80	25	3.20	895 - 1005
	90	20	3.30	

The average exposure factors for the study center for chest PA, lumbar spine AP and lumbar spine LAT are also presented in Table 4.9 for the purpose of comparison on how effective the dose-image optimization carried out by this study has been.

Table 4.9: Average Exposure Factors for the Study Center

Examination	V [kVp]	Q [mAs]	ESD [mGy]	EI
Chest PA	73	25	1.88	695
Lumbar spine AP	74	28	2.79	297
Lumbar spine LAT	74	56	5.34	552

4.8 Model Equation of EI, Q and V for Chest PA

To model the equation relating inverse of EI, Q and V for chest PA examination in order to be able to estimate acceptable values of each parameter, the experimental values were plotted in MATLAB and the graph is shown in Figure 4.32.

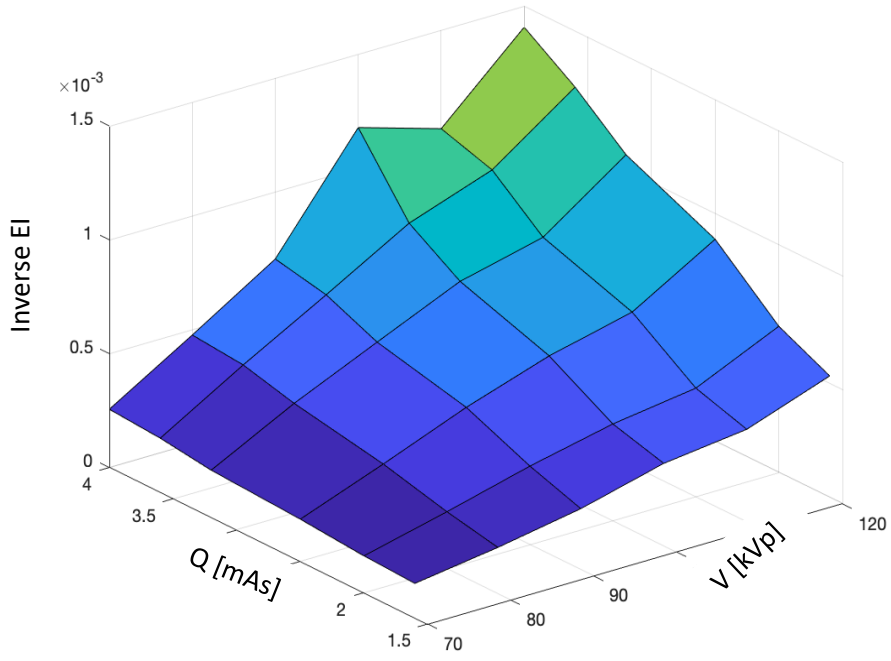

Figure 4.32: Inverse EI as Function of V and Q – Experimental Values.

From Figure 4.32, there was an experimental error in the inverse EI values at 100 and 110 kVp on 4 mAs. The rest of the values indicated linear correlation between inverse EI, V and Q. Based on measured EI as function of Q and V for Chest PA the following empirical model was manually fitted to the data:

$$\frac{1}{EI} = 6.4 \times 10^{-6} Q \times V - 3.4 \times 10^{-6} V - 4.0 \times 10^{-4} Q + 3.4 \times 10^{-4} \qquad 4.14$$

The values of the model inverse EI equation was plotted as shown in Figure 4.33.

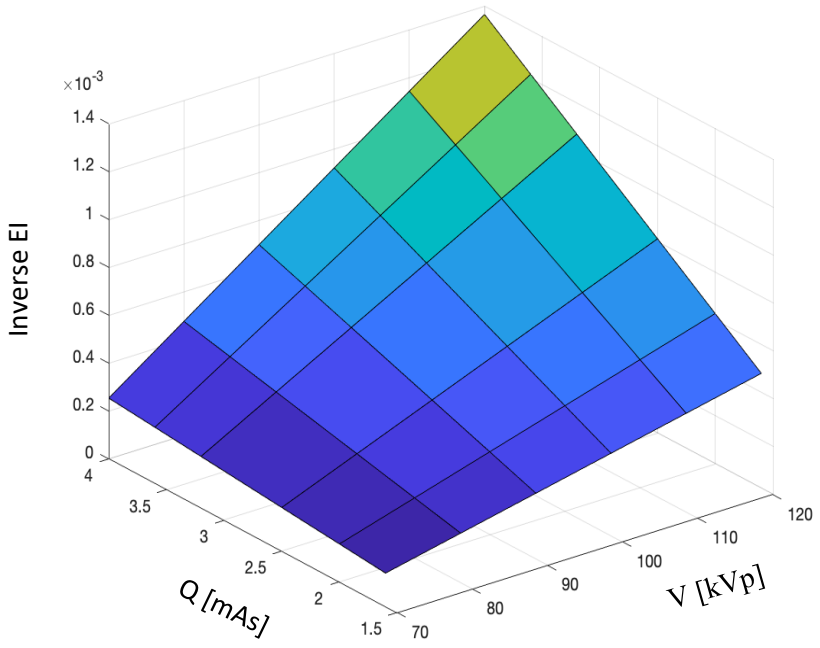

Figure 4.33: Inverse EI as Function of V and Q – Empirically Fitted Model.

The model contains linear relationships as well as a crossterm. The EI model did not deviate from the known relationship between mAs, kVp and dose, in particular there was no indication of a quadratic dependence on kVp for 1/EI. The empirical fitted model showed perfect correlation between inverse EI, V and Q. To validate, how well the developed model correlates to

experimental values, Figure 4.34 was developed to find the difference between the model values and the experimental values.

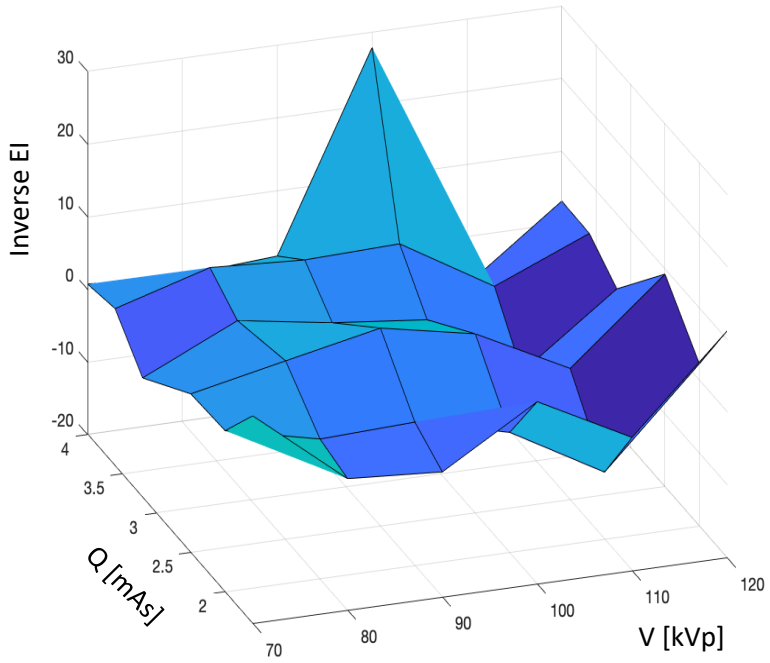

Figure 4.34: Deviation between Measured 1/EI and Model (2.9 % error).

The deviation between experimentally fitted values and the model was obvious at 100 and 110 kVp on 4 mAs. The median error deviation between the model and the empirical data was found to be 2.9%. This deviation was not as a result of defect of the model but mainly due to experimental errors as shown in Figure 4.32. EI values are susceptible to many factors such as read-out time, dirt on detector, and collimation of the radiation field. CR detectors lose some of their stored energy through phosphorescence and thus delay in read-out of the detector after the exposure would affect the intensity of the stored energy and the EI values. Again, detectors that are not cleaned for a long time would accumulate dirt which would affect the values of EI. These

are some of the reason why there were deviations in the experimental values and the model equation values.

The EI values recorded in all the three examinations (chest PA, lumbar spine AP and lumbar spine LAT) were outside the manufacturer's recommended values. Fuji ST. imaging plate was used for this study of which Fuji recommended values are 200 – 600 for general chest examinations and 100 – 400 for lumbar spine AP/LAT (Fuji medical systems 2014). Since EI depends on a number of factors, deviation from manufacturer's recommended values is expected in radiography. Studies conducted by other researchers also recorded EI values outside the recommended manufacturer's values (Mothiram et al, 2014: Lewis, Pieterse and Lawrence 2019). For this reason, it is important that each radiographic facility optimised its own EI values without completely depending on the manufacturer's values as a better option. Optimization management flow chart to be used in radiographic departments was developed to help protect patient from unnecessary radiation and this is shown in Figure 4.35.

4.9 Optimization Management Procedure

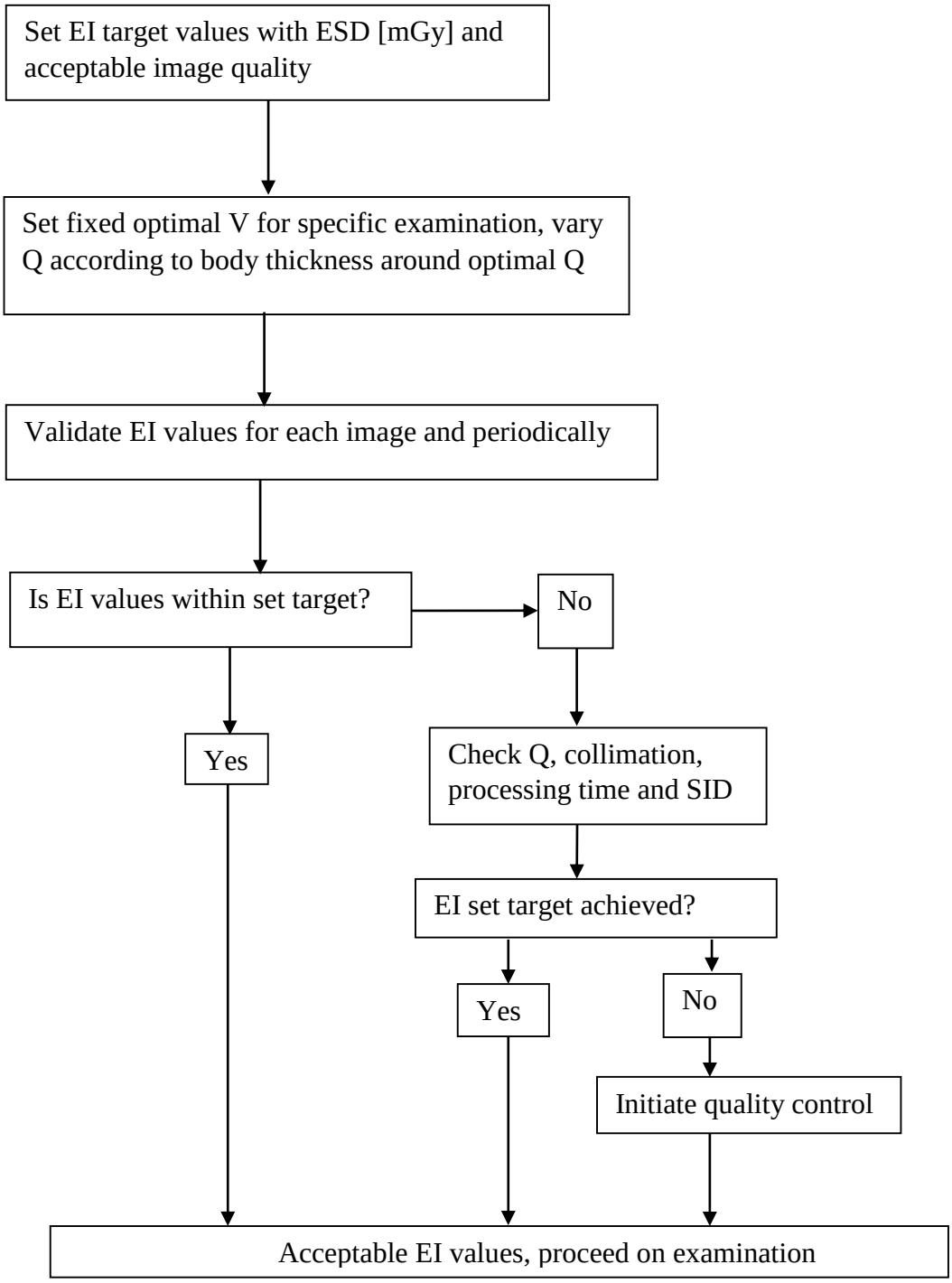

Figure 4.35: Optimization Management Procedure

This optimization strategy combines a number of techniques including image quality analysis, fixed V technique, quality control and patient radiation dose assessment which are very key elements in patient radiation protection. These combinations of techniques in the optimization strategy would provide a robust management system to ensure radiation safety in diagnostic radiography. Fixed V technique has been recommended in this strategy because radiation dose varies directly proportional to the square of V as shown in Figures 4.1 – 4.4. This means that, when V is doubled, radiation dose increases by a factor of four and thus V affects dose significantly than the Q which has direct proportionality to dose. In this case, varying V would have more potential to increase patient radiation those than varying Q.

Quality control tests to ensure effective and timely production of radiographic examinations must be a backbone in any optimization protocol. Quality control ensures that every equipment in the diagnostic chain works optimally to avoid unnecessary radiation dose to patients. Poor performance of X-ray equipment has been largely attributed to lack of proper quality control (Kharita, Khodr & Wannus, 2008)

The full implementation of this management strategy would require cooperation of different personnel such as radiographers, engineers, medical physicists and physicians. Optimization of patient radiation therefore requires proper collaboration of these professionals in order to achieve minimum radiation dose to patients.

4.10 Chapter Summary

The results and discussion are summarized as follows;

The tube output equations were modelled for all the five X-ray equipment. It was shown that the V^2 has direct proportional relationship with the tube output. It was found out that tube output varied from each X-ray machine.

All the X-ray equipment passed the quality control tests that were carried out. The quality control tests performed were kVp accuracy, kVp reproducibility, exposure reproducibility, exposure linearity and timer accuracy.

Entrance skin dose for nine (9) radiological examinations from five radiographic facilities were presented. The results showed variations in ESD from facility to facility. The variations were mainly due to variations in X-ray equipment output, selection of exposure factors, different SID values and lack of proper optimization protocol.

Optimal exposure factors were established for chest PA, lumbar spine AP, and lumbar spine LAT. The optimal exposure factors for chest PA were 90 kVp, 100 kVp and 110 kVp with 2.5 mAs, 2 mAs and 1.6 mAs respectively. 70 kVp and 22 mAs were obtained for lumbar spine AP while 80 kVp with 25 mAs and 90 kVp, 20 mAs were obtained for lumbar spine LAT.

Patient radiation dose reduction of 84.5% was achieved for chest PA. 29.3 and 38.2% reduction were achieved for lumbar spine AP and lumbar spine LAT respectively. The results also indicated that in CR imaging systems, overexposure of 64.6% and 60% are possible for chest PA, lumbar spine AP and lumbar spine LAT, respectively if proper optimization strategy is not instituted.

Model equation was developed to link applied voltage, Q and EI. The results also indicated that EI varied inversely proportional to the patient dose while image quality has linear relationship with the radiation dose. However, image quality does not increase significantly when the imaging detector received radiation that was enough to produce acceptable image quality. The image quality gradually deteriorates as the saturation limit of the detector is reached. CR image cannot be processed further when the saturation limit of the detector is reached and therefore calls for image rejection and repeat examination. EI values could be influenced by collimation, radiation exposure reaching the detector, readout time after exposure, SID and therefore setting EI values must be done carefully.

Optimization management flow chart based on setting target EI values was developed to achieve maximum radiation protection in diagnostic radiography. This optimization protocol requires that medical imaging professionals have to work in a team to be able to achieve maximum radiation protection for patients.

CHAPTER FIVE

SUMMARY, CONCLUSIONS AND RECOMMENDATIONS

5.0 Overview

In digital diagnostic radiography overexposure of patients could occur without being detected by radiographers, radiologists, or technologists. The wider dynamic range of the detector and the post processing algorithm of the digital systems have been identified as the cause of this overexposure. The brightness and contrast of digital radiography images are no longer dependent on the exposure factors. The exposure indicator which served as feedback to radiographers and technologists is only calibrated to indicate exposure to the detector and hence related to image quality. It has no direct indication of patient radiation entrance skin dose. This study therefore audit the patient radiation doses for nine radiological examinations. On the basis of the auditing, dose-image quality optimization procedure was used to determine the optimal exposure factors for chest PA, lumbar spine AP and lumbar spine LAT. Relationship between inverse EI, quantity of charge and applied voltage was investigated and model equation was developed to link these parameters for the purpose of optimization and patient radiation protection.

5.1 Summary

The aim of this study was to optimize patient radiation protection while maintaining the image quality in digital radiography examinations in Ghana. Entrance skin dose survey was conducted at five hospitals across Ghana for nine most common radiological examinations (chest PA, lumbar spine AP, lumbar spine LAT, pelvis AP, abdomen AP, skull AP, skull LAT,

cervical AP and cervical LAT). Patient ESD was estimated through mathematical equations using technical exposure parameters. Equations describing each X-ray tube output was developed for each five (5) X-ray equipment. The quality control results indicated that all the equipment were in good conditions for for clinical use. However, there were variations in the performance of these X-ray equipment. Requlr QC tests would ensure high image quality, reduce patient radiation dose and reduce repeat examinations.

The results of the study indicated that there were high variations in ESD of the same examinations across different radiological facilities. For chest PA, variations of up to 375.7 % was obtained. The variations in ESD were mainly due to differences in the selection of technical exposure factors across these facilities. Overexposure of 64.6 and 60.0 % for chest PA, lumbar spine AP and lumbar spine LAT, respectively were found to be possible if proper optimization protocols at radiological facilities are not implemented. This study also achieved 29.3, 38.2 and 84.5 % reduction in patient radiation dose for lumbar spine AP, lumbar spine LAT and chest PA, respectively for the study center and therefore encouraged the center to institute proper optimization protocols based on dose-image quality to protect patients.

The average ESD for the nine examinations were 0.66, 2.47, 3.77, 0.47, 0.49, 1.37, 1.29, 1.74, and 2.15 mGy for chest PA, lumbar spine AP, lumbar spine LAT, cervical spine AP, cervical spine LAT, skull PA, skull LAT, pelvis AP and abdomen AP, respectively. Optimal exposure factors for chest PA were 90 kVp; 2.5 mAs, 100 kVp; 2 mAs, and 110 kVp; 1.6 mAs. For lumbar spine AP, the optimal exposure factors were 70 kVp; 22 mAs while lumbar spine LAT were 80 kVp; 25mAs and 90 kVp; 20 mAs.

This study also indicated that, there was a linear relationship between ESD and Q and thus doubling the mAs doubled ESD. Also, there was inverse relationship between EI and ESD, therefore increase in ESD showed decrease in EI values, thus lower values of EI may indicate overexposure of patients. Again, it was also found that V has quadratic effects on X-ray tube output and thus doubling kVp increases the tube output by a factor of four. The relationship between inverse EI, V and Q was found to be linear from the developed mathematical model. This relationship indicated that, optimizing EI will indirectly optimize V, Q and ESD and therefore optimizing EI would provide effective means of radiation protection in digital radiography. Optimization management flow chart was also developed which centered on the ESD and EI optimization in order to protect patients. The optimization flow chart recommends auditing EI values for each image and periodically evaluate large EI values for different images.

5.2 Conclusion

From the results of this study the following conclusions are made:

All the X-ray equipment used in this study passed all the quality control tests that were performed, an indication that all the equipment were performing self- consistently. Equations describing each X-ray tube output was developed for each of the five (5) X-ray equipment. It was found that V has quadratic effect on the tube output.

ESD for chest PA, lumbar spine AP, lumbar spine LAT, cervical spine AP, cervical spine LAT, skull PA, skull LAT, abdomen AP and pelvis PA were estimated in five (5) radiographic facilities. The results show variations

in ESD for all the examinations considered. The reasons for these variations in ESD could be due to differences in exposure factors, tube output, patient thickness, and different X-ray equipment. This work also showed that high V with low Q technique could reduce patient radiation dose in chest PA examination as compared to low V with high Q.

Dose-image quality optimization was performed for chest PA, lumbar spine AP and lumbar spine LAT. Optimal exposure factors were recommended for these examinations in order to reduce patient radiation dose. The results of the dose-image quality optimization showed that over exposure of patients in computed radiography is likely to occur if proper optimization protocols are not established by the radiographic facilities. Effective patient radiation protection in radiological examinations require technical and daily operational levels of optimization, as well as fulfilling regulatory requirement.

Mathematical equation linking EI, V, and Q was developed. The model equation showed that inverse EI has linear relationship with V and Q, similar to the relationship between EI and ESD. Therefore, optimizing EI values would indirectly optimize ESD.

Optimization management flow chart based on setting EI target values was also developed in order to reduce patient radiation in diagnostic radiographic examinations. The optimization management flow chart combined techniques such as image quality analysis, QC, patient radiation dose assessment and fixed V. The full implementation of this optimization management chart would require the cooperation of different personnel such as radiographers, engineers, medical physicists and physicians.

5.3 Recommendations

The following recommendations are made to personnel in the radiology industry and the owners of the radiology department;

5.3.1 Personnel in the radiology industry

Patient protection in diagnostic radiography requires the collaborations of different professionals such as medical physicists, radiographers, radiologists, referring physicians, engineers, administrators of radiological facilities and the national regulatory authority. These professionals must work together to be able to identify challenges and develop comprehensive strategies to deal with patient radiation protection. The observation made during this research indicated that these professionals work more in isolation rather than in a team.

5.3.2 Owners of the radiology facilities

Radiographic facilities should conduct regular auditing of patient ESD and image quality in order to explore options of optimizing protocols to reduce patient radiation dose.

5.3.3 Nuclear Regulatory Authority (NRA)

NRA should establish regulatory framework that will ensure that patient radiation dose are audited regularly by the facilities owners.

5.3.4 Further Research Work

The optimal exposure factors that were established by this study were only for chest PA, lumbar spine AP and lumbar spine LAT. Further study could be extended to other examinations. The inverse exposure indicator values model that was developed was only for chest PA. Further study could

be extended to other examinations to investigate if similar relationships exist for the examinations.

REFERENCES

Abdelhalim, A. K. M., (2010). Patient dose levels for seven different radiographic examinations types. *Saudi Journal of Biological Sciences*, 17, 115-118.

Ackom, D., Inkoom, S., Sosu, E., Schandorf, C. (2017). Assessment of image quality and radiation dose to adult patients undergoing computed radiography examinations. *International journal of scientific research in science and technology*, 3(8): 89 – 94.

Adejoh, T., Ewuzie, O. C., Ogbonna, J. K., Nwefum, S. O., & Onuegbu, N. C. (2016). A Derived Exposure chart for computed Radiography in a *Nogroid population. Health*, 8: 953- 958.

Aggarwal, L. W. (2014). Biological effects of ionizing radiation. *Shodh Prerak*, 4(1), 343-348.

Aichinger, H., Dierker, J., Joite-Barfub, S., & Sabel, M. (2012). Radiation exposure and image quality in X-ray diagnostic radiology. Heidelberg, Berlin: Springer-Verlag.

Akaagerger, B. N., Akapa, C. T., & Ujah, F. O. (2014). Quality estimation of filtration of diagnostic X-ray at Federal Medical center and Bishop Murray hospital Makurdi using Half-value layer (HVL). *Advances in Physics and Theories and Applications*, 38, 1-6.

Akpochafor, M. O., Omajola, A. D., Soyebi K. O., Adeneye, S. O., Aweda, A. M., & Ajayi, B. H. (2016). Assessment of peak kilovoltage accuracy in ten selected x-ray centers in Lagos metropolis, south- western Nigeria. A quality control test to determine energy output accuracy of an ex-ray generator, *Journal of Health Research and Reviews*, 3(2): 60- 65.

Al – Qaroot, B., Hogg, P., Twiste, M., & Howar, D. (2014). A systematic procedure to optimise dose and image quality for the measurement of inter-vertebral angels from lateral spinal projections using cobb and superimposition methods. *Journal of X-ray Science Technology*, 22(5), 613 – 6325.

Alameen, S., Badrey, A. A. F., Abdullateaf, A. S., & Ahmed A. M. (2016). Assessment of ESAK and ED for Adult's patients examined by computed radiography. *International Journal of Medical Physics, Clinical Engineering and Radiation oncology*, 5:281- 28

Aldrich, E. J., Duran, E., Dunlop, P., & Mayo, J. R. (2006). Optimization of dose and image quality for computed radiography and digital radiography. *Journal of Digital Imaging*, 19(2), 126 – 131.

Alghoul, A., Abdalla, M.M., & Abubaker, H. M. (2017). Mathematical evaluation of entrance surface dose (ESD) for patients examined by diagnostic X-rays. *Open Access Journal of Science*, 1(1):8 – 11.

Aliasgharzadeh, A., Mihandoost, E., Masoumbeigi, M., Salimian, M., & Mohseni, M. (2015). Measurement of entrance skin dose and calculation of effective dose for common diagnostic X-ray examinations in Kashan, Iran. *Global journal of health science*. 7(5): 202-207.

Almen, A., Tingberg, A., Besjakov, J., & Mattsson, S. (2004). The use of reference image criteria in X-ray diagnostics: an application for the optimization of lumbar spine radiographs. *European Journal of Radiology*, 14, 1561 – 1567.

Alsleem, H., & Davidson, R. (2012). Quality parameters and assessment methods of digital radiography images. *The Radiographer*, 59(2), 46 - 55.

Alves, A. F. F., Alvarez, M., Ribeiro, S.M., Duarte, S.B., Miranda, J. R. A., & Pina, D. R. (2016). Association between subjective evaluation and physical parameters for radiographic images optimisation. *Physica Medical*, 32, 123-132.

American Association of Physicists in Medicine. (2002). Quality control in diagnostic radiology (AAPM Task Group No, 12, Report 74). Madison, USA: AAPM.

American Association of Physicists in Medicine. (2006). Acceptance testing and quality control of photostimulable storage phosphor imaging systems (Report of AAPM Task Group 10). Maryland, USA: AAPM.

American Association of Physicsts in Medicine. (2009). An exposure indicator for digital radiography (AAPM report No 116). College park,USA: AAPM.

Australian Radiation Protection and Nuclear Safety Agency. (2014). Fundamentals for protection against ionizing radiation (radiation protection series F-1). Yallabie, Australia: ARPNA.

Azzoz, R., Elshahat, K. M., & MonemRezt, A. R. (2014). Evaluation of quality control systems for x-ray machines at different hospitals using patient's radiological dose assessment technology. *IOSR Journal of Applied Physics*, *6*(5), 29-34.

Baker, M. (2012). Investigation into factors influence Fuji S-value using an Extremity phantom. *Journal of medical imaging and Radiation Sciences*, 43, 34- 37.

Barrett, H. H & Myers, K. (2004). Foundations of imaging science (1st Eds). New Jersey, John Wiley and sons Inc: USA.

Bansal, G. J. (2006). Digital radiography. A comparison with conventional imaging. *Postgraduate Medical Journal*, 82, 425-428.

Bath, M., & Mansson, G.L. (2007). Visual grading characteristics (VGC) analysis: a non- parametric rank – invariant statistical method for image quality evaluation. *The British Journal of Radiology*, 80, 169-176

Batista, W. O. G, & de Carvalho, A. G. (2016). Dosimetry and optimization in digital radiography based on the detail contrast resolution. Proceedings of the ISSSD Chiapas, Mexico: Tuxtla Gutierrez.

Betlazav, C., Banati, B.R., Liu. G.J., Middleton, J.R. (2016). The impact of high and low dose ionizing radiation on the central nervous system. *Redox Biology*, 9, 144-156.

Beyzadeoglu, M., Cuney, E., & Ozyigit, G. (2010). Basic Radiation Oncology. Berlin, Germany: Springer-Verlag Berlin Heidelberg. Pp. 71-102.

Bhat, A. (2018). Convenience sampling: Definition, method and examples. https://www.questionpro.com/blog/convenience-sampling [Accessed on 16/08/2018]

Bolus, E. N. (2001). Basic review of radiation Biology and terminology. *Journal of nuclear medicine technology*, 29, 67-73.

Brenner, D. J., & Hall, E. J. (2007). Computed Tomography- An increasing source of Radiation Exposure. *The New England journal of Medicine,* 357: 2277 -2284.

Bushberg, J. T. (2002). The essential physics of medical imaging (2nd Ed). Philadelphia, Lippincott Williams and Wilkins: USA.

Ching, W., Robinson, J., & McEntee, M., (2004). Patient –based radiographic exposure factors selection: a systematic review. *Journal of Medical Radiation Sciences*, 61, 176-190.

Ciraj, O., Markovic, S., & Kosutic, D. (2004). Patient dose from conventional diagnostic radiology procedures in Serbia and Montenegro. *The Journal of Preventive Medicine,* 12(3-4), 26-34.

Creswell, J. W. (2003). Research design; qualitative, quantitative, and mixed methods approach (2nd Ed). London, Sage publications Inc: UK.

Cunningham, I. A. (Ed.). (2000). Applied-systems theory, in handbook of medical imaging: Medical physics and psychophysics. Proceedings from the International Society for Optics and Photonics. Bellingham, USA: SPIE.

Davey, E., & England, A. (2014). AP versus PA positioning in lumbar spine computed radiography: Image quality and individual organ doses. *Radiography*, 21, 188- 196.

Davidson, A. R. (2006). Radiographic contrast-Enhancement Masks in Digital Radiography. Unpublished Doctoral thesis. The University of Sydney, New South Wales, Australia.

De-Crop, A. D., Bacher, K., Hoof, T. V., Duyck, P., Herde, D. K., Kiendys, U., Smeets, P. V., Smet, B. S, Thierens, H., Vergauwen, M., &

Verstraete, K., (2012). Correlation of contrast-detail analysis and clinical image quality assessment in chest radiography with a human cadaver study. *Radiology,* 262(1), 298-303.

Desouky, O., Ding, N., & Guangming, Z. (2015). Target and non-targeted effects of ionizing radiation. *Journal of radiation research and applied sciences,* 8, 247-254.

Do, H. K. (2016). General principles of radiation protection in fields of diagnostic medical exposure. *Journal of Korean medical science,* 31, 6-9.

Doi, K. (2006). Diagnostic imaging over the last 50 years: research and development in medical imaging science and technology. *Physics in Medicine and Biology,* 51, 5-27.

Donnellan, E., Collier, P., Desai, M., Griffin, B., Mccarthy, C. P., & Phelan, D. (2016). Radiation-induced heart disease: A practical guide to diagnosis and management. *Cleveland clinic journal of medicine,* 83(12), 914-922.

Doyle, P., Martin, C.J., & Gentle, D. J. (2005). Dose- image quality optimization in digital chest radiography. *Radiation protection dosimetry*, 114(1-3), 269 – 272.

Elgazzar, A. H., & Heger, N. (2006). Biological effects of ionizing radiation. Retrieved from http://www.eknygos.ismuni.it/springer/344/540-548.pdf.

Eng, J. (2005). Receiver operating characteristic analysis. Academic Radiology, 12(7), 909-916. European Society of Radiology. (2015).

Summary of the European Directive 2013/59/Euratom: essentials for health professionals in radiology. *Insights imaging*, 6, 411-417.

European commission (1996). European guidelines on quality criteria for diagnostic radiographic images. Report EUR 16261

Flannigan, A. W., Erickson, D., Magnuson, D., & Schneler, B. (2012). Artifacts in digital radiography. *American journal of Radiology*, 198, 156-161.

Franco, A., Ciccarelli, D., Durante, M., Fiordelisi, A., Iaccarino, G., Napolitano, L., Trimarco, B., & Sorriento, L. (2016). Rays Sting: the acute cellular effects of ionizing radiation exposure. *Translational Medicine*, 14(8), 42-53.

Fuji medical systems. (2014). FujiFilm medical systems CR users guide. (Www. Spectrumxray.com/sites/default/files/pdfs-CR-user-Guide.pdf.

Geijer, H., Norrman, E., & Persliden, J. (2009). Optimising the tube potential for lumbar spine radiography with a flat panel digital detector. *The British Journal of Radiology*, 82: 62 -68.

George, J., Eatough, J. P., Frain, G., Mountford, J. P., Oxtoby, J., & Koller, C. J. (2004). Patient dose optimization in plain radiography based on standard exposure factors. *The British Journal of Radiology*, 77: 858-863.

Gholami, M., Karami, V., & Nemati, F., (2015). The evaluation of conventional x-ray exposure parameters including tube voltage and exposure time in private and governmental hospitals of Lorestan province, Iran. *Iranian Journal of Medical Physics*, 12(2), 85-92.

Gibson, D. J., & Davidson, R. A. (2012). Exposure creep in computed Radiography: A Longitudinal study. *Academic Radiology*, 19(4), 458 - 462.

Graham, D. T., & Cloke, P.J. (2003). Principles of radiological physics (4th Ed). London, Churchill livingstone: UK.

Godfrey, L. D., Adeyemo, D. J., & Sadiq, U. (2015). Radiological kVp accuracy, reproducibility and consistency assessment of some hospitals in Zaria environs of Kaduna state, Nigeria. *Archives of Applied Science Research*, 7 (5), 27-31.

Grover, S. B., Kumar, J., Gupta, A., & Khanna, L. (2002). Protection against radiation hazards: Regulatory bodies, safety norms, doses limits and protection devices. *Nursing practices,* 12(2), 157 – 167.

Hart, D & Wall, B. F. (2002). Radiation Exposure of the UK population from medical and Dental X-ray Examinations. National Radiological Protection Board (NRPB-W4). Chilton, UK: Didcot.

Hart, D., Hillier, C. M., & Wall B. F. (2009). National reference doses for common radiographic, fluoroscopic and dental X-ray examinations in UK. *The British Journal of Radiology*, 82, 1-12.

Ibitola, G., Ilori, A.O., Ajanaku, O., & Utomewere, R. D. (2018). Entrance skin dose (Radiation) measurement and evaluation (for all age groups) at State specialist Hospital Okitipupa, Nigera. *Open Science Journal*, 3(2), 1 -14.

Ibrahim, U., Daniel, I. H., Ayaninola, O., Ibrahim, A., Hamza, A. M., & Umar, A.M. (2014). Determination of Entrance skin dose from

diagnostic X- ray of human chest at federal medical centre. *Nigeria Science world Journal*, 9(1), 14 -18.

Inah, B. G., Akintomide, A. O., Edim, U. U., Egbe, N. O., & Nzotta, C. (2013). A study of pelvic radiography image quality in a Nigerian teaching hospital based on the Commission European Communities (CEC) criteria. The South African Radiographer, 51(2), 15-18.

International Atomic Energy Agency (2004) Optimisation of the radiological protection of patients undergoing radiography, fluoroscopy and computed tomography (IAEA-TECDOC-1423). Vienna Austria.

International Atomic Energy Agency. (1996). International basic standards for protection against ionizing radiation and for the safety of radiation source. IAEA Safety series, Vienna.

International Commission on Radiation Protection (2016). The draft report on ethical foundations of the system of radiological protection. Ontario, Canada.

International Commission on Radiation Units and Measurements. (2005). Patient dosimetry for X-rays in medical imaging (ICRU Report 74). *Journal of ICRUs*, 5(2), 1-113.

International Commission on Radiological Protection. (1977). Recommendations of the International Commission on Radiological Protection (ICRP Publication, 26). Annals of ICRP 1(3).

International Commission on Radiological Protection. (1982). Protection of patient in diagnostic radiology (ICRP Publication 34). Pergaman press, Oxford, UK.

International Commission on Radiological Protection. (1991b). 1990 Recommendations of the International Commission on Radiological Protection (ICRP Publication 60). Annals of ICRP 21(1-3).

International Commission on Radiological Protection. (1996). Radiological protection and safety in medicines (Report 73). Annals of ICRP 26(2).

International Commission on Radiation Units and Measurements. (1996). Medical imaging – the assessment of image quality (ICRU report 54). Maryland, USA: ICRU.

International Commission on Radiological Protection. (2007). The 2007 recommendations of the International Commission on Radiological Protection (ICRP, Publication 103). Annals of the ICRP, 37 (2-4).

Jaworski, C., Kaye, D. M., Mariani, A. J., & Wheeler, G. (2013). Cardiac complications of thoracic irradiation. *Journal of the American College of cardiology*, 61(23), 2319-2328.

Jibiri, N. N., & Olowookere, C. J. (2016). Patient dose audit of the most frequent radiographic examinations and the proposed local diagnostic reference levels in southwestern Nigeria: Imperative for dose optimization. *Journal of Radiation Research and Applied Science*, 9, 274- 281.

Johnston, A. D & Brennan, C. P. (2002). Reference dose levels for patients undergoing common diagnostic x-ray examinations in Irish hospitals. *The British Journal of Radiology*, 73: 396-402.

Johnston, A. D., & Brennan, C. P. (2000). Reference dose levels for patients undergoing common diagnostic x-ray examinations in Irish hospitals. *The British Journal of Radiology*, 73, 396-402.

Jones, A. K., Heintz, P., Geiser, W., Goldman, L., Jerjian, K., Martin, M., Peck, D., Pfeiffer, D., Ranger, N., & Yorkston, J. (2015). Ongoing quality control in digital radiography: Report of AAPM imaging physics committee task group 151. *Medical Physics,* 42 (11), 6658 – 6670.

Kemerink, M., Dierichs, T. J., Dierichs, J., Huynen, H., Wildberger, E. J., van Engelshoven, J. M. A., & Kemerink, G. J., (2012). The application of X-rays in Radiology: From difficult & dangerous to simple and safe. *American Journal of Radiology*, 198: 754 -759.

Kenneth, K. R., (2004). Radiation protection principles of NCRP. *Health physics*, 87(3), 251-257.

Khan, F. M. (2003). The physics of radiation therapy (3rd ed.). Philadephia, USA: Lippincott Williams &Wilkins. Pp. 29-38.

Kharita, M. H., Khodr, M. S. & Wannus. K. M. (2008). A comparative study of quality control in diagnostic radiology. *Radiation protection dosimetry*, 2008: 1-5.

Khoshnazar, A. K., Hejazi, P., Mokhtarian, M., & Nooshi, S. (2013). Quality control of Radiography equipment in Golestan province of Iran. *Iranian Journal of medical Physics* 10 (1 -2), 37 -44.

Kim, K. R., Cui, H. Y., Jin, W. Y., Lee, J. S., Kaushhik, N., Kim, J. M.,Seong, K. M., Nam, S. Y., Suh, S. Y., & Yoo, C. K. (2015). Beneficial effects of low dose radiation in response to the oncogenic KRAs induced cellular transformation, *Scientific Reports*, 5(15809), 1-9.

Kim, M. S, Cho, C. L., Jung, H. J., Lee, E., Kim, W., Kim, J. H., Park, H. I., & Song, C. W. (2015). Radiological mechanisms of stereotactic body

radiation therapy and stereotactic radiation surgery. *Radiation oncology Journal,* 33(4), 265-275.

Korir, G. K., Wambani, J. S., & Ochieng, B. O. (2010). Optimization of patient protection and image quality in diagnostic radiology, *East African medical Journal*, 87 (3): 127- 138.

Korner, M., Pfeifer, J. K., Reiser, F. M., Treitl, M., Weber, C. H., & Wilth, S. (2007). Advances in Digital Radiography: Physical Principles and System Overview. *Radiographics*, 27 (3), 675-686.

Kothan, S. & Tungjai, M. (2011). An estimation of X-radiation output using mathematical model. *American Journal of Applied Sciences,* (9): 923-926.

Kotter, E., & Langer, M. (2002). Digital radiography with large-area flat-panel detector. *European Radiology*, 12, 2562-2570.

Kudr, J., & Heger, Z. (2015). Effects of ionizing radiation on nucleic acids and transcription factors. *Journal of Metallomics and Nanotechnologies*, 4, 22-29.

Lacerda, A. M. S., Oliveira, A. H. & Silva, A. T. (2007). The methodology for evaluating half-value layer and its influence on the diagnostic radiology. *Radiologia Brasileira,* 40(5), 331-336.

Lanca, L., & Silva, A. (2013). Digital radiography detectors: A technical overview. Retrieved from http:// www.springer.com/cda/content/ document/cda_downloaddocument/97814614506.[Accessedon 01/12/17].

Larcher, A. M., Lopez, O. P., Arias, C., Marechal, M. H., Alvarez, H. R., Garcia, F. N., Mucino, A. G., & Faller, B. (2008). Continuous

improvement of the Regulatory Framework for the control of medical Exposure. Paper presented at 12th International Congress of the International Radiation Protection Association, Buenos Aires, Argentina, and 19th -24th October, 2008.

Lewis, S., Pieterse, T., & Heather, L. (2019). Retrospective evaluation of exposure indicators: a pilot study of exposure technique in digital radiography. *Journal of medical Radiation Sciences*, 66, 38 – 43.

Little, P. M., Bouffler, D. S, de-Gonzalez, A. B., Tawn, E. J., & Wakeford, R. (2009). Risks associated with low doses and low dose rates of ionizing radiation: why linearity may be (almost) the best we can do. *Radiology, 25(1), 6-12.*

Loaz, O., Suliemun, A., & Yousef, M. (2015). Clinical evaluation of image quality for intravenous urography basis on European Commission guidelines on quality criteria in Sudan. *Scholars Journal of Applied Medical Sciences, 3*(3F), 1436- 1442.

Luckgy, D. T., & Lawrence, K. S. (2006). Radiation hormesis: The good, the bad, and the ugly. *Dose-response*, 4(3), 169-190.

Ludewig, E., Frame, M., & Richter, A. (2010). Diagnostic image-evaluating image quality using visual grading characteristics (VGC) analysis. *Veterinary Research Communications*, 34, 473-479.

Madan, R., Benson, R., Juka, P. K., Rath, G. K., & Sharma, D. N. (2015). Radiation induced heart disease: pathogenesis, management and review literature. *Journal of the Egyptian National Cancer Institute*, 27, 187-193.

Malone, J., Guleria, R., Craven, C., Horton, P., Jarvinen, H., Mayo, J., Reilly, G. O., Picano, E., Remedios, D., LeHeron, J., Rehani, M., Holmberg, O., & Czarwinski, R. (2012). Justification of diagnostic medical exposures: Some practical issues. Report of an International Atomic Energy Agency Consultation. *The British Journal of Radiology*, 85(2012), 523- 538.

Mana, S. (2011). Dose optimization for the quality control tests of X-ray equipment. Retrieved from http://www.intechopen.com. [Accessed on 16/09/17].

Manning- Stunley, A. S., Ward, A. J., & England, A. (2012). Options for radiation dose optimization in pelvic digital radiography: A phantom study. *Radiography*, 18, 256- 263.

Martin, C. J. (2007). Optimization in general radiography. *Biomedical imaging and Interventional Journal*, 3(2), 1-14.

Martin, C. J., Sutton, D. G., West, C. M., & Wright, E. G. (2009). The radiobiology/radiation protection interface in healthcare. *Journal of Radiological protection*, 29, 1-20.

Martin, E. J. (2006). Physics for radiation protection: A Handbook (2nd ed.). Weinheim, USA: Wiley- Vech Verlag GmbH and co. KGaA.

Massoud, E & Diab, H. M. (2014). Optimization of dose to patient in diagnostic radiology using Monte carlo method. *Journal of cell science and therapy, 5(1): 2-6.*

Matsumoto, M., Ota, S., Inone, S., Ogata, Y., Yamanoto, S., Ueguchi, T., & Johkoh, T. (2003). Analysis of entrance surface dose in general

radiographies using body mass index. *Japan Journal of Medical Physics,* 23(4): 232- 242.

Matton, J. S., & Smith, C. (2004). Breakthrough in Radiograph: Computed Radiography. Retrieved from https:// www.idexx.com/pdf/en_us/ equine/compendim-2004-jan-radiography.pdf. [Accessed on 24/11/17].

Mazzocch, S., Belli, G., Busoni, S., Gori, C., Menchi, I., Salucci, P., Taddeucci, A., & Zatelli, G. (2005). AEC Set-up optimization with computed radiography imaging. *Radiation protection dosimetry*, 117(1-3), 169-173.

McCollough, C. H. (1997). The American Association of Physicists in Medicine/ Radiological Society of North America physics Tutorial for Residents. *Radiographics*, 17, 967-984.

Mettler, F. A., Thomadsen, B. R., Bhargaran, M., Gilley, D. B., Gray, E. J., Lipoti, A. J., Mccrohan, J., Yoshizumi, T. T., & Mahesh, M., (2008). Medical Radiation Exposure in the U.S in 2006: preliminary results. *Health Physics*, 95(5), 502 -507.

Minaei, E. S., Firouzi, F., & Khosravi, H. R. (2014). Patient doses in radiographic examinations in Western and Eastern Azerbyjaan provinces of Iran. *Journal of paramedical Sciences*, 5(3): 77- 81.

Moore, C. S., Wood, T. J., Beavis, A. W., & Saunderson, J. R. (2013). Correlation of the clinical and physical image quality in chest radiography for average adults with a computer radiography imaging systems. *British Journal of Radiology*, 2013(86): 2- 12.

Moore, T. Q., Cohen, M., Don, S., Herrmann, T. M., John, D. S., Lehman, L., Morrison, G., MacDougall, R., Noble, L., & Strauss, J. K. (2012).

Image Gently: Using Exposure Indicators to improve paediatric Digital Radiography. *Radiologic Technology*, 84(1), 93-99

Mothiram, U., Brennan, C. P., Lewis, J. S., Moran, B., & Robinson, J. (2014). Digital radiography exposure indices: A review. *Journal of medical radiation science,* 61, 112-118.

Mould, R .F. (1995). Invited review: Rontgen and the discovery of x-rays. *The British Journal of Radiology,* 68: 1145 -1176.

Moy, J. P. (2000). Signal-to-noise ratio and spatial resolution in x-ray electronic imagers: is the MTF a relevant parameters? The International Journal of *Medical Physics Research and Practice,* 27(1), 86-93.

Mulubrihan, A., & Atnafu, A. (2001). Skin entrance dose to patients from routine P-A chest x-ray examinations, Radiology Departments, Tikur Anbessa Referral hospital. *Journal of health Development,* 15(2), 145-151.

Naji, A. T., Jaafar, M. S., Ali, E. A., & Al- Ani, J. S. K. (2017). Effect of backscattered radiation on x-ray image contrast. *Applied Physics Research*, 9 (1): 105- 114.

Nickoloff, E. L. & Berman, H. L. (1993), Factors affecting X-ray spectral. *Radiographics*, 13(6), 1337-1348.

Nielsen, K. M., Nielsen, H. M., Offersen, B. V., Vaage-Nilsen, M., & Yusuf, S. W. (2017). Short and long term radiation induced cardiovascular disease in patients with cancer. *Clinical Cardiology,* 40, 255-261.

Nyathi, T., Chirwa, F. T., & Merwe, D. G. (2010). A Survey of digital radiography practice in four South African Teaching hospitals: an

illuminative study. *Biomedical Imaging and Interventional Journal* 6(1), 1-6.

Oborska-Kumaszynska, D. (2011). Analog and Digital Systems of Imaging in Roentgeno diagnostics. Retrieved from https//www.fotospokojna. com/linki/www_cyfra/matryce.pdf. [Accessed on 27/11/17].

Obuchowski, A. N. (2005). Fundamentals of clinical research for radiologist ROC analysis. *American Journal of Radiology*, 184, 364-372.

Ofori, E. K., Antwi, K. W., Scutt, D. N., & Ward, M. (2013). Patient radiation dose assessment in pelvic x-ray examinations in Ghana. *OMICS Journal of Radiology*, 2(8), 1-5.

Ofori, E. K., Antwi, K. W., Scutt, D. N., Ward, M. (2012). Optimization of patient radiation in pelvic x-ray examination in Ghana. *Journal of Applied clinical medical physics*, 13(4):1-9.

Ofori, K., Ampene, A. A., Akrobortu, E., Gordon, S. W., & Darko E. O. (2014). Estimation of adult patient doses for selected X-ray diagnostic examinations. *Journal of Radiation Research and Applied Sciences*, 7, 459-462.

Ogundare, F. O., Balogun, A. F., & Uche, C. Z. (2004). Radiological parameters and radiation doses of patients undergoing abdomen, pelvis, and lumbar spine X-ray examinations in three Nigerian hospitals. *The British Journal of Radiology*, 77, 934-940.

Oliveira, A. C., Martins. A. P., Avelas, R. T., Santos, M. S. C. D., Martins, P. M., De- Francesco, S., Sa- Couto, P., & Ferreira, C. (2013).Visual grading analysis of image quality in pediatric abdominal images

acquired by direct radiography and computer radiography systems. *European Society of Radiology*, 1- 24.

Oluwafisuye, P. A., Olowookere, C. J., Jibiri, N. N., Bello, T. O., Alausa, S.K. & Efunwole, H.O. (2010). Quality control and environmental assessment of equipment used in diagnostic radiology. *International Journal of recent research and applied studies*, 3(2): 148-158.

Owolabi, A. S., Hussain, A. L., & Ogundare, F. O. (2005). Relationship between the exposure outputs of single-phase and three-phase diagnostic machines: Implications for patient exposure determination in developing countries. *Nigeria Journal of Physics*, 17, 203-212.

Palinkas, A. L., Horwitz, S. M., Green, A. C., Wisdom, J. P., Duan, N., & Hoagwood, K. (2015). Purposeful sampling for qualitative data collection & analysis in mixed method implementation research. *Adm Policy Ment Health*, 42(5), 533 – 544.

Panchbhail, A. S. (2015). Wilhelm Conrad Rontgen and the discovery of x-rays: Revisited after centennial. *Journal of Indian Academic oral medical Radiology, 27: 90 -95.*

Pierce, A. D., & Preston, D. L. (2000). Radiation - related cancer risks at low doses among atomic bomb survivors. *Journal of Radiation Research*, 154, 178-186.

Podgorsak, B. E. (2005). Radiation oncology physics: A Handbook for Teachers and students. Vienna, Austria; International Atomic Energy Agency.

Podgorsak, B. E. (2006). Radiation physics for medical physicists, Berlin, Germany; Springer-Verlag Berlin Heideliberg.

Rubai, S. S., Rahman, M.S., Purohit, S., Patway, M. K. A., Meaze, A. M. H, & Mamun, A. A (2018). Measurements of entrance sureface dose and effective dose of patients in diagnostic radiology. Biomedical Journal of Scientific and Technical Research, 12(1), 8924- 8928.

Sakurai, T., Kaku, Y., Kawamata, R., Kashima, K., Kozai, Y., Nakamura, K., & Saito M. (2010). Relationship between radiation dose reduction and image quality change in photosimulable phosphor luminescence X-ray imaging systems. *Dentomaxillofacial Radiology*, 39, 207-215.

Samei, E., Dobbins, J. T., Lo, J. Y., & Tornai, M. P. (2005). A frame work for optimizing the radiographic technique in digital X-ray imaging. *Radiation Dosimetry,* 114 (1-3). 220-229.

Schaner, D. A., & Linton, O. W. (2009). National Council on Radiation Protection and Measurements. Report shows substantial medical Exposure increase. *Radiology*, 253(2), 293 -296.

Schaetizing, R. (2003). Advances in digital radiography: RSNA categorical course in diagnostic radiology physics. Greenville, SC 29601.

Seeram, E., Bushong, S., Davidson, R., & Swan, H. (2016). Optimizing the exposure indicator as a dose management strategy in computed Radiography. *Radiologic Technology*, 87(4), 380 -391.

Seibert, A. J. (2004). X-ray imaging physics for nuclear medicine technologists. Part 1: Basic principles of X-ray production. *Journal of Nuclear Medicine Technology*, 32(3), 139-147.

Seibert, A. J. (1997). The American Association of physicists in Medicine/ Radiological Society of North America Physics Tutorial for Residents. *Radiographics*, 17(6), 1533-1557.

Seibert, A. J. (2009). Digital radiography: The bottom-line comparison of CR and DR technology. *Applied Radiology*, 5, 21-28.

Seibert, A. J., & Morin, L. R. (2011). The standardized exposure index for digital radiography: an opportunity for optimization. *Pediatric Radiology*, 41: 573 -581.

Seong, K. M., Jin, W. Y., Lee, D., Lee, S. S., Kim. J. M., Park, S., & Seo, S. (2016). Is the linear no-threshold dose-response paradigm still necessary for the assessment of health effects of low dose radiation? *Journal of Korean medical science, 31, 10-23.*

Sezdi, M. (2011). Dose optimization for the quality control tests of X-ray equipment. Www. research gate.net/…/x-ray –tube-output- changes-with-kvp-dose-values-from [Accessed on 20/08/2018].

Shannoun, F., Blettner, M., Schmidberger, H., & Zeeb, H. (2008). Radiation protection in diagnostic radiology. *Deutsches Arzteblatt International*, 105(3), 41-36.

Sharifat, I., & Oyeleke, I. O. (2009). Patient entrance skin doses at Minna and Ibadan for common diagnostic radiological examinations. *Bayero Journal of pure and Applied Sciences,* 2(1), 1-5.

Slapa, M., Dora, J., Drabik, W., Gutowski, R., Stras, W., Snopek, M., & Traczyk, M. (2002). X-ray tube with needle-like anode. *Nukleonika*, 4(3), 101-105.

Smith-Bindman, R., Lipson, J., Marcus, R., Kim, P. K., Mahesh, M., Gould, R., de Gonzalez, A. B., & Miglioretti, D. L. (2009). Radiation Dose Associated with common computed Tomography Examinations and

the associated Lifetime Attributable Risk of Cancer. *Arch International Medicine*, 22: 2078 -2086.

Sulieman, A. (2015). Current status of Radiation Dose Levels in Conventional paediatric Radiography: A review study. *Open Journal of Radiology*, 5: 104 -110.

Sun, Z., Lin, C., Tyan, Y., Hoong, K. N. (2012). Optimisation of chest radiographic imaging parameters: a comparison of image quality and entrance skin dose for digital chest radiography systems. *Clinical imaging*, 36, 279 – 286.

Sungital, Y. Y., Mode, S. S. L., & Maski, P. (2006). Diagnostic X-ray facilities as per quality control performances in Tanzania. *Journal of Applied Clinical Medical Physics*, 7 (4): 66-74.

Taha, M. T., Al-Ghorabie, F. H., Kutbi, R. A., & Saib W. K. (2015). Assessment of entrance skin doses for patients undergoing diagnostic X-ray examinations in King Abdullah medical city, Makkoh. *Journal of radiation research and Applied sciences* 8:100-103.

Tapiovaara, M. (2006). Relationships between physical measurements and user evaluation of image quality in medical radiology- A review (STUK-A219). Sateilyturvakeskus Stralsakerhetscentralen Radiation and Nuclear Safety Authority, Helsinki/Finland. 1-62.

Thurston, J. (2010). NCRP Report no. 160: Ionizing radiation exposure of the population of the United States. *Physics in Medicine and Biology*, 55(20), 6327-6335.

Tingberg, A. (2000). Quantifying the quality of medical X-ray images. Unpublished Doctoral thesis. Lund University. Malmo-Sweden.

Tung, C. J., Lo, H. S., & Tsai H. Y. (2001). Determination of guidance levels of dose for diagnostic radiography in Taiwan. *American Association of Physicists in medicine,* 28(5). 850-857.

Uffmann, M., & Schaefe-Prokop, C. (2009). Digital radiography: The balance between image quality and required radiation dose. *European Journal of Radiology, 72, 202-208.*

United Nations Scientific Committee on Effects of Atomic Radiation. UNSCEAR. (2008). Report to General Assembly with scientific annexes. Volume 1. United Nations. New York, 2010.

United Nations Scientific Committee on Effects of Atomic Radiation. (2000). Sources and effects of ionizing radiation (UNSCEAR Report Volume 1). United Nations, New York.

United Nations Scientific Committee on Effects of Atomic Radiation. (2006). Effects of ionizing radiation (Report volume 1 annexes A& B). United Nations, New York.

Veldkamp, J. H. W., Geleijns, J., & Lucia, J. M. K. (2009). Dose and perceived image quality in chest radiography. *European Journal of Radiology*, 72, 209-217.

Verdum, F. R., Aroua, A., Bochud, F., Gudinchet, F., Menli, R., & Schnyder, P. (2008). Radiation risk: what you should know to tell your patient. *Radiographics*, 28(7), 1807-1816.

Victor, A. G., (2000). Statistical approach for image quality evaluation in daily medical practice. *Medical Physics*, 27(1), 94-100.

Vodovatov, A. V., Bernhardsson, C., Drozdov, A. A., Kamishanskaya, G. I. (2017). Quality assessment of digital X-ray chest images using an anthropomorphic chest phantom. *Journal of Physics*, 808, 1 – 6.

Walker, W. (2015). The strengths and weaknesses of research designs involving quantitative measurements. *Journal of Research in Nursing*, 10(5), 571-582.

Wagner, R. F., Beiden, S. V., & Campbell, G. (2001). Multiple-reader studies, digital mammography computer-aided diagnosis and the holy grail of imaging physics. Proc. SPIE 4320, 611-618.

Wambani, J. S., Onditi, E. G., Korir, G. K., & Korir, J. K. (2015). Patient doses in general radiography examinations. *The South African Radiographer*, 53 (1): 22- 26.

Waters, H. (2011). The first X-ray, 1895. Retrieved from; https://www.the-scientist.com/foundations/first-x-ray-1895-42279.

Wang, Z., Sheikh, H. R., & Simoncelli, E. P. (2004). Image quality assessment: From error visibility to structural similarity. *IEEE Transactions on Image Processing*, 13(4). 600-612.

Ween, B., & Jacobsen, A. J. (2015). Sharpness and noise in digital chest radiographs, Assessed by visual rating. Radiography open, 2(1), 30-51.

Williams, B. M., Krupinsui, A. E., Strauss, J. K., Breeden, K. W., Rozeszotarski, M. S., Applegate, K., Wyatt, M., Bjork, S., & Seibert, J.A. (2007). Digital Radiography image quality: Image Acquisition. *Journal of the American College of Radiology*, 4(6), 371 -388.

Winslow, F. J., Hyer, D. E., Fisher, F. R., Tien, C. J., Hintenlang, D. E. (2009). Construction of anthropomorphic phantom for use in dosimetry studies. *Journal of Applied clinical medical physics,* 10 (3), 195 – 204.

Yacoob, H. Y., Hariwan, A. M. (2017). Assessment of patients X-ray doses at three Government hospital in Duhok city lacking requirements of effective quality control. *Journal of Radiation Research and Applied Sciences,* 10: 183-187.

Yusuf, S. W., Daher, I. N., & Sami, S. (2011). Radiation –induced heart disease: A clinical update. *Cardiology Research and practice*, 2011, 1-9.

Zink, E. F. (1997). The American Association of physicists in Medicine/Radiological Society of North America Physics Tutorial for Residence. *Radiographics,* 17(5), 1259-12685.

APPENDICES

APPENDIX A

DATA COLLECTION INSTRUMENT FOR ESD SURVEY – CHEST PA AT HP1

Patient No	V [kVp]	Q [mAs]	T [ms]	W [kg]	H [cm]	FDD [cm]	FSD [cm]	ESD [mGy]	Body thickness [cm]	Age	Sex
1.	102	5.00	10	60	151	150	127	0.649	23	24	F
2	102	3.60	7.1	70	160	150	126	0.475	24	65	F
3	102	3.60	7.1	82	150	150	124	0.490	26	63	F
4	102	2.80	5.6	85	150	150	123	0.388	27	49	M
5	102	2.80	5.6	62	151	150	127	0.364	23	55	M
6	102	2.80	5.6	84	140	150	122	0.394	28	43	F
7	100	2.00	4.0	47	150	150	130	0.238	20	43	F
8	100	2.00	4.0	65	170	150	128	0.245	22	82	M
9	100	1.80	3.6	55	160	150	129	0.217	21	32	M
10	104	1.80	3.6	50	151	150	129	0.236	21	22	M
Aveg	101.6	2.84	5.6	66	141	150	126.5	0.369	23.5	47.8	-
Min	102	1.80	3.6	47	140	150	122	0.217	20	22	-
Max	104	5.00	10	85	170	150	129	0.649	28	82	-

APPENDIX B

DATA COLLECTION INSTRUMENT AND RESULTS FOR PHANTOM STUDIES – LUMBAR SPINE AP

Image No	Q [mAs]	V [kVp]	Dose(mGy)	EI	VGAS
13	16	70	1.411	592	0.601
22	18	70	1.586	527	0.634
2	20	70	1.762	515	0.847
42	22	70	1.941	679	0.847
4	25	70	2.203	527	0.846
40	28	70	2.467	565	0.846
5	32	70	2.819	409	0.848
10	36	70	3.172	283	0.848
27	40	70	3.524	252	0.845
7	45	70	3.965	225	0.849
42	50	70	4.406	241	0.852
26	16	80	1.894	409	0.845
28	18	80	2.131	348	0.846
3	20	80	2.367	459	0.848
50	22	80	2.604	439	0.850
1	25	80	2.959	258	0.853
51	28	80	3.314	348	0.855
36	32	80	3.788	283	0.856
33	36	80	4.262	175	0.856
18	40	80	4.735	152	0.857
32	45	80	5.327	191	0.855
41	50	80	5.919	163	0.855
24	16	90	2.441	215	0.846
25	18	90	2.746	348	0.848
23	20	90	3.051	171	0.850
52	22	90	3.356	236	0.851
14	25	90	3.814	132	0.852
53	28	90	4.271	179	0.852
16	32	90	4.882	103	0.852
12	36	90	5.492	94	0.736
29	40	90	6.102	82	0.736
31	45	90	6.865	73	0.658
44	50	90	7.628	66	0.658
15	16	100	3.052	191	0.846
17	18	100	3.433	68	0.845
19	20	100	3.815	98	0.845
54	22	100	4.196	126	0.846
30	25	100	4.768	88	0.846
55	28	100	5.341	96	0.736
9	32	100	6.104	94	0.736
34	36	100	6.867	57	0.658
6	40	100	7.630	55	0.658
8	45	100	8.583	48	0.658
39	50	100	9.537	39	0.656
Reference image	28	74	2.794	297	0.840

APPENDIX C

DATA COLLECTION INSTRUMENT AND RESULTS FOR PHANTOM STUDIES – LUMBAR SPINE LAT

Image No	Q [mAs]	V [kVp]	Dose(mGy)	EI	VGAS
2	16	70	1.528	2198	0.855
26	18	70	1.719	2148	0.858
28	20	70	1.910	1915	0.862
44	22	70	2.101	2704	0.862
4	25	70	2.388	1486	0.865
46	28	70	2.674	1667	0.868
5	32	70	3.057	1154	0.871
10	36	70	3.439	1028	0.871
27	40	70	3.821	895	0.868
7	45	70	4.299	836	0.866
42	50	70	4.776	780	0.866
3	16	80	2.050	2099	0.565
24	18	80	2.307	2148	0.575
38	20	80	2.563	2005	0.652
45	22	80	2.820	1236	0.682
1	25	80	3.204	1005	0.853
43	28	80	3.589	1236	0.855
36	32	80	4.101	695	0.857
33	36	80	4.614	711	0.860
18	40	80	5.127	649	0.865
32	45	80	5.768	679	0.865
41	50	80	6.409	504	0.865
23	16	90	2.642	1154	0.745
21	18	90	2.973	960	0.750
17	20	90	3.303	895	0.854
42	22	90	3.634	695	0.858
14	25	90	4.129	649	0.860
41	28	90	4.625	664	0.862
16	32	90	5.285	527	0.866
12	36	90	5.946	439	0.871
29	40	90	6.607	429	0.872
31	45	90	7.433	303	0.872
44	50	90	8.259	318	0.871
19	16	100	3.304	895	0.855
15	18	100	3.717	798	0.858
20	20	100	4.130	679	0.862
40	22	100	4.543	649	0.862
30	25	100	5.163	409	0.865
37	28	100	5.783	303	0.868
9	32	100	6.609	439	0.871
34	36	100	7.435	283	0.871
6	40	100	8.261	241	0.868
8	45	100	9.294	220	0.866
39	50	100	10.327	290	0.866
Reference image	56	74	5.349	552	0.851

APPENDIX D

DATA COLLECTION INSTRUMENT AND RESULTS FOR PHANTOM STUDIES – CHEST PA

Image No	Q [mAs]	V[kVp]	Dose (mGy)	EI	VGAS
32	1.6	70	0.110	6638	0.120
10	2.0	70	0.137	6195	0.147
3	2.5	70	0.171	5396	0.171
20	3.2	70	0.220	4809	0.400
15	3.6	70	0.247	4189	0.432
22	4.0	70	0.275	3909	0.451
11	1.6	80	0.147	4921	0.348
33	2.0	80	0.184	4000	0.378
19	2.5	80	0.230	3105	0.460
7	3.2	80	0.295	2524	0.461
12	3.6	80	0.332	2198	0.463
18	4.0	80	0.369	2099	0.465
25	1.6	90	0.190	3733	0.355
28	2.0	90	0.237	2898	0.656
6	2.5	90	0.297	2148	0.830
13	3.2	90	0.380	1787	0.831
29	3.6	90	0.428	1521	0.832
2	4.0	90	0.475	1419	0.833
8	1.6	100	0.237	2767	0.765
1	2.0	100	0.297	2355	0.831
14	2.5	100	0.371	1706	0.833
21	3.2	100	0.475	1387	0.835
36	3.6	100	0.535	1154	0.840
5	4.0	100	0.594	565	0.841
16	1.6	110	0.290	2466	0.832
35	2.0	110	0.363	2099	0.843
23	2.5	110	0.453	1486	0.835
27	3.2	110	0.581	1236	0.835
24	3.6	110	0.653	1005	0.837
9	4.0	110	0.726	938	0.837
31	1.6	120	0.348	1871	0.834
17	2.0	120	0.435	1556	0.835
26	2.5	120	0.544	1127	0.836
4	3.2	120	0.696	938	0.838
34	3.6	120	0.783	798	0.840
30	4.0	120	0.870	711	0.840
Reference image	25	73	1.887	695	0.628

APPENDIX E

IMAGE QUALITY CRITERIA ASSESSMENT FOR CHEST PA

You have been provided with test images marked with numbers. Please evaluate each anatomical criterion according to their degree of visibility as shown.

Anatomical Criteria for Chest PA		Clearly confident that the criterion is fulfilled (5)	Somewhat confident that the criterion is fulfilled (4)	Indecisive whether criterion is fulfilled or not (3)	Somewhat confident that the criterion is not fulfilled (2)	Clearly confident that the criterion is not fulfilled (1)
1	Visualization of the spine through the heart shadow					
2	Visually sharp production of trachea					
3	Visually reproduction of proximal bronchi					
4	Visually sharp reproduction of the diaphragm					
5	Reproduction of the whole ribcage above the diaphragm					
6	Visually sharp reproduction of lateral costo-phrenic angles.					

APPENDIX F

IMAGE QUALITY CRITERIA ASSESSMENT FOR LUMBAR SPINE AP

You have been provided with test images marked with numbers. Please evaluate each anatomical criterion according to their degree of visibility as shown.

Anatomical Criteria for Lumbar spine AP		Clearly confident that the criterion is fulfilled (5)	Somewhat confident that the criterion is fulfilled (4)	Indecisive whether criterion is fulfilled or not (3)	Somewhat confident that the criterion is not fulfilled (2)	Clearly confident that the criterion is not fulfilled (1)
1	Reproduction of the sacro-iliac joints					
2	Visually sharp reproduction of the pedicles					
3	Reproduction of the transverse process					
4	Reproduction of the spinous process					
5	Reproduction of the intervertebral spaces					
6	Reproduction of the adjacent soft tissues					

APPENDIX G

IMAGE QUALITY CRITERIA ASSESSMENT FOR LUMBAR SPINE LAT

You have been provided with test images marked with numbers. Please evaluate each anatomical criterion according to their degree of visibility as shown.

Anatomical Criteria Lumber spine LAT		Clearly confident that the criterion is fulfilled (5)	Somewhat confident that the criterion is fulfilled (4)	Indecisive whether criterion is fulfilled or not (3)	Somewhat confident that the criterion is not fulfilled (2)	Clearly confident that the criterion is not fulfilled (1)
1	Reproduction of the pedicles					
2	Reproduction of the intervertebral foramina					
3	Visualization of the spinous process					
4	Visually sharp reproduction of the intervertebral spaces					
5	Visually sharp reproduction of the cortex and trabecular structures.					